

**Translocation of water and nutrients
during growth and fructification of
*Agaricus bisporus***

PhD thesis Utrecht University, Utrecht, The Netherlands (2024)

The research described in this thesis was performed within the Microbiology group of Utrecht University, Padualaan 8, 3584 CH Utrecht, The Netherlands.

Copyright © 2024 by K. C. Herman. All rights reserved.

Cover design: Sandra Tukker
Printed by: Ridderprint
ISBN: 978-94-6483-942-5

Translocation of water and nutrients during growth and fructification of *Agaricus bisporus*

Transport van water en nutriënten gedurende de groei en
fructificatie van *Agaricus bisporus*
(met een samenvatting in het Nederlands)

Proefschrift

ter verkrijging van de graad van doctor aan de Universiteit Utrecht op gezag
van de rector magnificus, prof. dr. H.R.B.M. Kummeling, ingevolge het besluit
van het college voor promoties in het openbaar te verdedigen op

woensdag 17 april 2024 des middags te 4.15 uur

door

Koen Clement Herman

geboren op 17 januari 1993
te Leiden

Promotor:

Prof. dr. H.A.B. Wösten

Copromotoren:

Dr. L.G. Lugones

Dr. R. Bleichrodt

Beoordelingscommissie:

Prof. dr. W. de Boer

Dr. J. Dijksterhuis

Prof. dr. G.A. Kowalchuk

Prof. dr. E.E. Kuramae

Prof. dr. J.B.M. Middelburg

“We accept the reality with which we’re presented.”
The Truman show (1998)

*“As being is to becoming, so is intellect to opinion.
And as intellect is to opinion, so is science to belief,
and understanding to the perception of shadows.”*
The Republic, book VII (534a), Plato

Contents

	Scope of the Thesis	9
Chapter 1	General introduction	13
Chapter 2	Cycling in degradation of organic polymers and uptake of nutrients by a litter-degrading fungus	31
Chapter 3	Growth induced translocation effectively directs an amino acid analogue to developing zones in <i>Agaricus bisporus</i>	57
Chapter 4	Water requirements of <i>Agaricus bisporus</i> during growth and fructification	77
Chapter 5	Colonisation of compost by wild type and commercial <i>Agaricus bisporus</i> strains assessed by a scanning imaging method	93
Chapter 6	Summary and General Discussion	105
Appendix	References	117
	Nederlandse Samenvatting	131
	Curriculum vitae	137
	List of Publications	139
	Dankwoord	141

Scope of the Thesis

Mushrooms of *A. bisporus* (known as white buttons or “champignons”) are produced in the Netherlands on a compost that is topped with a casing layer. This thesis describes the colonization of the compost by the vegetative mycelium of *A. bisporus* as well as the transport of water and nutrients within this mycelium and to the developing mushrooms. Understanding how developing mushrooms acquire food and water via their supporting mycelial network could provide leads for a more efficient mushroom production.

Chapter 1 reviews the literature to provide a comprehensive view on how fungi obtain and translocate water needed for their development. *Agaricus bisporus* growing on compost and casing soil is taken as an example to discuss water relations during fruiting in detail.

Colonization of compost by *A. bisporus* was studied in **Chapter 2**. Bursts in O₂ consumption, CO₂ production, and temperature were observed during colonization. Sequencing of RNA isolated during, after, and in between these 2.5 - 5 hour bursts revealed different expression patterns. Genes encoding ligninolytic enzymes were highly expressed before and during a burst, (hemi-)cellulolytic genes and genes involved in microbial biomass degradation were upregulated during and after a burst, while sugar and amino acid transporters were highly expressed after the burst. These transcriptomic data support the view that *A. bisporus* cycles through degradation of lignin, degradation of (hemi-) cellulose and microbial biomass, and uptake of breakdown products.

In **Chapter 3** the amino acid analogue ¹⁴C-aminoisobutyric acid was used as a radioactive tracer to study translocation of nutrients during growth and development of mushrooms in *A. bisporus*. The translocation speed of ¹⁴C-AIB was 3.68 and 3.47 mm * h⁻¹ in *A. bisporus* mycelium in compost and casing, respectively. A 1.8 fold faster translocation velocity of the tracer was observed when compost was inoculated at one side of the compost (directional growth) instead of mixing the inoculum through the substrate as is routinely done in commercial mushroom growth. This was accompanied by the formation of more cords (i.e. bundles of aggregated hyphae containing wider vessel hyphae) and translocation of more ¹⁴C-AIB over longer distances towards developing mushrooms.

To better understand the flow of water towards mushrooms, the water potential (Ψ), osmotic potential (Ψ_{osm}) and the water content were determined of the casing and the different layers of compost during substrate colonisation and fructification. Additionally, the matric potential was inferred from the difference between the water potential and osmotic potential (Ψ_{mat}) (**Chapter 4**). It was shown that Ψ_{osm} of the compost and casing layer determines the water potential in the beginning of cultivation, whilst the matric potential becomes increasingly important in later stages, most notably in the casing soil. In addition, it was shown that the casing layer and the bottom compost layer are the most and least important in supplying water to mushrooms, respectively. Notably, the Ψ difference cannot explain the flow of water from the compost towards mushrooms. This may be explained by differences in turgor pressure in the mycelium during fructification.

Chapter 5 describes the colonisation of compost by commercial and wild type strains of *A. bisporus* by using a scanning imaging method. By taking the mean gray value as a marker for biomass we showed that some strains of *A. bisporus* followed a logistic growth profile, whilst others do not. All strains colonized the compost evenly, except strain MES 01808 that showed a bimodal distribution. The maximum colonisation and mushroom yield showed a positive correlation when data of strain MES 01808 was not taken into account. Together, data indicate that the degree of colonisation is a predictor for mushroom yield. Additionally, we suggest that an even colonisation is a more favourable trait over an uneven colonisation for mushroom production.

The results are discussed in **Chapter 6**.

1

General Introduction

Koen C. Herman, Robert-Jan Bleichrodt

This chapter has been published as: Herman, K.C., Bleichrodt, R., 2022. Go with the flow: mechanisms driving water transport during vegetative growth and fruiting. *Fungal Biol. Rev.* 41, 10-23

Abstract

Fungi need water for all stages of life. In fact, mushrooms consist of 90 % of water. Fungi degrade organic matter by secreting enzymes. These enzymes need water to break down the substrate. For instance, when the substrate is too dry, fungi are known to transport water from moist areas to arid areas by hydraulic redistribution. Once nutrients are freed from the substrate, they are taken up by transporters lining the cell membrane. Thereby, an intracellular osmotic potential is created that is greater than that of the substrate, and water follows by osmosis. Aquaporins facilitate water uptake at cold temperatures. Since fungi possess a cell wall, the cell volume will not increase by water uptake, but the cytoplasm will exert higher pressure on the cell wall, thereby building up turgor. Fungi have tightly coordinated osmotic regulatory controls via the HOG pathway. When water is getting scarce, this pathway makes sure enough osmolytes are synthesized to allow sufficient water uptake for maintaining turgor homeostasis. The fungal network is interconnected and allows water flow when small pressure differences exist. These pressure differences can be the result of growth, differential osmolyte uptake/synthesis or external osmotic conditions. Overall, the water potential of the substrate and fungal tissues determine whether water will flow, since water flows from an area of high- to a low water potential area. In this review we aim to give a comprehensive view on how fungi obtain and translocate water needed for their development. We have taken *Agaricus bisporus* growing on compost and casing soil as a case study, to discuss water relations during fruiting in detail. Using the current state-of-the-art we found that there is a discrepancy between the models describing water transport to mushrooms and the story that water potentials tell us.

1. Introduction

From the moment a fungal spore germinates, the fungus depends on water for its growth (Heaton et al., 2010), substrate degradation (Guhr et al., 2015), nutrient uptake, reproduction, and spore dispersal (Dressaire et al., 2016). Mushrooms even consist of ≥ 90 % water (Kalberer, 1985). It is not clear in which part(s) of the mycelium water is taken up, while this has huge implications for the extent and direction of water and nutrient transport. Some imply that water must be taken up in the colony centre or along the hyphae in the colony (reviewed by Fricker et al., 2017), while others suggest that this happens at the hyphal tips (reviewed by Lew, 2011; Tegelaar, 2017, 2020). If water is only taken up at the hyphal tip, the mass flow observed towards the colony margin (Lew, 2005), would not be possible, since it would counteract the sub-apical pressure differences needed for tip-directed mass flow. On the other hand, if the centre of the colony is the sole zone of water uptake, this would counteract the observed oscillations and bidirectionality in transport directions (Tlalka et al., 2007; Muralidhar et al., 2016; Schmieder et al., 2019). This suggests that these proposed models may be incomplete and could co-exist or that water uptake is regulated in space and time and could be heterogeneous between single hyphae. Although extensive efforts have been made to understand the water relations in *A. bisporus* cultures, it is not clear how water would be transported from compost to the mushrooms, since mushrooms have higher water potential than the compost (Kalberer, 1983, 1985, 1987, 2006) and water should flow from areas with high to low water potential

(see Text box 1).

In this review, that focusses mainly on saprotrophic mushroom forming fungi, we explore what factors influence water uptake and transport in the vegetative mycelium and transport to the mushrooms, and how water availability in the substrate may limit mushroom formation in *Agaricus bisporus* as an example.

2. Water uptake and transport

2.1 Aquaporins

Water needs to be transferred over the fungal cell membrane in order to enter the cell. Although the cell membrane is permeable to water, aquaporins increase membrane permeability and allow control by gating. Four classes of fungal aquaporins have been proposed based on phylogenetic analysis: orthodox aquaporins, aquaglyceroporins, SIP-like aquaporins and X intrinsic proteins (Verma et al., 2014). However, basidiomycetes only possess orthodox aquaporins and / or aquaglyceroporins (Xu et al., 2013; Verma et al., 2014).

Orthodox aquaporins do only allow permeation of water molecules. The crystal structure of Aqy1 of *Pichia pastoris* indicates that water molecules can be taken up in single file, but that water is not allowed to exit the cell. Gating is regulated by changing membrane tension and phosphorylation (Soveral et al., 2008; Fischer et al., 2009). Aquaglyceroporins transport water and polyols such as glycerol (Nehls and Dietz, 2014), but also urea and arsenite (Heller et al., 1980). They show the highest number of functional subgroups in fungi compared to all other organisms that have been investigated (Verma et al., 2014), indicating that they have specialized roles. Remarkably, some aquaglyceroporins found in the basidiomycete *Laccaria bicolor* are better water transporters than the orthodox aquaporins (Dietz et al., 2011; Xu et al., 2013). For example, yeast aquaglyceroporin Fps1 closes in response to hyperosmotic conditions in a HOG pathway dependent manner (Tamás et al., 1999; Lee et al., 2013). Genomic analysis of *A. bisporus* showed only four aquaporin genes. They all belong to the aquaglyceroporin class. Homologs of these genes influence membrane water permeability in the basidiomycete *L. bicolor* (Dietz et al., 2011). The function of these missing orthodox aquaporins might thus be taken over by the aquaglyceroporins in *A. bisporus* (Nehls and Dietz, 2014).

Expression analysis showed that aquaporins are upregulated during fruiting body formation in *L. bicolor* and *Flammulina filliformis*. High transcript levels are found during the primordial stage. In later stages, either the stipe or cap show high expression of aquaporins (Nehls and Dietz, 2014; Xu et al., 2016; Liu et al., 2020). These studies provide interesting evidence on the role of aquaporins during fructification. Studying which aquaporins are expressed where and when, and their gating will improve our understanding of water uptake and transport in fungi.

2.2 Osmoregulation

Turgor is regulated by the HOG pathway (Reiser et al., 2003; Schaber et al., 2010). The HOG pathway not only responds to osmotic stress, but also to stresses such as cold (Panadero et al., 2006), citric acid (Lawrence et al., 2004) and heat (Winkler et al., 2002). The HOG pathway structure of *Saccharomyces cerevisiae*, as well as a timeline following hyperosmotic shock have been previously reviewed (Hohmann, 2002; O'Rourke et al.,

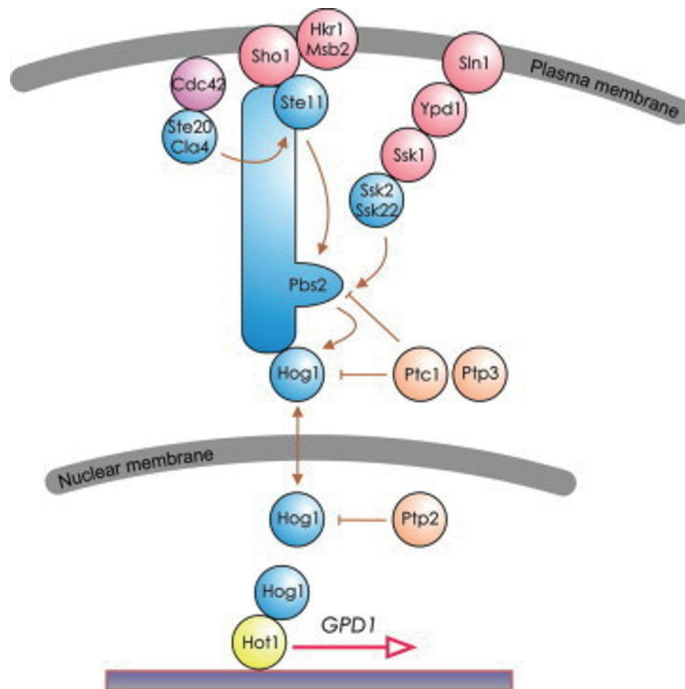


Figure 1. Signal transduction in the yeast HOG pathway. Membrane-localised sensors and regulators are shown in red, protein kinases in blue, protein phosphatases in orange and transcription factors in yellow. Two branches converge at the level of Pbs2 to activate Hog1, which accumulates in the nucleus under stress. Ste11, Ssk2 and Ssk22 are MAPKKs, Pbs2 a MAPKK and Hog1 the MAPK in the system. See text for further details. Used with permission of [John Wiley and Sons], from [Hohmann, S., 2009. Control of high osmolarity signalling in the yeast *Saccharomyces cerevisiae*. FEBS Lett. 583, 4025–4029]; permission conveyed through Copyright Clearance Center, Inc.

2002; Hohmann et al., 2007; Saito and Posas, 2012). The HOG pathway consists of two branches that sense osmotic changes differently (Fig. 1). These branches are termed the Sln1 and Sho1 branch and integrate their signal transduction at the MAPKK Pbs2, which in turn activates the MAPK Hog1 (Maeda et al., 1995). The HOG pathway in yeast encompasses an immediate response aimed at maintaining vital cellular processes, followed by a more long-term transcriptional response to counteract the hyperosmotic conditions. The fast response involves mediating ion fluxes (Proft and Struhl, 2004; Lew, 2011), whilst the transcriptional response induces the synthesis of compatible solutes, such as glycerol, which lowers the internal osmotic potential (see Text box 1) (Albertyn et al., 1994).

Considerably less is known about the HOG pathway in filamentous fungi. Comparative genomic analysis between yeast species, filamentous ascomycetes, and the basidiomycete *Ustilago maydis*, highlights a ‘consensus’ HOG pathway consisting of the Sln1 and the Sho1 branch converging on Pbs2. However, designs of both branches differ notably in the pathway input (Krantz et al., 2006a, 2006b). The Sho1 branch in these fungi presumably does not function in response to osmotic changes, but functions in the filamentous growth pathway (Krantz et al., 2006a). Indeed, the HOG pathway of *Aspergillus nidulans* is solely

Text box 1: Water potential (ψ)

The water potential is the sum of all forces that work on water. When unobstructed, water flows from an area with high water potential to an area having a lower water potential. This can be sometimes tricky to imagine, since the water potential can be between zero and a negative value. Thus, water would flow from an area with a water potential of e.g. -2 MPa to an area of -4 MPa. When a substrate dries out, as a consequence of water usage by the fungus or evaporation, the water potential will drop. The relationship between gravimetric water content and water potential is not linear and can be depicted in a soil-water characteristic curve (Tuller and Or, 2005).

The water potential is given by the following equation (Eq. 1):

$$\Psi = \Psi_{osm} + \Psi_{\Pi} + \Psi_g + \Psi_h + \Psi_{mat} \quad (Pa = kg \cdot m^{-1} \cdot s^{-2} = Nm^{-2}) \text{ where:}$$

The osmotic potential (Eq. 2) $\Psi_{osm} = -i \cdot \Phi \cdot C \cdot R \cdot T$, where i is the ionization constant or Van't Hoff factor (the number of molecules that the substance disintegrates in when dissolved in water), Φ is the osmotic coefficient (is the deviation of a solvent from ideal behaviour, which is usually close to 1 (mounir et al., 2020)), C is the molarity ($mol \cdot L^{-1}$), R is the gas constant ($8314 L \cdot Pa \cdot K^{-1} \cdot mol^{-1}$), and T is the absolute temperature (K).

the (hydrostatic) pressure potential Ψ_{Π} or turgor is the internal pressure of the cell and is usually positive, in contrast to all other water potential factors that are negative. If a cell is at equilibrium with a bath of pure water at atmospheric pressure, then its turgor pressure is equal to its osmotic pressure (Beauzamy et al., 2014). However, this holds only for a cell that is not constrained by a rigid cell wall, which fungi do possess. In walled fungi the turgor becomes increasingly greater with higher osmotic potential differences, since the cell wall gets more rigid at higher internal pressures. The turgor pressure can be measured using atomic force microscopy (Arnoldi et al., 2000; Bovio et al., 2019) or a pressure probe (Lew, 2005).

The gravitational potential (Eq. 3) $\Psi_g = \frac{m \cdot g \cdot h}{v}$, where where m is the mass (kg), g is the gravitational acceleration ($9.81 m \cdot s^{-2}$), h is the height difference (m), and v is the volume (m^3). The gravitational potential ψ_i in a mushroom bed is negligible, since 1 kg of water transported over 0.25 m height difference, results in a pressure of just $(1 \cdot 9.81 \cdot 0.25) / (1 kg / 997 kg m^3) = 0.0025 MPa$.

The humidity potential (Eq. 4) $\Psi_h = \frac{RT}{V_w} \ln(RH)$, where R is the gas constant, T is the absolute temperature (K), V_w is the partial molar volume of liquid water ($18E-6 m^3 \cdot mol^{-1}$), and RH is the relative humidity of the air as a fraction, thus 80% RH = 0.8. The humidity potential ψ_h quickly drops with decreasing relative humidity of the air (Fig. 2). In fact, the low water potential of air (-70 MPa at 60 % RH and 22 °C) is usually the biggest factor for water loss, due to evaporation. In plant research the concept of the soil plant atmosphere continuum explains why and how water flows from the soil via root uptake through the plant and ends up in the air. Soil, root, stem, leaves, and air have increasingly lower water potentials (Taiz et al., 2014). This ensures a continuous flow of water through the system in which nutrients can be transported.

The matric potential ψ_{mat} is defined as the attractive forces between water and the soil, such as capillary pressure exerted by van der Waals and electrostatic forces, given by the Young-Laplace equation (Eq. 5), $\psi_m = -\frac{2\gamma \cos(\theta)}{r}$, where γ is the surface tension of water ($N \cdot m^{-1}$), θ is the contact angle between the water and soil at the air-soil-water interface ($^\circ$), and r is the radius of the pore in hydrophilic soils (m). Usually, the matric potential is not calculated, but determined by subtracting the measured osmotic potential from the water potential. In hydrophobic soils, the matric potential (Eq. 6) $\Psi_{mat} = \Psi_{\Pi} + \Psi_{os}$, where Ψ_{Π} is the hydrostatic pressure, and Ψ_{osm} is osmotic potential, but in this case these cannot be dissected experimentally (Whalley et al., 2013).

Water potential can be measured by several methods. For example, thermocouple psychrometry relies on the relation between the vapour pressure and the water potential of a sample. Water with a higher concentration of solutes has a lower vapour pressure, and thus in a closed chamber the surrounding air has a lower humidity. In a closed chamber, where temperature and pressure are in equilibrium, the humidity can be determined in various ways using a thermocouple (Boyer, 1995). From the humidity readings the water potential is calculated.

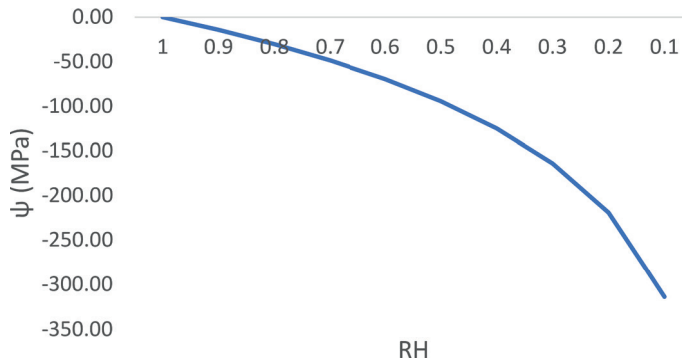


Figure 2. Relation between the water potential (ψ) of air and relative humidity (RH), calculated using eq. 4 in Text box 1.

activated by proteins orthologous to the Sln1 branch of *S. cerevisiae* (Furukawa et al., 2005).

The sensor Sln1 is the only hybrid histidine kinase in *S. cerevisiae*. Fungal histidine kinases generally have sensor functions to respond to a variety of stresses (Bahn et al., 2007). Most basidiomycetes have multiple histidine kinases, implying a more complex input of extracellular signals. A classification system of these proteins was proposed by Lavín et al. (2010). *A. bisporus* has four hybrid histidine kinases, one of which is a type IA (AGABI2DRAFT_228355; Lavín et al., 2013). The hybrid histidine kinase type IA Tco1/Nik1 has been shown to regulate the HOG pathway in *Cryptococcus neoformans* (Bahn et al., 2006). The hybrid histidine kinase Le.Nik1 was found to be important during fruiting body formation in *Lentinula edodes*. Expression of Le.Nik1 increases as primordia mature into fruiting bodies. High amounts of transcripts are found in the trama cells, which support the gills and expand rapidly by absorption of water during the later stages of fruiting body development (Szeto et al., 2008). This suggests that the HOG pathway not only mediates the regulation of osmotic potential during vegetative growth but also in the development of fruiting bodies. Functional analysis of this pathway should be done in *A. bisporus* to provide definitive conclusions. We will discuss how fruiting bodies of *A. bisporus* generate their osmotic potential in section 3.7.

2.3 Turgor and tip-directed bulk flow

Filamentous fungi maintain turgor for optimal growth, but also differences in turgor pressure exist in a fungal colony. Eamus and Jennings (1984) have proposed pressure-driven mass flow as a mechanism for translocation of water and solutes in the direction of the growing hyphal tips in basidiomycetes. This flow is achieved by small pressure differences along the hyphae that result from differential (i) osmolyte take up, including ions and nutrients (Lew, 2005); (ii) osmolyte synthesis, such as glycerol (Lew, 2011); (iii) extracellular pressure differences resulting from differential osmotic or matric potentials (see Text box 1) (Amir et al., 1995; Muralidhar et al., 2016); or (iv) growth (Heaton et al., 2010; Lew, 2011).

Various filamentous fungi, for example *Armillaria mellea*, *Phallus impudicus*, *Phanerochaete velutina*, *Penicillium chrysogenum*, and *Serpula lacrymans* all show a higher

turgor pressure at the centre of the colony compared to the periphery (Luard and Griffin, 1981; Granlund et al., 1985; Eamus and Jennings, 1986). The turgor pressure could be temporarily reversed in *S. lacrymans* grown on Perspex by adding 2 M glucose solution to the woodblock inoculum (Thompson et al., 1985). This decreased the growth speed (Clarke et al., 1980). Applying hyperosmotic treatment in front of the colony margin causes a pressure drop within the leading hyphae. As a result, mass flow velocity increases towards the hyphal tip. When applied behind the colony margin, mass flow velocity towards the front decreases and causes water outflow from the hyphae (Lew, 2005, 2011; Abadeh and Lew, 2013). This further supports the view that water taken up in the centre drives bulk flow of water and solutes towards the colony margin (Heaton et al., 2010).

Contrasting with this view is the self-sustaining apical compartment. When the second compartment of hyphae was ruptured, by an UV laser pulse, the hyphal tip continued its growth at a similar rate as before when it was still attached to the colony (Tegelaar and Wösten, 2017; Tegelaar et al., 2020). This shows that tips can take up all the water required for their growth and are not dependent on the colony centre, at least in case of an emergency. Subjecting *P. chrysogenum* to hyperosmotic conditions (-10 MPa) results in a lower osmotic potential (-10.3 MPa) of the hyphae. The periphery has lower osmotic potential than the centre of the colony, both under normal and hyperosmotic conditions (Luard, 1982a, 1982b). If the colony margin has the lowest osmotic potential, then water could be taken up most efficiently here. This assumes that the entire colony is equally permeable to water. The observations of oscillatory or bidirectional transport patterns also contrast with the view of tip-directed bulk flow. Rapid pulsatile fluxes of the amino acid analogue ^{14}C labelled α -aminoisobutyrate are observed in *Phanerochaete velutina*. This nutrient analogue is transported along routes that rapidly changed in direction (Tlalka et al., 2002, 2003, 2007). In *C. cinerea* distinct trunk hyphae propagated cellular signals and nutrients bidirectionally. Dynamic opening and closing of septa was proposed as a mechanism to revert bulk flow (Schmieder et al., 2019).

We highlight the debate on how the uptake of water would generate pressure-driven mass flow. Lew (2011) states that it is likely that water is maximally taken up at the tip and tapers off towards the colony centre, but this would short circuit the pressure differences needed for tip-directed bulk flow. Yet, water uptake at hyphal tips is supported by the lower osmotic potential of the colony margin (Luard and Griffin, 1981). Fricker et al. (2017) argue that water could be taken up anywhere along the mycelium and that the turgor gradient mediates bulk flow. Indeed, there is evidence for a higher turgor pressure in the colony centre (Luard and Griffin, 1981; Eamus and Jennings, 1984; Thompson et al., 1985). The bidirectional or oscillatory patterns in transport of nutrients (Tlalka et al., 2003; Muralidhar et al., 2016; Schmieder et al., 2019) further complicate the long-standing view of tip directed bulk flow (Eamus and Jennings, 1984). Therefore the site of water uptake in a mycelium is of critical importance in understanding turgor pressure differences and bulk flow. Identifying the locations and unravelling dynamics of water uptake / loss and subsequent pressure differences, should provide the starting point to resolve these seemingly contrasting models and observations.

3. Water requirements during fruiting body formation in *A. bisporus*

3.1 Commercial culturing of *A. bisporus*

To provide an overview of the water balance of *A. bisporus* during fruiting, we first describe how the fungus is commercially cultivated. *A. bisporus* is grown on compost that is based on a mixture of horse / chicken manure, wheat straw, gypsum and water (Gerrits 1988). Composting knows 2 phases in which bacteria convert (hemi)cellulose (Jurak 2015; Jurak et al. 2015b) and thermophilic fungi are selected (Straatsma and Samson, 1993). This makes the compost selective for *A. bisporus* (Ross and Harris 1983; Straatsma et al. 1989, 1994b). Spawn, usually rye colonised with mycelium, is mixed through the compost. *A. bisporus* colonizes the compost in 16 days, feeding on lignin, (hemi)cellulose and/or bacteria (Jurak 2015; Jurak et al. 2015b; Vos et al., 2017a). The colonised compost is transported to the grower, where it is applied as a ~ 25 cm thick layer and topped with a 5 cm thick casing layer (Fig. 3), composed of peat and lime. After colonisation of the casing layer, primordia formation is induced by lowering the air temperature and CO₂ levels by ventilation (Visscher, 1988). Few of the primordia develop into mature mushrooms, that are harvested in 2 - 3 flushes at weekly intervals.

Previously, typical water contents of compost and casing soil were 50 - 56 % and 67 - 69 %, respectively (Gerrits, 1971; Kalberer, 1985). Of note, the casing soil that is nowadays used, has a higher water content of 80 % at a water potential of 0 MPa. This may impact the conclusions that are drawn below, when applied to modern day casing. Previously, casing contained 2 volumes black peat, 2 volumes black soil and 1 volume ground chalk or lime cakes (Kalberer, 1985; or similar, Kalberer, 1990b), while presently casing contains only peat and lime (Vos et al., 2017a).

Mushrooms contain more than 90 % water (Kalberer, 1987), thus their water supply is paramount for development. In the next paragraphs we will describe from which layers (*i.e.* casing and compost) in the culture the mushrooms take their water, what the mechanism is for driving this water uptake/transport, and discuss which factors may limit mushroom development in relation to water availability.

3.2 The casing layer and compost differentially supply mushrooms with water

A 5-6 cm thick casing layer on ~ 17.5 cm compost contributes on average 33 % of the water in mushrooms of the first flush, whilst a thinner 3 - 3.5 cm casing layer decreases this contribution to 16 % (Kalberer, 1983, 1985). These observations are similar to those of



Figure 3. *Agaricus bisporus* mushroom culture. Colonised compost is topped with a layer of casing soil to produce mushrooms. In some studies, the compost was subdivided in three equal sized layers (Top, Middle and Bottom) to analyse their individual water content or water/osmotic potentials.

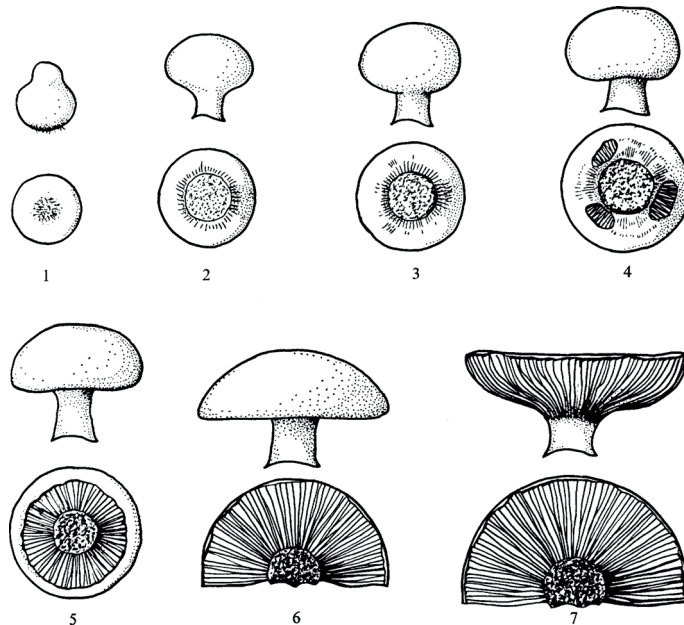


Figure 4. Appearance of sporophores at stages 1 to 7. Used with permission of [Microbiology Society], from [Hammond, J. B., Nichols, R., 1976a. Carbohydrate metabolism in *Agaricus bisporus* (Lange) Sing; changes in soluble carbohydrates during growth of mycelium and sporophore. *J. Gen. Microbiol.* 93, 309–320]; permission conveyed through Copyright Clearance Center, Inc.

Gerrits (1968) and Flegg (1974). Moreover, subsequent flushes draw more water from the casing, until in the third flush almost equal parts of the water are taken from the compost and the casing (Kalberer, 1985). The water content after the second flush was 54.1 % for casing and on average 71.1 % for compost. Together, this shows that although casing has a lower water content, mushrooms preferentially take water from the casing. This is because the osmotic potential of casing (-0.26 MPa) is higher than that of compost (-1.33 MPa on average; Kalberer, 1987; see also Text box 1), since casing has a lower solute concentration. Thus, water can be more easily extracted from the casing than from the compost by the mycelial network to supply the mushrooms.

Interestingly, mushrooms harvested from a thin casing layer or young mushrooms (stages 1-2, Fig. 4) show higher dry matter contents than mushrooms harvested from a thick casing layer or old mushrooms (stages 5 - 7, Fig. 4). This is in agreement with the facts that young and old mushrooms take 37 % and 46 % of their water from casing, respectively, and that mushrooms take less water from a thinner casing layer (Kalberer, 1983), since compost contains many nutrients, while casing is nutrient poor. Thus, mushrooms grown on thicker casing layers, take more water from the casing, thus relatively less nutrients, and as a result have lower dry matter contents. Over three flushes combined, yields are 1.16 fold higher on thick casing compared to thin casing layers, but this could not be explained by higher water content of the mushrooms (1.01 fold; (Kalberer, 1985). Either more or bigger mushrooms developed on the thick casing layer.

3.3 *The vegetative mycelium supplies mushrooms differentially depending on the compost depth*

For all three flushes, most water is lost from the top layer of compost (Fig. 3), followed by the middle layer, while the bottom layer hardly contributes to supplying the mushrooms with water (Kalberer, 1983, 1985). Flegg (1981) showed that the top layer of the compost also supplies most nutrients to the mushrooms. *A. bisporus* was shown to transport water from zones of abundant to zones of scarce water availability by hydraulic redistribution, to aid substrate degradation (Guhr et al., 2015). However, the mycelium of the bottom compost layer does not seem to transport water to the layers above. In compost the mycelium forms a fine network of mainly individual hyphae, while in casing predominantly bundles of hyphae (cords) are formed, of which some hyphae have higher diameters (Cairney, 1990). Volume flow rate in pipes is mainly dependent on their diameter (see Herman et al., 2020; Chapter 3). Therefore, it is likely that the distance from the lower compost layer is so far located from the mushrooms, that the resistance of the fungal network therein is too high to sufficiently transport to the mushrooms. Supporting this, we found that a network architecture having predominantly cords showed 5 fold more nutrient transport to mushrooms than a network of predominantly fine mycelium (Herman et al., 2020; Chapter 3).

3.4 *Evaporation by the mushrooms and the casing layer*

By evaporation from the casing and through the mushrooms, and the mushroom harvest itself, the cultures lose water. Although relative humidity is usually kept between 95 - 99 %, air still has a lower water potential (Eq. 4 in Text box 1: -7.0 to -1.4 MPa at 22 °C; Fig. 2) than that of the casing and mushrooms (Kalberer, 1987), thereby stimulating evaporation. Evaporation totals 9 - 50 % of the water content of the harvested mushrooms, depending on the conditions (San Antonio and Flegg, 1964; Kalberer, 1987). Evaporation from the casing is constant over a large range of gravimetric water contents (Flegg, 1974). Mushrooms evaporate at the same rate as a free water surface. This is independent on age, developmental stage or air temperature (San Antonio and Flegg, 1964). 2 cm diameter mushrooms (stage 1, Fig. 4) evaporate 1 ml / day, while 6 cm diameter mushrooms (stage 4 - 5, Fig. 4) evaporate 2 - 4 ml / day, which equals up to 3 mg / cm² / h. When evaporation is increased to 6 - 8 mg / cm² / h, growth ceases and the pileus becomes cracked, scaly and discoloured. This indicates that the hyphal network attached to the mushroom can only supply up to 3 mg / cm² / h plus the water needed for expansion of the mushroom.

Thus, the rate of water transport to mushrooms must be greater than their evaporation rate, otherwise mushrooms cannot expand exponentially in volume (Straatsma et al., 2013). This suggests that reducing evaporation may increase expansion rate. However, when mushrooms are grown under water saturating conditions, mushrooms expand at the same rate as mushrooms under control conditions (Mader, 1943; Riber Rasmussen, 1959). This shows that evaporation is not required for mushroom expansion. Nevertheless, evaporation by the mushroom is important for spore dispersal (Dressaire et al., 2016).

3.5 *Effect of watering*

Watering can increase the moisture content of the casing and to a certain degree that of the compost (Kalberer, 1985), since water percolates through the casing layer into the compost (Fig. 3). Colonisation of the casing layer is markedly affected by watering. In relatively dry

casing, the mycelium grows dense, while in wetter casing the mycelium forms thick hyphal cords leaving areas of uncolonized casing (Flegg, 1962, 1974). Watering the casing layer shows a positive correlation with yield (Flegg, 1974). This suggests that cord formation correlates with mushroom yield. It is not clear whether this is due to better transport connections between the compost and the mushrooms or serves better water uptake from the casing.

Mushroom cultures that are given the same amount of water, but with different watering regimes, do not affect yield by more than 10 %. Yet, yield is optimal when watering is applied at regular intervals, during colonisation of the casing and fructification. When watering is delayed, yield is reduced and the casing is covered with more mycelium. When no water is applied, still 2 / 3 of the yield is obtained compared with regular watering, indicating that the substrate stores a considerable water reserve that supplies mushrooms under development (Flegg, 1975). At any point in development, the amount of water given to the casing has to be ~ 50 % of the wet weight of the fruiting bodies at that time, to keep the water level in casing constant. Watering of cultures results in higher moisture levels of the casing, top and middle compost layers (see Fig. 3). The yield is significantly higher in watered than in unwatered cultures, but this is only when harvesting after 3 weeks after filling, but not earlier. Fruiting bodies from watered cultures have significantly lower dry matter contents than unwatered cultures (Kalberer, 1990b).

3.6 *Hydrophobins: friend and foe*

Fungi secrete hydrophobins that assemble at the air-water interface. This help the fungus escape from the substrate into the air to bridge gaps within the substrate or to form reproductive structures (Wösten, 2001). During cultivation of *A. bisporus* both the compost, but predominantly the casing soil become more and more hydrophobic, which hampers water uptake after watering (Bleichrodt, unpublished results), thus reducing water availability for mushroom production. On the other hand, casing soil contains cells or pockets filled with water (Noble et al., 1999). Once the casing soil is dried out too much, these pockets cannot be regenerated by watering. Hydrophobins may coat these pockets or coat water-filled gaps in the compost. The hydrophobins would lower the surface tension of water, thus lowering the capillary forces of walls of air pockets, thereby increasing the matric potential (see Text box 1), and thus free up scarce water for the fungus. This said, matric potential is quite low in commercial mushroom compost (Kalberer, 2006), thus this only comes into play at lower water availability. Thus paradoxically, on one hand hydrophobins might help to 'squeeze' out the last bits of water from the substrate, while on the other hand, they prevent water uptake by the casing and compost during watering, since they repel water. More research is needed to discover the role of hydrophobins in water uptake of mushroom cultures.

3.7 *Mushrooms pull water from the vegetative mycelium by creating an osmotic potential*

Mushrooms synthesise compatible solutes to produce an osmotic potential that drives water flow from the supporting mycelial network to these fruiting bodies. These solutes are usually sugars, like fructose, arabinose and trehalose or polyols (i.e. sugar alcohols), such as mannitol and arabitol. The abundance and ratio of these is dependent on the species (Hong and Kim, 1988; Reis et al., 2012; Heleno et al., 2009, 2012). *A. bisporus*' main osmolyte is mannitol and comprises 30-60 % of the mushroom dry weight (Hammond

and Nichols, 1976a; Tan and Moore, 1994; Stoop and Mooibroek, 1998).

Enzymes that are involved in compatible solute synthesis, such as trehalose phosphorylase (TP), mannitol dehydrogenase (MD), glucose-6-phosphate dehydrogenase (G6PD), and glycogen phosphorylase (GP) are developmentally regulated in contrast to hexokinase (HK) that is active during glycolysis (Wells et al., 1987; Wannet et al., 1999). The former three enzymes have higher levels in aerial hyphal aggregates, that precede primordium formation, than in vegetative mycelium. Before fruiting the mycelium accumulates high trehalose, glucose and sucrose levels, that drop during fruiting, but mannitol levels do not increase in the vegetative mycelium (Hammond and Nichols, 1976a; Wannet et al., 1999). Trehalose translocates to the fruiting bodies and each molecule is then rapidly converted to a glucose and a glucose-1-phosphate molecule by TP (Wannet et al., 1998), thereby potentially doubling the osmotic potential. These serve as carbon source for growth and for synthesis of the osmolyte mannitol via fructose through MD (Wannet et al., 1999). Mannitol mainly accumulates in the stipe and pileus of mushrooms (Hammond and Nichols, 1976a). Higher G6PD and MD activities are consistently found in stage 1 - 2 sporophores (see Fig. 4) harvested between flushes, while their activity is minimal during flushes (stage 2) and as a result mannitol and trehalose levels are highest in stage 1 sporophores harvested between flushes (Hammond, 1981). Hammond and Nichols (1979) present conflicting evidence that mannitol levels are highest during flushes.

Glycogen has also been detected in mushrooms (Hammond and Nichols, 1979), but it is unclear if it is produced in the mycelium and translocates to the mushrooms and is then converted to glucose to serve mannitol synthesis, or whether glucose is transported and converted to glycogen and stored in the mushrooms until needed. Glycogen levels of mycelium and fruiting bodies appear to be similar (Hammond, 1979) and can reach up to 22 % of the dry weight (Hammond and Nichols, 1979). In another study, levels of young mushrooms were lower (stage 1 - 2 Fig. 4; 2 - 4 % of the dry weight) than that of mature opened mushrooms (stage >5 Fig. 4; 5 - 8 %; Hammond and Nichols, 1976b), indicating that glycogen is not degraded to build up an osmotic potential on one hand. On the other hand, small mushrooms that emerge just before a flush show maximum glycogen levels (Hammond and Nichols, 1979). Moreover, the sum of their peak trehalose and glycogen levels correlates with the yield of the first flush (Hammond and Nichols, 1979). This indicates that both trehalose and glycogen are converted to produce osmolytes, to pull water from the mycelium to support mushroom expansion during flushes.

This leads to a model in which the mycelium prepares for fruiting during before/inter flush stages, where it accumulates sugars and trehalose in the vegetative mycelium. When mushrooms form, these compounds are then transported to the mushrooms by (i) growth induced bulk flow and converted into osmolytes such as mannitol which pull water from the supporting mycelium; or (ii) uptake / synthesis of nutrients / osmolytes in the vegetative mycelium that attract water by osmosis from the substrate. The latter creates an over pressure in the mycelium that pushes water to the mushrooms. These forces work in harmony to supply the exponentially growing mushrooms (Straatsma et al., 2013) with water and nutrients. It is not clear in what ratio cell division and cell expansion contribute to mushroom expansion. The facts that more mature mushrooms have higher water contents (Kalberer, 1983) and that mushrooms before a flush have higher mannitol levels (Hammond, 1981) indicate that expansion is mostly due to cell expansion by water uptake.

Interestingly, total free sugar (alcohol) content is correlated with mushroom size (Table S1). Large mushrooms have 3x higher sugar (alcohol) content than smaller mushrooms ($p = 0.009$, t-test). Since larger mushrooms drain more water from their substrate than small mushrooms, they need to accommodate the drop in water potential of the substrate, by creating a more negative osmotic potential. The higher level of free sugar (alcohols) in larger mushrooms would facilitate this.

When NaCl or PEG is added to casing soil, which decreases osmotic- and matric potential (see Text box 1), respectively (Ramirez et al., 2004), mushroom yield is reduced (Kalberer, 1990a; Stoop and Mooibroek, 1998). Moreover, cropping is delayed, and mushrooms have higher dry weight percentages (Kalberer, 1990a). Interestingly, total crop dry weight is similar of controls and in experiments when salt is added to the casing soil. Moreover, NADP-dependent mannitol dehydrogenase (MtDH; EC 1.1.1.138) shows increased activity, abundance and *MtDH* mRNA accumulation after salt addition, indicating that mannitol levels increase. Additionally, *MtDH* transcript level is increasing during mushroom maturation (Stoop and Mooibroek, 1998). This shows that *A. bisporus* can regulate the mushroom osmotic potential depending on the water potential of the substrate, at least between certain limits. When the substrate becomes too dry, no more mushrooms will develop on the bed. This explains why subsequent mushroom flushes have lower yields.

The big open question remains: what determines which primordia or pins will develop into fully mature mushrooms? After colonization of casing soil and venting, thousands of mushroom initials develop per m^2 while only a few of these mature. Previously, it has been hypothesized that a certain compound needs to reach a threshold to induce mushroom maturation (Chanter and Thornley, 1978; Chanter, 1979). This compound could be trehalose and/or glycogen. However, it is not clear what determines which pins will receive most. A plausible explanation would be that primordia tap into different parts of the mycelial network. The differential network architecture could then determine which primordia receive most trehalose by cytoplasmic bulk-flow.

3.8 Mushrooms should not get water from the compost according to the story the water potential tell

To look into why mushrooms prefer taking relatively more water from the casing than from compost, we have to look at the water potential of the respective layers in the mushroom culture and of the mushrooms (see Text box 1). If not obstructed, water would freely move from areas with high water potential to areas with lower water potential.

The osmotic potential of casing press juice is -0.07 MPa at filling and -0.26 MPa after the second flush (Kalberer, 1987). Since casing matric potential is very small (0.04 MPa; Noble et al., 1999), the casing osmotic potential is a good approximation of its water potential (see also Text box 1). Watering was performed so that the moisture content of the casing was brought to about the same level as before each flush, but the top compost layer decreased in water content over time (Kalberer, 1987). Top, middle and bottom compost layers (Fig. 3) shows osmotic potential changes from -1.46 to -2.16 MPa, -1.71 to -2.44 , and -1.43 to -1.55 , respectively, before flush 1 until the end of flush 4. The water content changes from 63.3 % to 50.4 %, 60.1 % to 51.7 %, and 63.1 % to 65.1 %, respectively (Kalberer, 2006). Since changes in water content are quite similar for the top and middle layer, while the middle layer shows lowest water and osmotic potentials, this indicates that

the middle layer produces more osmolytes. The bottom layer did not lose water, indicating that it is not supplying water to the mushrooms, as found earlier by Kalberer (1985). However, the higher the thickness of the compost bed, the higher the yield is (Leyh and Blok, 2017). Thus, since the bottom layer is not supplying water to the mushrooms, it must have another function. For example, the bottom layer of compost transports nutrients to the developing mushrooms (Herman et al, 2020; **Chapter 3**).

The water potential of mushrooms is on average -0.72 ± 0.10 MPa, while the osmotic potential was -1.13 ± 0.13 MPa (Kalberer, 2006). The pressure potential of mushrooms (as derived by subtracting the osmotic potential from the water potential) are on average 0.4 MPa during the cropping process (see Text box 1). However, this ignores the matric potential of the mushroom tissue. Thus, in practice the pressure potential could be even greater (see Text box 1). However, in plant tissues matric potential is close to zero at physiological water contents (Wiebe, 1966). Using the data of Kalberer (1987), we found a correlation of 0.9 between the yield and the osmotic potential of the caps of the mushrooms. The osmotic potential of the caps increases (i.e. become less negative) during each following flush (Kalberer, 1987), suggesting that osmolytes (or precursors thereof) transport to the mushrooms decreases due to lowering of the osmotic potential of the compost.

The water potential of the casing is always higher (> -0.26 MPa; Kalberer, 1987) than that of the mushrooms (-0.72 MPa), suggesting that mushrooms can readily take up water from the casing. In contrast, the water potential of the compost (< -1.40 MPa) is always lower than that of the mushrooms (-0.72 MPa; Kalberer, 2006). It is therefore contradictory, that mushrooms take most of their water from the compost (Kalberer, 1983, 1985, 1987) since the water potential differences would oppose this water transport. However, to our knowledge the water / osmotic potential and pressure potential of the mycelium within the compost and casing have never been measured during fruiting. Pressure potential ranged from 0.86 - 3.32 MPa in mycelium of other fungi and were on average 2.03 MPa (Luard and Griffin, 1981). If *A. bisporus* mycelium would have similar pressure potential during fruiting, it is likely that the vegetative mycelium (turgor 2.03 MPa) pushes water into the expanding mushrooms (turgor 0.4 MPa) due to their differential internal pressure. Internal pressure is dependent on the osmotic potential, and this is usually close to that of the substrate (Luard, 1982b; Lew, 2011). Thus, the vegetative mycelium needs to accommodate its osmotic potential during decreasing water potential of the compost during cropping to maintain turgor to push water to the mushrooms. The mushrooms keep synthesising sugar (alcohols) to maintain low osmotic potential to pull water from their supporting mycelial network. Thus, both work in harmony to generate water transport to the mushrooms.

4. Conclusion

We have a clear understanding of the importance of water and its translocation during the fungal life cycle. However, there are contrasting views and observations regarding water transport in the vegetative mycelium, but also to the mushrooms. To complete

the picture, it is key to unravel when, where and how much water is taken up and how this is regulated, but also where water exits the translocation pathway as exudation or water vapor. Single cell measurements are required to understand the phenomenon of bi-directional translocation and oscillations observed in fungal colonies. According to the current account of the water potential data during fruiting, we cannot explain the rapid translocation of water from the compost to the mushrooms. We point to the internal pressure of the mycelium during fructification as the missing link in the story of water potential.

Acknowledgements

This work was in part funded by NWO TTW grant ‘Traffic control’ [15493].

Supplemental material

Table S1. The relation of total free sugar (alcohol) content and mushroom size.

Species	Sugar (alcohol) level (% of dry weight)	Mushroom size	Reference
<i>Agaricus bisporus</i>	46.3 (mannitol)	large	Tan and Moore, 1994
<i>Letinula edodes</i>	21.1-30.6 (mannitol)	large	Tan and Moore, 1994
<i>Pleurotus ostreatus</i>	9.53	large	Hong and Kim, 1988
<i>Cortinarius glaucopus</i>	19.72	large	Heleno et al., 2009
<i>Fistulina hepatica</i>	12.82	large	Heleno et al., 2009
<i>Hygrophoropsis aurantiaca</i>	13.40	small	Heleno et al., 2009
<i>Hypholoma capnoides</i>	1.96	small	Heleno et al., 2009
<i>Laccaria laccata</i>	6.45	small	Heleno et al., 2009
<i>Lactarius salmonicolor</i>	13.83	large	Heleno et al., 2009
<i>Lepista inversa</i>	6.18	small	Heleno et al., 2009
<i>Russula delica</i>	18.62	large	Heleno et al., 2009
<i>Suillus mediterraneensis</i>	8.10	large	Heleno et al., 2009
<i>Tricholoma imbricatum</i>	17.09	large	Heleno et al., 2009
<i>Coprinopsis atramentaria</i>	6.19	small	Heleno et al., 2012
<i>Lactarius bertillonii</i>	13.32	large	Heleno et al., 2012
<i>Lactarius vellereus</i>	27.18	large	Heleno et al., 2012
<i>Rhodotus palmatus</i>	32.86	large	Heleno et al., 2012
<i>Xerocomus chrysenteron</i>	9.98	large	Heleno et al., 2012

2

Cycling in degradation of organic polymers and uptake of nutrients by a litter-degrading fungus

Koen C. Herman, Aurin M. Vos, Robert-Jan Bleichrodt, Robin A. Ohm, Karin Scholtmeijer, Heike Schmitt, Luis G. Lugones, Han A. B. Wösten

This chapter has been published as: Vos, A.M., Bleichrodt, R.J., Herman, K.C., Ohm, R.A., Scholtmeijer, K., Schmitt, H., Lugones, L.G., Wösten, H.A.B., 2021. Cycling in degradation of organic polymers and uptake of nutrients by a litter-degrading fungus. *Environ. Microbiol.* 23, 224–238.

Abstract

Wood and litter degrading fungi are the main decomposers of lignocellulose and thus play a key role in carbon cycling in nature. Here we provide evidence for a novel lignocellulose degradation strategy employed by the litter degrading fungus *Agaricus bisporus* (known as the white button mushroom). Fusion of hyphae allows this fungus to synchronize the activity of its mycelium over large distances (50 cm). The synchronized activity has a 13 - hour interval that increases to 20 h before becoming irregular and it is associated with a 3.5 - fold increase in respiration, while compost temperature increases up to 2 °C. Transcriptomic analysis of this burst-like phenomenon supports a cyclic degradation of lignin, deconstruction of (hemi-) cellulose and microbial cell wall polymers, and uptake of degradation products during vegetative growth of *A. bisporus*. Cycling in expression of the ligninolytic system, of enzymes involved in saccharification, and of proteins involved in nutrient uptake is proposed to provide an efficient way for degradation of substrates such as litter.

Introduction

Mushroom forming fungi play a key role in nature and human society (Grimm and Wösten, 2018). For instance, they produce edible and medicinal fruiting bodies and play a pivotal role in cycling of carbon in nature. The latter is illustrated by the fact that they are the main decomposers of lignocellulose, the most abundant terrestrial organic material. This complex is found in wood and litter and consists of cellulose, hemicellulose, and lignin. Brown rot fungi mostly modify lignin and degrade carbohydrates, while white rots simultaneously degrade lignin and carbohydrates or selectively (i.e. predominantly) degrade lignin (Worrall et al., 1997; Riley et al., 2014; Schilling et al., 2015). Brown and white rot wood degrading fungi use different types of radical chemistry to modify and degrade lignin (ten Have and Teunissen, 2001; Hammel et al., 2015), thereby exposing (hemi-) cellulose to the action of carbohydrate-active enzymes (CAZyS; enzymes involved in breakdown or synthesis of polysaccharides).

Recently, it was found that the mycelium of mushroom forming brown rot fungi spatially separate the radical generating Fenton chemistry from CAZyS (Zhang et al., 2016, 2019; Presley and Schilling, 2017; Castaño et al., 2018). The outer 5 mm of the colony of brown rots like *Postia placenta* generate •OH radicals using the Fenton reaction, while the inner 15-35 mm regions of the colony secrete the bulk of (hemi-) cellulases. This spatial separation would prevent inactivation of these enzymes by radical oxygen species generated by Fenton chemistry. In addition, the radical pre-treatment of cell walls may facilitate the activity of CAZyS (Castaño et al., 2018; Zhang et al., 2019).

White rots may also make use of Fenton chemistry to attack lignocellulose, but it is not the main mechanism. These fungi mineralize lignin using a ligninolytic system that includes oxidoreductases like lignin peroxidase, manganese peroxidase (MnP), and / or versatile peroxidase, and possibly laccase (LCC) as well (ten Have and Teunissen, 2001; Hammel et al., 2015). The peroxidases use H₂O₂ that is generated by oxidases like glyoxal oxidase, but it may also arise from secondary reactions with organic acids like oxalate (Kersten and Kirk, 1987; Urzúa et al., 1998). As a result, small radical intermediates are produced that penetrate lignocellulose and attack lignin directly or indirectly by

facilitating secondary reactions, possibly including lipid peroxidation in the case of MnP (Hofrichter, 2002). Radicals generated by the ligninolytic system of white rots may result in a gentler radical treatment of lignocellulose as not all radical species that are associated with white rot match the reactivity of $\bullet\text{OH}$ radicals. This may explain why white rots have been described to produce their ligninolytic system together with (hemi-) cellulases. For example, the white rot *Trametes versicolor* expresses genes related to ligninolytic and (hemi-)cellulolytic activity in a region 15–35 mm from the colony hyphal front (Presley et al., 2018; Zhang et al., 2019). The white rots *Phanerochaete chrysosporium* and *Stereum hirsutum* have a delayed onset of ligninolytic activities (Moukha et al., 1993; Korripally et al., 2015; Presley et al., 2018) and expression of (hemi-) cellulolytic genes in *P. chrysosporium* occurs in both younger and older mycelium (Korripally et al., 2015). In contrast, *Pleurotus ostreatus* separates the bulk of (hemi-) cellulases from its ligninolytic system by producing (hemi-) cellulases 15–20 mm from its hyphal front while its ligninolytic system is most active in the 0–5 mm and 30–35 mm region of its colony (Zhang et al., 2019). Together, white rots show differences in their spatial expression of ligninolytic and (hemi-)cellulolytic activities.

Soil-inhabiting saprotrophs like the litter-decomposer *Agaricus bisporus* (the white button mushroom) are, like white rots, capable of extensive lignin degradation (Osono, 2007; Jurak et al., 2015b). The genomes of litter-degrading and white rot fungi indicate differences in their ligninolytic machinery, possibly relating to the difference in wood and litter environments (Floudas et al., 2020). Yet, the enzymatic system enabling the decomposition of lignin by *A. bisporus* includes MnP and LCC that are thought to play an important role in lignin breakdown by some white rot fungi as well. The expression of CAZYs and their activities throughout the life cycle of *A. bisporus* have been relatively well studied. This fungus is grown commercially on a horse manure based compost (Grimm and Wösten, 2018) that is produced in two phases. *A. bisporus* is introduced at the end of Phase II (PII), which starts the vegetative growth period during Phase III (PIII). After topping the PIII-end compost with a casing layer and changing environmental conditions, fruiting is induced (Phase IV [PIV]). It is generally assumed that *A. bisporus* degrades the lignocellulose in the substrate by means of (hemi-) cellulases, LCC and MnP (Bonnen et al., 1994; Patyshakuliyeva et al., 2015). About 40 % of the lignin, 6 % of the xylan (part of the hemicellulose), and 6 % of the cellulose is degraded during PIII relative to PII (Kabel et al., 2017). In addition, a significant part of the microbial population is consumed in PIII (Vos et al., 2017a; Carrasco et al., 2020). Xylan and cellulose are preferentially degraded during PIV with approximately 48 % and 33 % cellulose and xylan being removed after fruiting, respectively, while minor amounts of lignin are removed. Loss of lignocellulose in compost in time is in agreement with overall expression patterns of ligninolytic and (hemi-) cellulolytic genes (Patyshakuliyeva et al., 2015).

So far, physiology and gene expression studies have not been performed at short time intervals during the different phases of the life cycle of *A. bisporus* such as during PIII. Here, we performed such studies, revealing that the expression profile of *A. bisporus* during its vegetative growth is in line with its mycelium cycling through degradation of lignin, degradation of polysaccharides, and uptake of degradation products. This cycling, which is accompanied by respiratory bursts, is synchronized over a large distance within the mycelium and is proposed to enable *A. bisporus* to efficiently degrade litter.

Material and Methods

Strain and growth conditions

A. bisporus strains A15 (Sylvan, Netherlands) and Bisp015 were grown in PII-end compost (CNC Grondstoffen, Milsbeek, the Netherlands) at 25 °C unless otherwise indicated. Compost was inoculated with either rye based A15 (Gift from CNC Grondstoffen) or Bisp015 spawn (Basidiomycete culture collection WUR, Wageningen, the Netherlands) or with PIII compost. Respiration measurements were done in 1 litre bottles using 50 g PII-end compost that was either or not inoculated with 10 spawn grains. Temperature was monitored either in boxes or in square Petri dishes. In the latter case, square Petri dishes (12 x 12 x 1.2 cm) were filled with 57.6 g PII compost on one side and 11.5 g PIII compost on the other side from which the PII compost was colonized. Growth in boxes was done using 1 kg (30 x 20 x 22 cm boxes), 8 kg (40 x 60 x 20 cm boxes), or 16 kg (40 x 60 x 22 cm boxes) PII-end compost that was inoculated with 8, 64, or 75 gr of spawn, respectively. The 1 and 8 kg compost boxes that were used to monitor temperature dynamics during PIII were covered with plastic film containing 50 3-mm-wide holes m⁻². The 16 kg compost boxes were used to monitor temperature dynamics both during PIII and PIV under cultivation conditions described previously (Vos et al., 2017a).

Quantification of CO₂, O₂, temperature and growth

Correlation of CO₂ production and O₂ consumption was done using a respirometer (Biometric Systems, Germany) with optical CO₂ and O₂ sensors. In short, CO₂ and O₂ was measured using biological triplicates at t=0 and t=2.5 h, after which the air in the flask was refreshed. This was repeated 170 times during a 425 h period. Data were converted to molar amounts of produced CO₂ and consumed O₂, correcting for temperature and pressure.

Growth in compost was measured by placing 12-cm-square Petri dishes in a flatbed scanner (Epson V300 / V370, Seiko Epson Corporation, Shinjuku, Tokyo, Japan). Compost was scanned every hour. These images were produced in 16-bit grayscale intensity at 2400 dpi resolution (10.6 µm pixel size). The grey values were quantified in a 3.8 x 0.5 cm window around a Pt100 (class B) temperature sensor probe (1.83 x 6 mm; Sensing Devices LLC, Lancaster, USA) that had been placed inside the 2 cm layer PII compost in the middle of the square Petri dish before placing the dish in the scanner. Temperature was logged by connecting the temperature probe to a real-time clock (RTC) DS1307 module, a micro-SD module, a MAX31865 RTD module, and an Arduino Nano according to manufacturer's instructions. Temperature was measured every 5 min, while the mean grayscale intensity within the temperature probe area was quantified over time using ImageJ. The scanner was covered with a 5 cm thick-walled polystyrene box to minimize the effect of the incubator hysteresis.

Arduinos (<https://www.arduino.cc/>) equipped with temperature (DS18B20; Dallas Semiconductor, USA) or CO₂ (MG811; Sandbox Electronics, Finland) sensors were used to measure and correlate changes in temperature and CO₂ levels in box experiments. To this end, the temperature sensor was placed 2 cm below the compost surface, while the CO₂ sensor was placed 5 cm above the compost.

Vegetative incompatible strains (A15 / Bisp015) and vegetative compatible strains (A15 / A15 and Bisp015 / Bisp015) were grown together in duplo in a 40 x 60 cm compost box

filled with 16 kg compost. The compost was divided in 4 areas, 2 of which were inoculated with A15 and two with Bisp015 in diagonal positions. Two thermocouple probes (Type T; Copper / Constantan) were placed per separate area (8 probes in total). Temperature changes were recorded using a DT85 Series 2 Data logger (Cambeep, Cambridge, United Kingdom), every 10 min starting on day 1 of cultivation and ending at day 18.

RNA isolation

RNA was isolated from 7.5 gr colonized compost of box cultures (30 x 20 x 22 cm) after 130-145 h of incubation (Fig. S1). Samples (biological triplicates) were taken from the immediate surroundings of a temperature sensor during and after a burst and in between bursts (i.e., 0.5, 4.5, and 8.5 h after a burst started, respectively). Compost was crushed using mortar and pestle under liquid nitrogen and ground to a fine powder for 1 min at 30 Hz using a tissuelyser II with a steel grinding jar pre-cooled with liquid nitrogen (Qiagen, Venlo, Netherlands). RNA was extracted using a modified method described by Patyshakuliyeva et al. (2014). For each sample, 200 mg compost powder was transferred to 7 ml extraction buffer (4 M guanidinium thiocyanate, 25 mM sodium citrate, pH 5.0, 0.5 % N-lauroyl sarcosine, 0.1 M β -mercaptoethanol), shaken vigorously, and incubated for 10 min at RT. Next, 7 ml of chloroform:isoamyl alcohol (24:1) was added, mixed by vortexing, and incubated for 2 min. Phases were separated by centrifugation for 15 min at 4500 g and 6.5 ml of the aqueous phase was transferred to an ultracentrifugation tube (Ultra-Clear, open-top; Beckman coulter) filled with a 2 ml cushion of 5.7 M CsCl in 25 mM sodium citrate, pH 5.0. The tube was topped with 7 ml 0.8 M guanidine thiocyanate, 0.4 M ammonium thiocyanate, 0.1 M sodium acetate, pH 5 (TS buffer). RNA was pelleted by centrifugation for 24 h at 4 °C and 104.000 g in a SW28.1 swing out rotor (Beckman Coulter, Brea, CA, USA). RNA was taken up in 100 μ l H₂O and 500 μ l TS buffer was added. RNA was precipitated with 0.8 volume isopropanol, washed with 70 % ethanol, and further purified using a Qiagen RNeasy Mini Kit. RNA quality and quantity was assessed using gel electrophoresis and a Qubit Fluorometer.

RNA sequencing and analysis

Strand-specific mRNA-seq libraries for the Illumina platform were generated and sequenced at BaseClear BV (Leiden, The Netherlands). High-quality total RNA (checked and quantified using a Bioanalyzer (Agilent, Santa Clara, CA, USA) was used as input for a dUTP library preparation method (Parkhomchuk et al., 2009; Levin et al., 2010). For dUTP library preparation the mRNA fraction was purified from total RNA by polyA capture, fragmented and subjected to first-strand cDNA synthesis with random hexamers in the presence of actinomycin D. The second-strand synthesis was performed incorporating dUTP instead of dTTP. Barcoded DNA adapters were ligated to both ends of the double-stranded cDNA and subjected to PCR amplification. The resulting library was quality checked and quantified using a Bioanalyzer (Agilent). The libraries were multiplexed, clustered, and sequenced on an Illumina HiSeq 2500 (HiSeq Rapid SBS v2 chemistry) with a single-read 50 cycles sequencing protocol and indexing. At least 10 million 50 bp single reads were generated per sample.

FASTQ sequence files were generated using bcl2fastq2 version 2.18. Initial quality assessment was based on data passing the Illumina Chastity filtering. Subsequently, reads containing PhiX control signal were removed using an in-house filtering protocol. In

addition, reads containing (partial) adapters were clipped up to minimum read length of 50 bp. Remaining reads were subjected to a second quality assessment using the FASTQC quality control tool version 0.11.5 (<http://www.bioinformatics.babraham.ac.uk/projects/fastqc/>) and deposited in NCBI GEO with accession number GSE124976. HISAT version 2.1.0 (Kim et al., 2015) was used to align sequence reads to the Agabi_varbisH97_2 version of the *A. bisporus* H97 genome (Morin et al., 2012; Sonnenberg et al., 2020), which was obtained from MycoCosm (Grigoriev et al., 2014). Cuffdiff (version 2.2.1), which is part of Cufflinks (Trapnell et al., 2010), was used to identify reads mapping to predicted genes and to identify differentially expressed genes. The bias correction method was used while running Cuffdiff (Roberts et al., 2011). Cuffdiff normalizes the expression level of each predicted gene to fragments per kilobase of exon model per million fragments (FPKM). In addition to Cuffdiff's requirements for differential expression the following requirements were applied: a ≥ 2 -fold change and a minimal expression level of 10 FPKM in at least one of the samples. Therefore, genes with an fpkm < 10 in a sample point were only included in the set of differentially expressed genes when meeting the aforementioned conditions in another sample point. Quality of these results was analyzed using CummeRbund (Goff et al., 2013). All expression data can be found in Dataset S4 (see online version: <https://doi.org/10.1111/1462-2920.15297>).

Functional annotation

Conserved protein domains were predicted using PFAM version 31 (Finn et al., 2016) and mapped to the corresponding gene ontology (GO) terms (Hunter et al., 2009). Proteases were predicted using the MEROPS database (Rawlings et al., 2016) with a blastp E-value cut-off of 10^{-5} . Secretion signals and transmembrane domains were predicted using SignalP 4.1 (Petersen et al., 2011) and TMHMM 2.0c (Krogh et al., 2001), respectively.

The previously identified *A. bisporus* CAZYS and proteins involved in carbon metabolism (Patyshakuliyeva et al., 2013, 2015) were further annotated and supplemented as described in Supplementary Text 1 (see online version). Over- and under-representation of functional annotation terms in sets of differentially regulated genes were identified using the Fisher Exact test. The Benjamini-Hochberg correction was used to correct for multiple testing using a p-value < 0.05 .

Results

Respiratory bursts in compost

The CO₂ production and O₂ consumption of PII-end compost inoculated with *A. bisporus* variety Sylvan A15 (A15) was monitored using a respirometer. Non-inoculated and sterilized PII-end compost served as a control to exclude the activity of microorganisms other than *A. bisporus*. The CO₂ production and O₂ consumption were determined every 2.5 h during a 425 h measurement period. Measurements started after a 5-days pre-incubation at 25 °C to allow the *A. bisporus* inoculum to (start to) form an interconnected mycelium. Total CO₂ produced gr⁻¹ of sterile compost, non-inoculated compost, and inoculated compost was 52, 227, and 831 μmol during the 425 h period, respectively (Fig. 1A). The CO₂ production rate decreased over time from 1 to 0.3 $\mu\text{mol h}^{-1} \text{g}^{-1}$ in compost without *A. bisporus* A15, while $\leq 0.23 \mu\text{mol CO}_2 \text{h}^{-1} \text{g}^{-1}$ compost was released from sterile

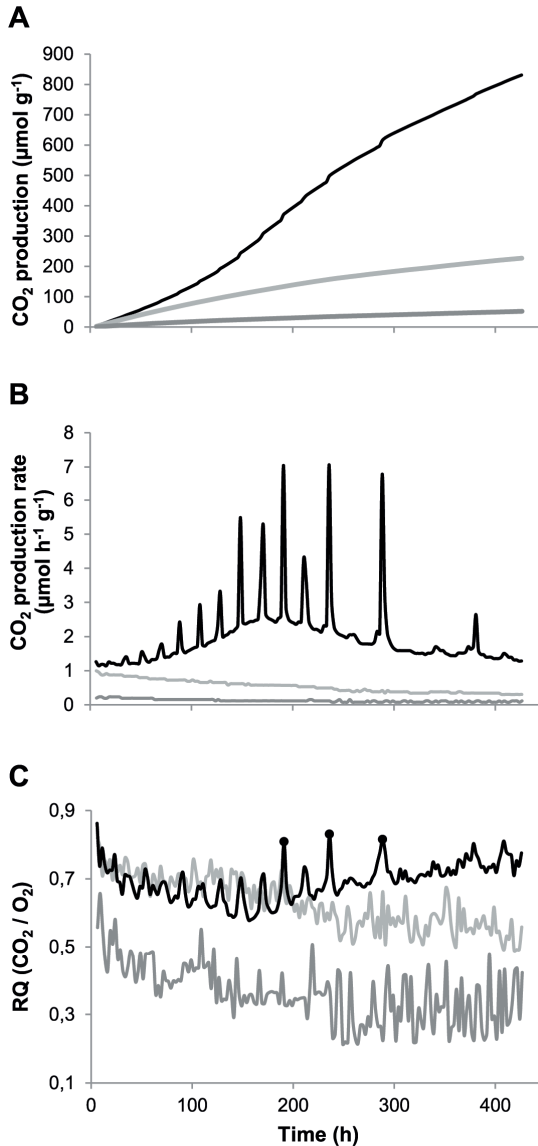


Figure 1. Cumulative CO₂ production (A), CO₂ production rate (B), and respiratory quotient (C) by sterile compost (dark grey), compost without *A. bisporus* (light grey), and compost inoculated with *A. bisporus* (black). O₂ levels were below 17.97 % (the limit at which O₂ could be measured) at time points indicated with a black dot (C), resulting in an underestimation of the actual O₂ consumption and therefore overestimation of the RQ.

compost (Fig. 1B). In contrast, CO₂ production in compost with *A. bisporus* A15 increased from 1.2 to 2.6 μmol h⁻¹ g⁻¹ substrate during the first 180 h and then decreased to 1.3 μmol h⁻¹ g⁻¹ compost. This was accompanied by distinct respiratory bursts of 2.5-5 h (Fig. 1B). The CO₂ production rate during the bursts increased up to 3.5 fold as compared to

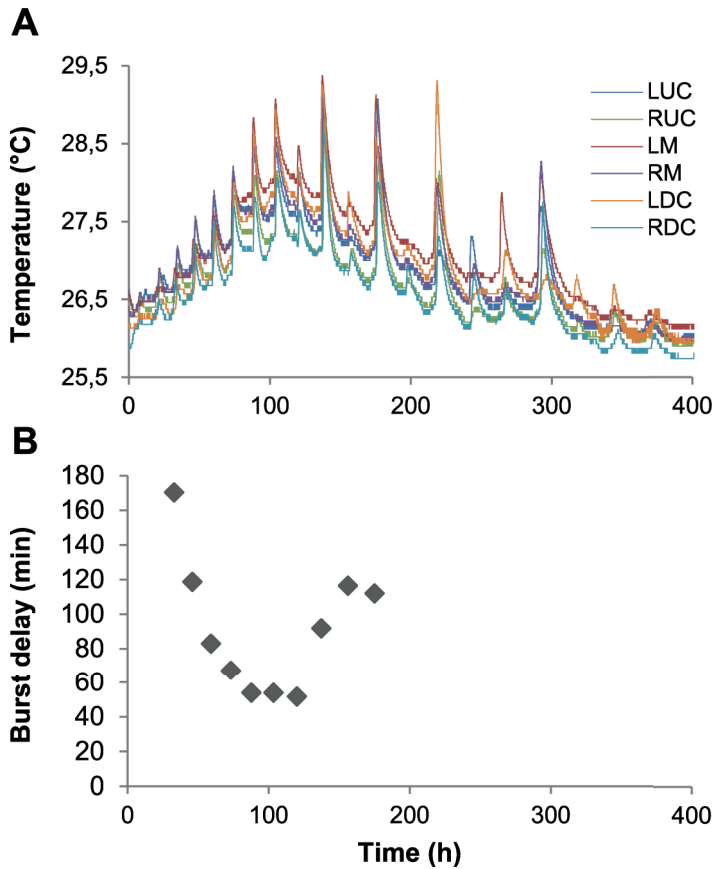


Figure 2. Compost temperature measured by 6 sensors spaced 15-25 cm apart in a 40 x 60 cm box (A) and the maximum peak delay between the sensors during a burst (B). LUC = left upper corner, RUC = right upper corner, LM = left of the middle, RM = right of the middle, LDC = left bottom corner, RDC = right bottom corner.

the intermediate periods. These intermediate periods had an initial length of 13 h and increased to 20 h. The interval became irregular as illustrated by an increase to 50 and 90 h after 200 and 240 h, respectively. No respiratory bursts were observed in the absence of *A. bisporus* A15 but they were produced in sterilized compost inoculated with this fungus (Fig. S2). However, growth of *A. bisporus* A15 in sterilized compost was slow, likely due to the absence of an active microbiome (Straatsma et al., 1994b), coinciding with low CO₂ production.

The respiratory quotient (RQ; mol CO₂ released / mol O₂ consumed) in non-inoculated compost decreased from 0.8 to 0.55 during the 450 h measurement period (Fig. 1C), while it decreased in sterilized compost from 0.6 to 0.3. In the latter case this was probably due to decrease in CO₂ release due to abiotic reactions. During the colonization of *A. bisporus* A15 the maximal RQ decreased from 0.8 to 0.65 during the first 150 h period and then increased to 0.8 again in the following 350 h (Fig. 1C). At three time points the O₂ levels were below 17.9 %, the lower limit of detection of the respirometer, resulting

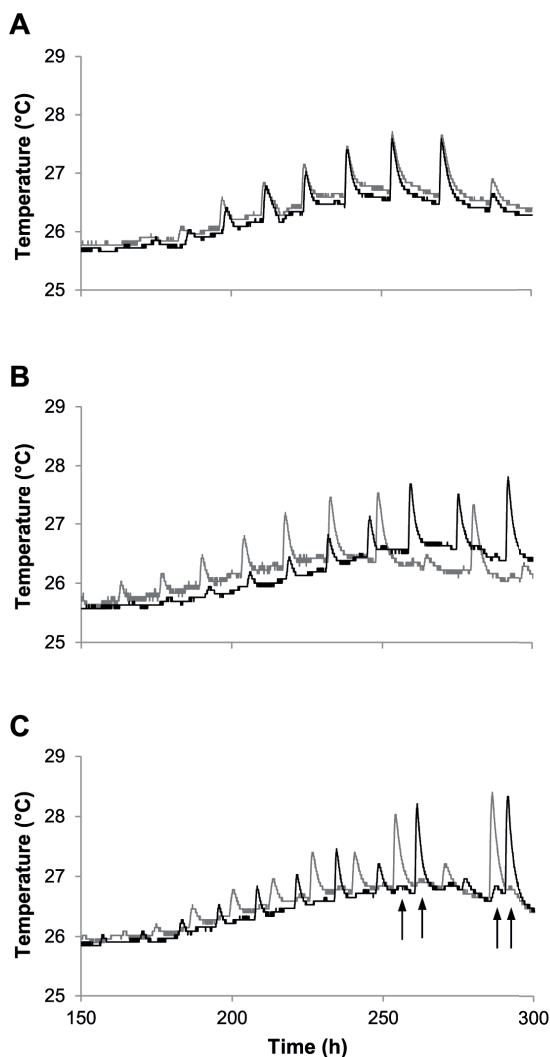


Figure 3. Typical temperature profiles of two parts of compost (dark and light grey) pressed together (A), placed 3 cm apart (B), or separated by aluminium foil (C). Arrows indicate where heat transfer through the aluminium foil was detected by the temperature sensor. Each experiment was performed 5 times. The average difference between two temperature sensors picking up a burst (i.e. the time delay of a burst) for each condition was tested using Mann-Whitney U, $P < 0.05$.

in an underestimation of the actual O_2 consumption and overestimation of the RQ (Fig. 1C, black dots). The RQ was up to 0.13 higher during bursts as compared to the pre-burst minimum of 0.58.

CO_2 production correlated with an increase in compost temperature. Temperature increase was detected 30 min after the start of a respiratory burst, peaked 45-90 min later, and took 2-8 h to normalize to pre-peak temperature (Fig. S3). Hence, monitoring compost temperature can be used to monitor respiratory bursts. This was adopted to

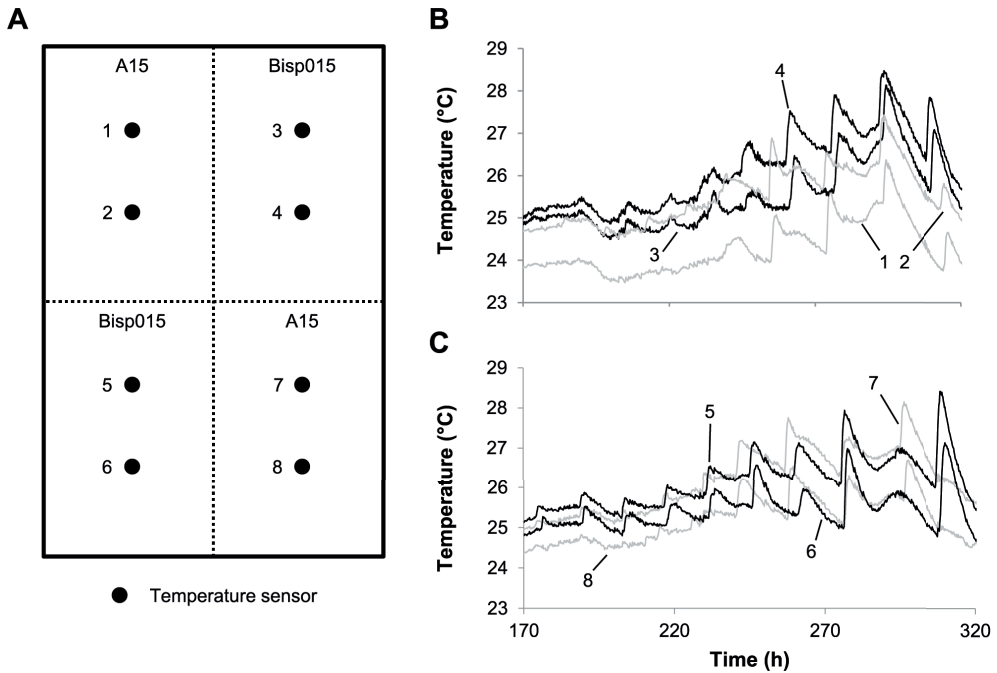


Figure 4. Experimental setup (A) and typical temperature profile of compost divided in four areas, two of which were inoculated with A15 (B and C, black lines) and two with Bisp015 (B and C, grey lines) in diagonal positions in a box. Numbers in panel B and C relate to the location of temperature sensors in panel A. The temperature profiles of A15 and Bisp015 in panel B and C are representative of two independent experiments.

monitor respiratory bursts during PIII and PIV of a semi-commercial *A. bisporus* A15 cultivation. Respiratory bursts were observed between day 10 and 16 of PIII (Fig. S4) and followed a similar pattern as observed in small scale lab cultivations. They were also observed during colonization of casing and the 1st flush but not during the 2nd flush.

Synchronization of respiratory bursts is mediated by hyphal fusion

The respiratory bursts observed during colonization of compost by *A. bisporus* A15 are suggestive of synchronized mycelial action in the compost. This synchronization was characterized using 6 temperature sensors that had been placed 15-25 cm apart in a 40 x 60 cm box containing 8 kg inoculated PII-end compost. *A. bisporus* A15 was allowed to colonize the compost for 8 days at 25 °C before temperature measurements were started. Respiratory bursts occurred during the first 400 h of a 700 h measurement period (Fig. 2A). They resulted in a temperature increase of up to 2 °C in a 1.5-3 h period. Different maximum temperatures detected by the different sensors resulted from local differences in the level of colonization by *A. bisporus*, insulation of the sensor by the compost, and mycelial activity. Initially, the maximum time delay between all sensors measuring a burst was 170 min (Fig. 2B). This decreased to 50 min between 33 and 88 h after the measurements had been started (Fig. 2B), showing that heat production by the mycelium synchronized over at least 50 cm (the largest distance between the sensors). No pattern

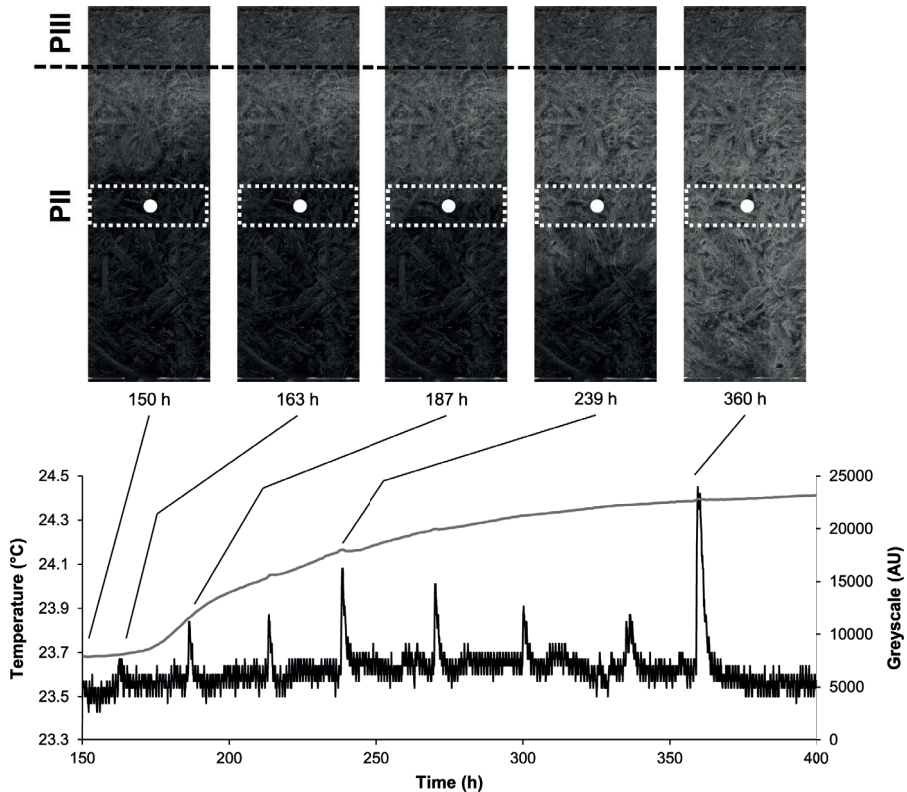


Figure 5. Compost temperature (black line) and mycelial growth expressed as grey value (grey line, based on the area in the white dashed boxes) during growth of *A. bisporus* from PIII compost into fresh PII compost (border indicated by the dashed line). Scans of the compost after 150, 163, 187, 239, and 360 h are shown with the position of the temperature sensor indicated (white dot). These data are representative of two independent experiments.

was observed in the order sensors measured a burst. The maximum time delay of the sensors picking up a burst increased to 116 min after a 120 h measurement period, while after measuring growth for 198 h not all sensors picked up a burst anymore with one exception at 218 h. After this time point bursts became erratic.

To obtain information on the nature of the synchronization in compost two aliquots of 1 kg *A. bisporus* A15 inoculated PII-end compost were placed next to each other (i.e. physically touching each other), 3 cm apart, or were separated by aluminium foil. In the latter case, transfer of heat could occur but hyphae of the two parts could not interact. The temperature in the center of both parts of compost was monitored for 300 h after 8 days of culturing (Fig. 3). The average time between sensors in the two parts of compost picking up a burst was lower when the parts were in physical contact (38 min) when compared to those placed 3 cm apart or separated by aluminium foil (3 h 50 min and 4 h 33 min, respectively; Mann-Whitney U, $p < 0.05$). This suggests that interaction of mycelium is required for the observed synchronization.

Hyphae of *A. bisporus* colonies that are vegetatively compatible can fuse to form a larger

colony (O'Connor et al., 2020). The use of two incompatible strains allows to distinguish between proximity of hyphae or hyphal fusion being required for synchronization of bursts over large distances. To this end, compost was divided in 4 areas of which two were inoculated with *A. bisporus* A15 and two with *A. bisporus* Bisp015 in diagonal positions in a 40 x 60 cm box. The mycelium of *A. bisporus* A15 anastomoses with hyphae of other *A. bisporus* A15 colonies forming a single mycelium (Fig. S5). However, *A. bisporus* A15 does not anastomose with hyphae of *A. bisporus* Bisp015 as these strains show a vegetative incompatibility, i.e. do not fuse likely due to different alleles in vegetative incompatibility genes (O'Connor et al., 2020) (Fig. S5). Temperature sensors placed in an area containing only 1 of both strains synchronized, while no synchronization of bursts was observed between areas containing A15 and areas containing Bisp015 (Fig. 4A and 4B). This shows that anastomosis is required to synchronize the activity of the mycelial colony.

Respiratory bursts occur in sub-peripheral zones of the mycelium

In all previous experiments the inoculum of *A. bisporus* was homogeneously distributed throughout the compost. Therefore, it is not possible to distinguish if bursts occur at the hyphal front of a colony or if older parts of the mycelium contribute to these bursts. To distinguish between these options, growth of *A. bisporus* A15 containing PIII compost into fresh PII compost in a square Petri dish was monitored using a flatbed scanner and a temperature sensor. Biomass was distinguished by increased whitening of the compost and the temperature sensor was placed in the middle of the PII compost to monitor the bursts in a moving hyphal front. The linear growth rate of the hyphal front was 8.8 mm d⁻¹. After 163 h a small temperature increase was observed when the mycelial front had approached the temperature sensor to 8.1 mm (Fig. 5). This was followed by bursts starting 9 h after the mycelium had reached the temperature sensor. The hyphal front had grown 3.6 mm past the sensor at this moment. Bursts were separated by 23-36 h periods. Notably, bursts continued after the mycelial front had passed the probe up to 5.7 cm. At this moment, hardly any biomass was produced anymore at this location as shown by the low increase in whitening of this area. Moreover, respiratory bursts were not accompanied by increased growth as the increase and decrease in grayscale value around bursts was caused by condensation of water and its evaporation. Together, the data indicate that the whole colony of *A. bisporus* (i.e. the hyphal front and older parts of the colony) contribute to the respiratory bursts observed in previous experiments.

Reorganization of gene expression during respiratory bursts

The physiological characterization of vegetative growth of *A. bisporus* revealed a burst-like phenomenon not previously observed in fungi growing in complex substrates. RNA was isolated from biological triplicates during, after, and in between bursts (0.5 h, 4.5 h, and 8.5 h after a burst started, respectively) to investigate the process underlying these bursts (Fig. 6A). Out of the 10438 predicted genes encoded by the *A. bisporus* genome, 4731 were differentially expressed (i.e. ≥ 2 -fold up or down-regulated, with an fpkm > 10 in at least 1 of the 3 conditions and a q-value < 0.05 ; Fig. 6B). The differentially expressed genes consisted of 1425 genes without annotation, 139 of which encode proteins with a predicted signal sequence for secretion. Differential expression may be a result of de

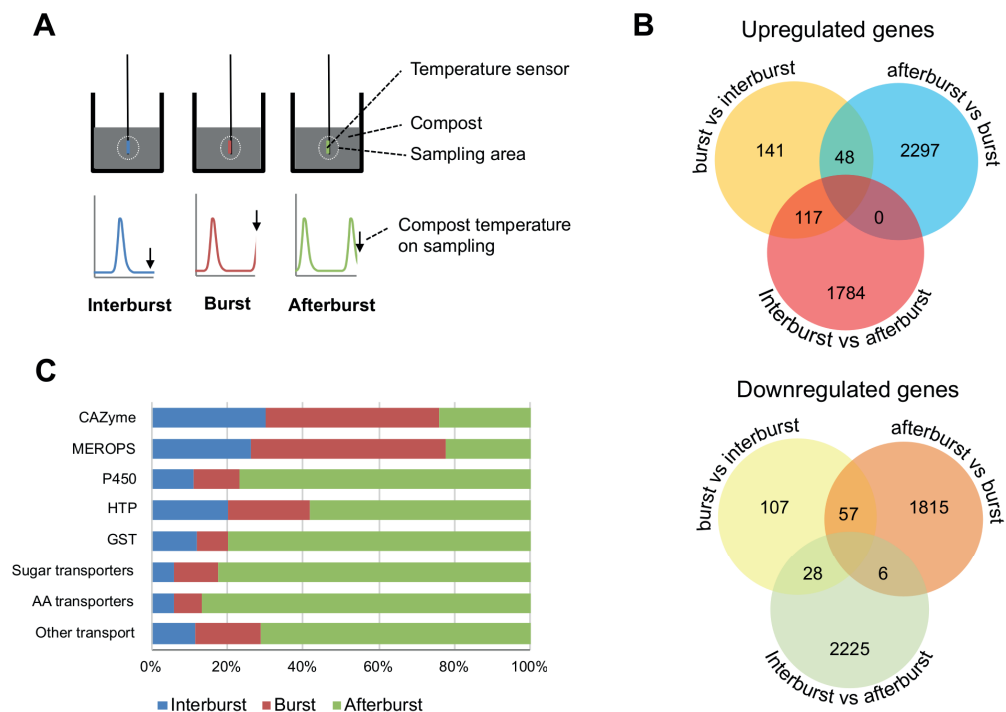


Figure 6. Schematic representation of experimental setup for the transcriptome analysis of respiratory bursts (A) and analysis of differentially expressed genes. Samples were harvested in between bursts (end of blue line), during bursts (end of red line), or after a burst (end of green line). For each point, RNA was isolated from three biological replicates. Up- (B, top panel) and down- (B, lower panel) regulated genes before a burst, during a burst, and after a burst (i.e. greater than or equal to twofold up or downregulated, with an fpkm > 10 in at least one of the three conditions and a q-value < 0.05). Relative abundance of FPKM of differentially expressed genes annotated as CAZyS, MEROPS proteases, P450 enzymes, heme-thiolate peroxidases (HTP), glutathione-S-transferase (GST), sugar transporters, amino acid transporters, and other transporters (C).

novo RNA synthesis but also of RNA turnover. Therefore, *A. bisporus* regulation of gene expression during bursts may include degradation of specific transcripts. A total of 197 GO terms and 69 Pfam domains were over- and / or under-represented in sets of up- or down-regulated genes (Dataset S1, see online version). Cell cycle (i.e. cell division and / or nuclear division) and translation related GO terms were overrepresented and underrepresented, respectively, in upregulated genes after a burst relative to during a burst, while GO terms related to transcription and the cell membrane were overrepresented in genes upregulated after a burst when compared to the other two samples. The GO term related to metabolic processes was overrepresented in genes upregulated during the bursts relative to the inter-burst samples and in downregulated genes after a burst relative to the other two samples. Furthermore, cell wall related GO terms were overrepresented in genes downregulated during a burst when compared to the inter-burst samples. Proteins with a predicted secretion signal were overrepresented in both upregulated and downregulated genes during a burst compared to the inter-burst samples. In addition, these proteins were

overrepresented in downregulated genes after a burst relative to the other two samples. The differential expression of cyclins after a burst points to a synchronized cell cycle (Supplementary Text 2, see online version). It is not clear which functions these cyclins have, i.e. whether they are involved in nuclear division or in growth.

Expression of CAZyS and proteases was increased during a burst, while enzymes with a potential role in metabolism of lignin derived products (P450, Heme-thiolate peroxygenase [HTP], β -etherase), and sugar, amino acid, and other transporters were highly expressed after a burst (Fig. 6C). Putative sugar transporter genes (Pfam 00083) were overrepresented in the downregulated genes during the inter-burst relative to after a burst (Dataset S1; see online version). Indeed, the majority of differentially expressed sugar transporters were upregulated after a burst (Fig. 6C; Dataset S7, see online version; 19 out of 33). In addition, differentially expressed amino acid / peptide transporter genes were mostly upregulated after a burst (20 out 26; Fig. 6C; Dataset S7, see online version; Pfam 03169, 00854, 01490, 00324, and 13520). From the remaining 50 differentially expressed transporter genes (annotated with Pfam 07690; Fig. 6C; Dataset S7, see online version) 36 were upregulated after a burst. These genes included putative nicotinic acid and thiamine transporter genes and transporter genes putatively involved in secretion of toxins (Pfam 06609; Alexander et al., 1999). The combination of transporters and secreted proteins being differentially expressed points to changes in the extracellular availability of free sugars. Therefore, the CAZyS were analysed in more detail. Expression values of each differentially expressed CAZy family were summed to identify general patterns in their expression (Fig. 7). The number of differentially regulated genes in each CAZy class can be found in the figure description.

Downregulation of the ligninolytic system after bursts

MnPs and LCCs (AA2 and AA1_1) were highly expressed before and during bursts but downregulated up to 367 fold for the most highly expressed LCCs after bursts (Fig. 7A; Dataset S2 and S3, see online version). Similarly, glyoxal oxidases (GLOX; AA5_1) and alcohol oxidases (AO; AA3_3) were down-regulated (3.5-194 fold) after a burst and upregulated 2.3-58 fold in between bursts. Putative aryl alcohol oxidases, glucose 1-oxidases, and pyranose dehydrogenases (AA3_2) were upregulated after a burst and downregulated in the interburst samples. Expression of fatty acid desaturases (Protein ID 194591 and 193825; Dataset S4, see online version) peaked after a burst, being upregulated 13.6-243 fold compared to a burst and the inter-burst. These data show that genes encoding the ligninolytic machinery are actively expressed before and during bursts, while they are downregulated after bursts except for fatty acid desaturases.

Polysaccharide deconstruction CAZyS are upregulated during respiratory bursts

Cellulase genes (Fig. 7B; Dataset S2 and S3, see online version) were upregulated during and after bursts relative to in between bursts. Putative endo- and exo-acting cellulases like GH5_5, GH6, GH7, GH45, and the LPMO AA9 dominated the expression of cellulases during bursts, while the endoglucanase GH12 genes together with AA9 and GH45 were dominantly expressed after bursts. Hemicellulases peaked in expression during bursts

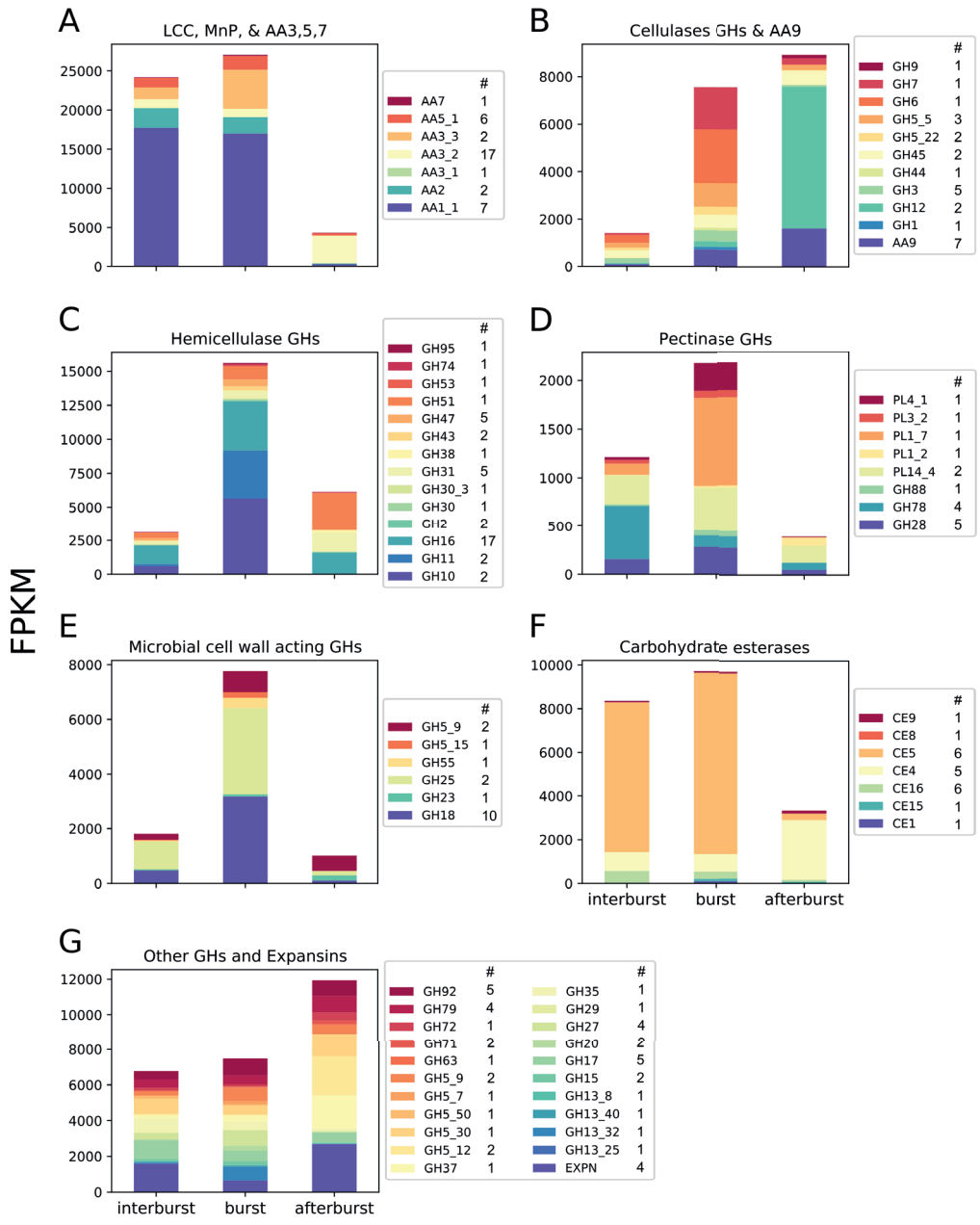


Figure 7. Expression values (FPKM) of differentially expressed classes of CAZYs related to lignin degradation (A), cellulose degradation (B), hemicellulose degradation (C), pectin degradation (D), microbial cell wall degradation and remodelling (E), carbohydrate esterases (F), other GHs and expansins (G). Bars represent expression values before (inter-burst) during (burst) and after bursts (after burst). The number of differentially expressed genes that are considered for each CAZY class are listed in the legend of each subfigure.

and were dominated by putative endo-acting hemicellulases like GH10, GH11, and GH16 while after bursts GH16, GH31, and GH51 were dominantly expressed (Fig. 7C). Similar to the ligninolytic system pectinases were downregulated after bursts (Fig. 7D). In between bursts the GH78 and the PL14_4 pectinase families were dominantly expressed while the PL4_1, PL1_7, PL14_4, and GH28 pectinase families were most highly expressed during bursts. Glycoside hydrolase families acting on microbial cell walls were upregulated during bursts (Fig. 7E) and their expression was dominated by lysozyme and chitinase families GH18 and GH25, and putative β -1,3-glucanases and β -1,6-glucanases (GH5_9, GH5_15, and GH55). Putative cutinases of the carbohydrate esterase family CE5 were dominantly expressed in between and during bursts (Fig. 7F; Dataset S2 and S3, see online version). The CE5 family was downregulated after bursts while the putative chitin deacetylases of the CE4 family were upregulated after a burst. Finally, expression of expansins was lower during bursts compared to the samples in between and after bursts (Fig. 7G). From these data it is clear that genes involved in degradation of hemicellulose and microbial cell walls are primarily expressed during bursts while cellulases are also expressed after a burst.

Sets of protease genes are upregulated during and after respiratory bursts and in inter-burst periods

Upregulation of amino acid and peptide transporters after bursts point to increased extracellular availability of these nutrients at this stage. MEROPS protease genes were enriched in the upregulated genes during a burst, in the downregulated genes after a burst and the upregulated genes during the inter-burst (Dataset S1, see online version). Specifically, sets of protease genes were expressed during, after and in between bursts (Dataset S5, see online version). For example, 19 out of 23 and 49 out of 54 protease genes upregulated during and after a burst, respectively, were most highly expressed at that sample point. The highly expressed serine protease gene SRP1 (Burton et al., 1997; Heneghan et al., 2016) (Protein ID 194648) that is implicated in nitrogen acquisition from humic-rich substrates was upregulated 3.5 fold during a burst and 372 fold downregulated after this event. Together, this suggests a highly differentiated role for proteases in vegetative growth of *A. bisporus*.

Expression of metabolic genes support a repeated reorganization of fungal metabolism

A total of 15 out of 59 genes involved in glycolysis, the pentose phosphate pathway (including genes involved in conversion of pentoses to D-xylulose), and the galactose pathway changed expression more than 5 fold during cycling (Dataset S8, see online version). For example, the pyruvate kinase (EC 2.7.1.40), ribose-phosphate pyrophosphokinase (EC 2.7.6.1) and ribulose-phosphate 3-epimerase (EC 5.1.3.1) genes were upregulated 37, 10, and 16 fold after a burst, respectively. Furthermore, 7 out of 21 genes involved in the TCA cycle changed expression ≥ 5 fold of which 4 were downregulated after a burst and 2 were upregulated after a burst. A predicted trehalose phosphorylase (EC 2.4.1.231 / 2.4.1.64) and mannitol-1-phosphate dehydrogenase (EC 1.1.1.17) gene were upregulated 3.8 and 13 fold, respectively, after a burst. This indicates

that the metabolism of *A. bisporus* is regulated in a cyclic way during most of the vegetative growth in compost.

The secreted oxalate decarboxylase (Kathiara et al., 2000) (EC 4.1.1.2) and intracellular formate dehydrogenase (EC 1.17.1.9) genes were downregulated 5.3 and 105 fold, respectively, after a burst and stably expressed in between and during bursts. Two glyoxalase genes (Pfam 00903) and a putative glyoxylate reductase gene (EC 1.1.1.26) were also downregulated after a burst (5.6-39 fold), while the putative glyoxylate reductase gene and a glyoxalase gene were upregulated before and during a burst (2.3-17.9 and 2.2-2.5 fold, respectively). This shows that genes involved in oxalate metabolism are downregulated after bursts.

Discussion

Growth of filamentous fungi in complex substrates is associated with respiration (i.e. production of CO₂ and O₂ consumption) and heat production, yet these variables are rarely measured. Here, a respirometer and temperature electrodes were used to study the vegetative growth of *A. bisporus* in compost revealing bursts of temperature and respiratory activity. Respiratory cycles with periods varying between 7.5 and 22.5 h (i.e. distinct from a circadian type of rhythm) have been observed during colonization of malt extract and wood blocks by the brown rot fungi *Neolentinus suffrutescens* (*Lentinus lepideus*), *Gloeophyllum trabeum* (*Lenzites trabea*), *Postia placenta* (*Poria monticola*), and *Coniophora puteana* (Damaschke and Becker, 1966; Smith, 1973). This indicates that respiratory patterns are widespread in basidiomycetes. However, the increase in respiration during bursts produced by *A. bisporus* is more dramatic (up to 3.5-fold) compared to the wave-like respiratory patterns of brown rot fungi (up to 0.3-fold). Bursts of *A. bisporus* became increasingly synchronized over a distance of at least 50 cm and required anastomosis of hyphae as the burst produced by incompatible strains A15 and Bisp015 did not synchronize. The loss of synchronization in late vegetative growth of A15 may reflect loss of mycelial interactions, possibly due to lysis of hyphae. Older parts of the mycelium participated in bursts as they were observed until the outer region of the mycelium had passed the temperature sensor 5.7 cm. Thereafter, the mycelium had reached the edge of its substrate and bursts were no longer observed. Growth of the hyphal front may, therefore, be important for the occurrence of bursts in older parts of the mycelium.

Compost temperature increased up to 2 °C in 1.5 to 2 h during bursts corresponding to the release of up to 5 kJ energy kg⁻¹ compost when assuming a water content of 60 %. Thornton's Rule shows that O₂ consumption can fully explain the temperature increase observed in compost (Thornton, 1917; Hansen et al., 2004) (Supplementary text 3, see online version; Table S1, S2). The decrease in RQ from 0.8 to 0.65 in the period where respiratory bursts are most regular (Fig. 1C, first 150 h) fits with the formation of oxidized compounds like oxalic acid that are formed around hyphae of *A. bisporus* during its vegetative growth (Atkey and Wood, 1983) and preferential lignin mineralization during PIII (Kabel et al., 2017). Lignin mineralization accounts for approximately 84 % of the total heat production during PIII (Supplementary text 3, see online version; Table S3, S4), while the total O₂ consumption during bursts is 21 % of total O₂ consumption (Table S1). Therefore, lignin degradation cannot occur solely in bursts as oxygen consumption does

not match what is expected from lignin loss.

Transcriptomic data, obtained in between, during, and after bursts, supports the view that *A. bisporus* cycles through degradation of lignin, (hemi-) cellulose and microbial biomass, and uptake of breakdown products using a synchronized vegetative growing mycelium. The ligninolytic system of *A. bisporus* is active before and during these bursts while (hemi-) cellulolytic genes and genes encoding microbial biomass degrading activities are upregulated during and after this event. The active expression of sugar and amino acid transporters after a burst indicates that carbon influx occurs at this time whereafter nutrients are likely redistributed throughout the mycelial network (Herman et al., 2020; **Chapter 3**). Indeed, genes involved in glycolysis and the pentose phosphate pathway were upregulated (up to 37 fold) after a burst. In addition, expression of trehalose phosphorylase and mannitol-1-phosphate dehydrogenase genes was increased after bursts too (up to 13 fold). Therefore, trehalose and mannitol may not only play a role in mushroom formation (Hammond and Nichols, 1976a) but also in carbon storage and transport within the mycelial network.

The increase in respiration and the oscillations of the RQ around the time bursts occur (e.g. from 0.58 to 0.71) show that there is increased mineralization of more oxidized substrates during a burst. This could be explained by the consumption of sugars (RQ = 1) but also mineralization of oxalic acid (RQ = 4). This link between bursts and oxalate metabolism is supported by downregulation of putatively secreted oxalate decarboxylase and formate dehydrogenase after bursts (up to 105 fold). Thus, the bursts and RQ oscillations could relate to mineralization of extracellular oxalic acid. Free energy conservation in oxalate (or sugar) metabolism produces ATP that would be required for synthesis of secreted proteins like CAZYS during bursts. Protein production is an energy intensive process (Stouthamer, 1973). Hence, protein synthesis could partly explain the temperature increase (O_2 consumption) during bursts. Protein secretion could be facilitated by formation of new (small) branching hyphae or cell wall remodeling of older mycelium (Wösten et al., 1991; Krijgsheld et al., 2013). Furthermore, a burst was observed in the 1st flush of a semi-commercial cultivation but not in the 2nd flush. Possibly relating to previous observations where low expression of CAZYS was found in samples taken during the 2nd flush (Patyshakuliyeva et al., 2015).

In line with downregulation of the ligninolytic system, MnP, LCC, glyoxal oxidases, and alcohol oxidase genes were downregulated up to 194-fold after a burst together with oxalate metabolism. This fits with degradation of lignin (and humic compounds) before and during bursts, where ligninolytic action of a synchronized mycelium increases accessibility of carbohydrates together with pectinase and cutinase genes. As with white rot fungi, ligninolytic action of *A. bisporus* should include the production of extracellular radical species. Indeed, there is evidence for radical generation by *A. bisporus* in compost based on the presence and generation of H_2O_2 in compost water extracts (Savoie et al., 2007; Vos et al., 2017b). In addition, components involved in Fenton chemistry, like Fe^{2+} and H_2O_2 , but also molecules that are required for extracellular lipid peroxidation, e.g. unsaturated lipids, glyoxal oxidase, and MnP, are presumably present in compost. Analysis of iron-species and experiments with $^{14}/^{13}C$ -labeled lignin or fatty acids combined with pyrolysis-GC-MS and NMR (Wood, 1983; Van Erven et al., 2019) may provide insights in the chemistry of lignin and humic acids degradation by *A. bisporus*. These insights may pave the road in understanding the radical chemistry employed by this fungus *in situ*

(i.e. a role of Fenton chemistry and / or lipid peroxidation) during its cultivation process as well as during bursts. Recent insights in the decay strategy of brown rot fungi points to the production of hydroxyl radicals by their hyphal front while the bulk of (hemi-) cellulases is produced by older mycelium (Zhang et al., 2016, 2019; Presley and Schilling, 2017; Castaño et al., 2018). H_2O_2 and other radical species can damage proteins involved in polysaccharide deconstruction and spatial separation of radical generation and (hemi-) cellulases can protect these CAZYs from oxidative damage (Zhang et al., 2016; Castaño et al., 2018). In addition, the pre-treatment of plant cell walls with Fenton chemistry derived radicals or a ligninolytic system allows a more efficient (hemi-) cellulose deconstruction by CAZYs (ten Have et al., 2003; Arantes et al., 2012). Therefore, temporal cycling in ligninolytic and cellulolytic activities by *A. bisporus* may enable the repeated pre-treatment of compost and protect extracellular proteins from radical species, resulting in a more efficient substrate decomposition when compared to a spatial separation of ligninolytic and cellulolytic activities.

Acknowledgements

This research was supported by the Dutch Technology Foundation STW (Grants 11108 and 15493), which is part of the Netherlands Organization for Scientific Research (NWO), and which is partly funded by the Ministry of Economic Affairs.

Supplemental Material

Table S1. Additionally released CO₂ (Add. CO₂) and O₂ (Add. O₂) during bursts observed in the respirometer (Fig. 1). kJ released per burst was calculated assuming 455 kJ mol⁻¹ O₂ (Hansen *et al.*, 2004) the ratio of metabolic heat rate to the rate of CO₂ production and the ratio of metabolic heat rate to the rate of O₂ uptake (R q/RCO₂ and R q/RO₂, respectively. Total CO₂ production and O₂ consumption was 831 and 1205 mmol kg⁻¹ compost, respectively. The total O₂ production during bursts was 255.15 mmol kg⁻¹ compost and the total of additional O₂ released during bursts was 95.65 mmol kg⁻¹ compost.

Burst	Total mmol O ₂ consumption kg ⁻¹ compost per burst	Additional CO ₂ mmol kg ⁻¹ compost per burst	Additional O ₂ mmol consumption kg ⁻¹ compost per burst	RQ*	Calculated heat release in kJ kg ⁻¹ compost per burst
33 h	9.63	0.85	0.83	1.03	0.38
50 h	10.70	1.22	1.65	0.74	0.75
68 h	12.41	1.59	2.10	0.76	0.96
88 h	8.71	2.07	2.84	0.73	1.29
108 h	11.00	2.99	4.56	0.65	2.08
128 h	20.53	4.30	5.08	0.84	2.31
148 h	19.52	7.78	10.45	0.74	4.76
170 h	31.68	9.40	10.85	0.87	4.94
191 h	32.29	11.96	12.96	0.92	5.90
211 h	27.26	7.56	8.85	0.85	4.03
236 h	31.83	13.82	15.13	0.91	6.88
288 h	31.09	14.50	17.08	0.85	7.77
380 h	8.55	2.49	3.27	0.76	1.49

*respiratory quotient of the additionally released CO₂ and consumed O₂.

Table S2. Average (and standard deviation) of the duration of temperature increase, temperature increase, kJ released per burst assuming 60 % water content, and mmol O₂ kg⁻¹ compost released per burst. Values represent the average of the 6 sensors in Fig. 2 for a burst around a time point. The maximum values for one of the peaks at 218 h are shown.

Burst	Period of T* increase (min)	dT**	Heat release in kJ kg ⁻¹ compost per burst	mmol O ₂ kg ⁻¹ compost per burst
73 h	49.3 (6.3)	0.81 (0.06)	2.02 (0.15)	4.44 (0.34)
88 h	51.9 (5.6)	0.83 (0.12)	2.06 (0.31)	4.53 (0.67)
103 h	48.9 (6.6)	0.89 (0.14)	2.22 (0.36)	4.87 (0.79)
120 h	41.1 (6)	0.44 (0.07)	1.11 (0.18)	2.44 (0.39)
137 h	59.4 (3.1)	1.51 (0.05)	3.78 (0.12)	8.3 (0.26)
156 h	46.7 (11.3)	0.23 (0.14)	0.57 (0.34)	1.25 (0.75)
175 h	69.8 (7.7)	1.39 (0.26)	3.47 (0.64)	7.63 (1.42)
218 h	85.5 (14.5)	1.13 (0.7)	2.82 (1.76)	6.2 (3.86)
Maximum (218 h)	94.1	2.31	5.78	12.69

*temperature in °C; **increase in compost temperature in °C.

Table S3. Estimates of lignin, cellulose, and hemicellulose heat production upon mineralization. Numbers are based on data from (Ioelovich, 2018) and Thorntons Rule (Thornton, 1917).

Monomer	Monomer formula	Monomer MW	Mol O ₂ per mol mineralized monomer	Heat production in kJ mol ⁻¹ based on (Ioelovich, 2018)	Heat production in kJ mol ⁻¹ based on Thorntons Rule
Lignin	C _{10.24} H _{12.48} O _{3.24}	188.29	11.74	-5452	-5342
Cellulose	C ₆ H ₁₀ O ₅	162	6	-2988	-2730
Hemicellulose	C ₅ H ₈ O ₄	132	5	-2477	-2275

Table S4. Estimated heat production as a consequence of lignin, cellulose, and hemicellulose loss during a typical PIII. Values for the PIII mass balance were taken from (Jurak et al., 2015b). Conversion to heat production are based on Table S3.

Component	PII mass balance (g)	PIII mass balance (g)	Loss relative to PII (g)	% loss during PIII	mol "monomer" ^p	kJ heat kg ⁻¹ compost [*]	O ₂ ^{**} mol kg ⁻¹
Total (with Klason lignin)	787	708	79	10.0%		-1305	-2.9
Lignin (pyrogram based)	208	91	117	56.3%	0.62	-3387	-7.4
Lignin (klason based)	252	214	38	15.1%	0.20	-1100	-2.4
Cellulose	197	186	11	5.6%	0.07	-114	-0.2
Hemicellulose	110	104	6	5.6%	0.04	-91	-0.2

^{*}Based on Ioelovich (2018). ^{**}Based on Thornton's rule.

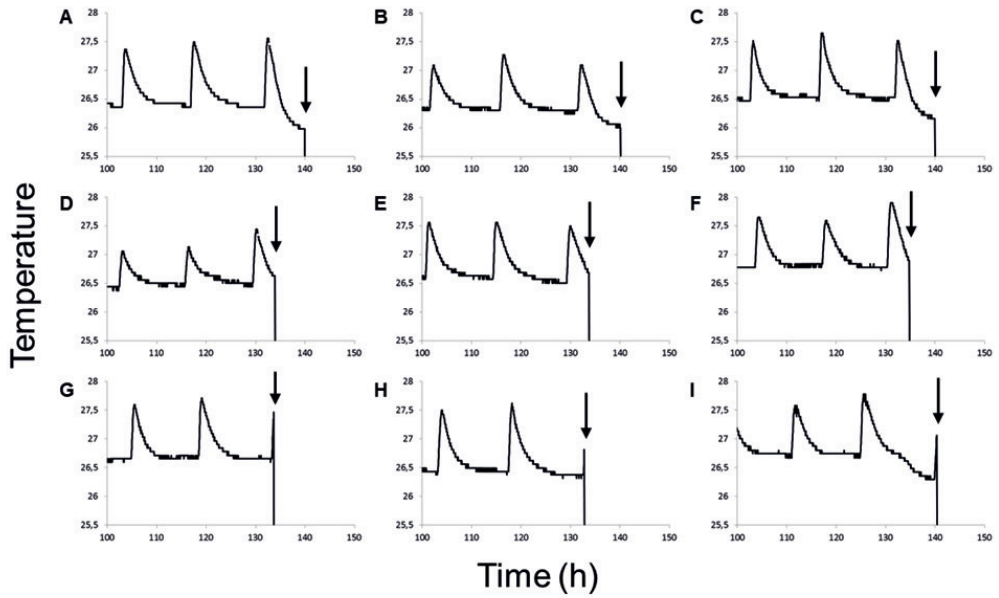


Figure S1. Temperature profiles of PIII compost used for RNA isolation in triplicate of inter-burst (A-C), after-burst (D-F), and burst (G-I) stages. Harvesting was done at time points indicated with an arrow. Temperature measurements were started 4 days after inoculation.

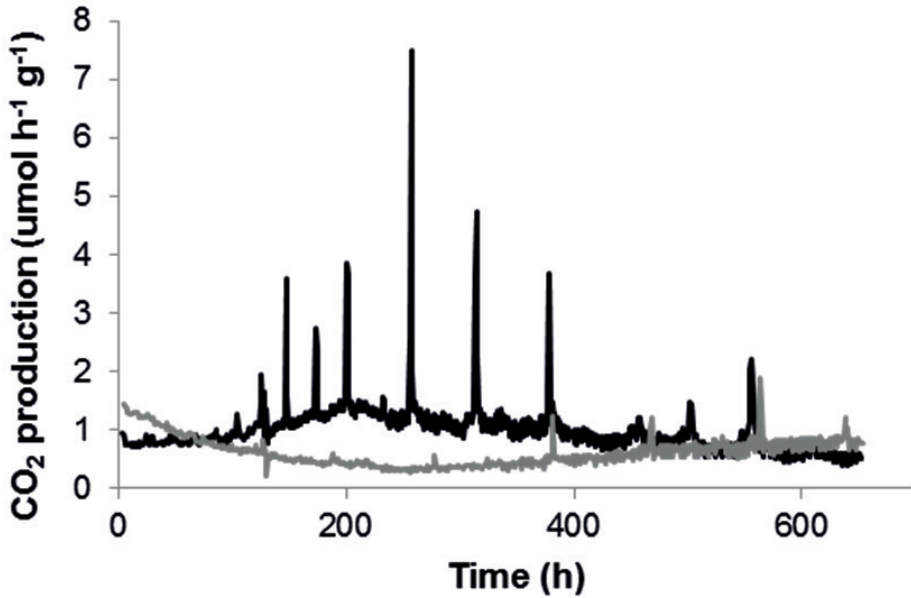


Figure S2. CO₂ production rate of 10 g PII-end compost that had (grey line) or had not (black line) been sterilized prior to inoculation with 4 spawn grains of *A. bisporus*. CO₂ production was monitored after pre-growth at 25 °C for 3 days.

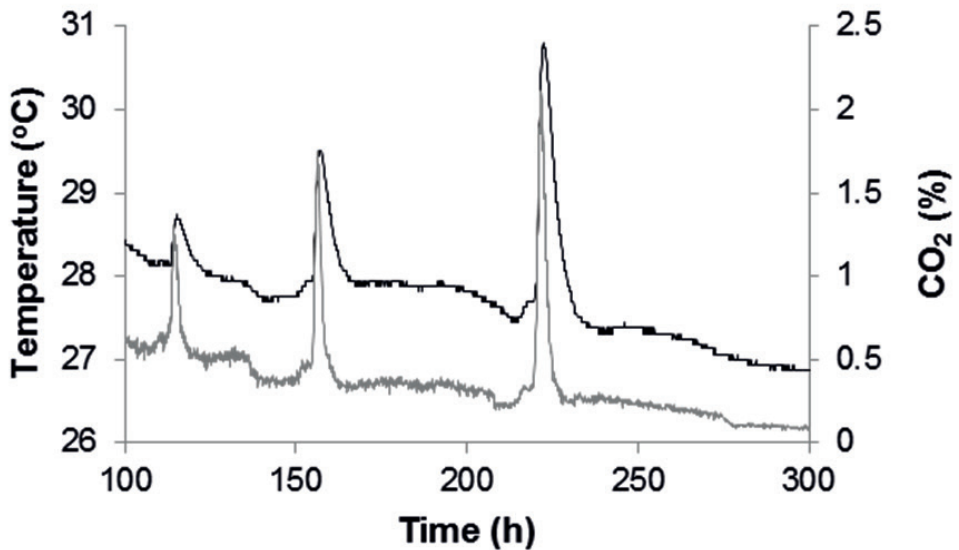


Figure S3. Respiratory bursts in 1 kg compost as measured by monitoring changes in temperature (black) and CO₂ (grey).

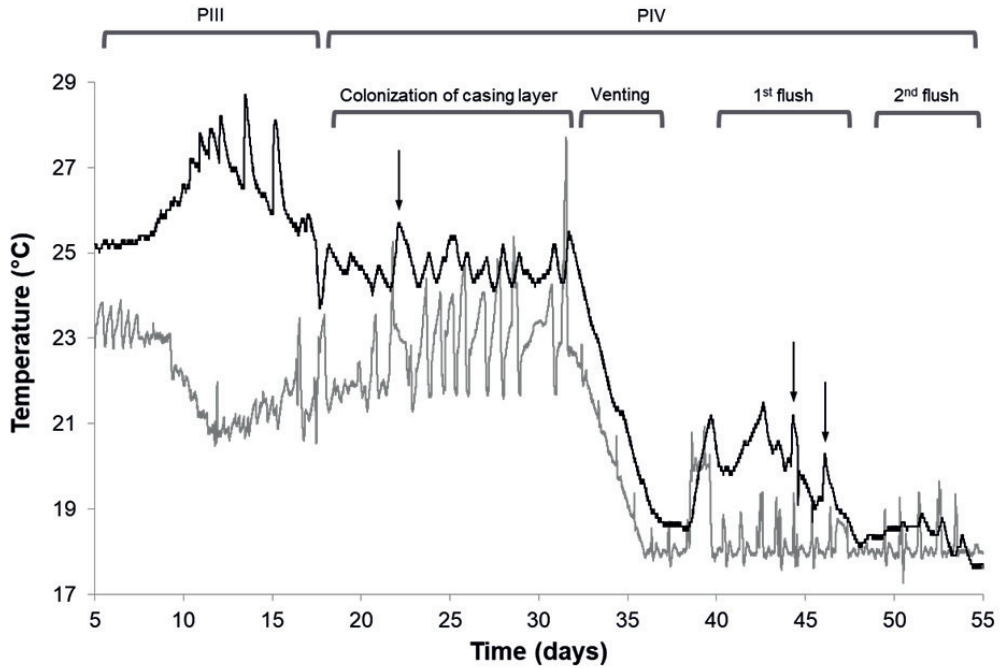


Figure S4. Temperature profile of compost (black line) and air in the incubation room (grey line) during vegetative growth (PIII and colonization of casing layer) and mushroom production (Venting, 1st flush, and 2nd flush) of *A. bisporus*. Respiratory bursts occurring in PIV are indicated with an arrow. These temperature peaks cannot be explained by peaks in the temperature of the incubation room.

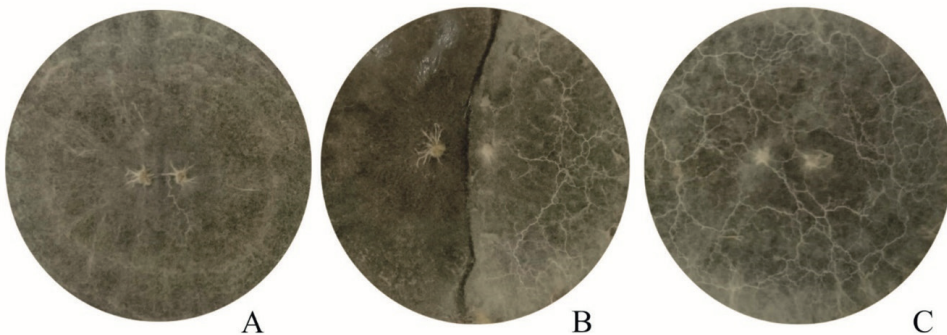


Figure S5. Examples of a compatible interactions of strain A15 (A), incompatible interaction of strains A15 and Bisp015 (B) and compatible interaction of strain Bisp015 (C).

3

Growth induced translocation effectively directs an amino acid analogue to developing zones in *Agaricus bisporus*

Koen C. Herman, Han A.B. Wösten, Mark D. Fricker, Robert-Jan Bleichrodt

This chapter has been published as: Herman, K.C., Wösten, H.A.B., Fricker, M.D., Bleichrodt, R.J., 2020. Growth induced translocation effectively directs an amino acid analogue to developing zones in *Agaricus bisporus*. *Fungal Biol.* 124, 1013–1023.

Abstract

The vegetative mycelium of *Agaricus bisporus* supplies developing white button mushrooms with water and nutrients. However, it is not yet known which part of the mycelium contributes to the feeding of the mushrooms and how this depends on growth conditions. Here we used photon counting scintillation imaging to track translocation of the ^{14}C -radiolabeled metabolically inert amino acid analogue α -aminoisobutyric acid (^{14}C -AIB). Translocation to the periphery of the mycelium was observed in actively growing vegetative mycelium with a velocity of up to 6.6 mm h^{-1} , which was 30 fold higher than the growth rate. Furthermore, ^{14}C -AIB translocated to neighboring colonies after fusion by anastomosis depending on the relative growth rate in these colonies. When mushrooms started to develop, translocation of ^{14}C -AIB was redirected to the fruiting bodies via mycelium and hyphal cords. More abundant mycelial cord formation and a 5 fold higher rate of translocation was observed for cultures growing directionally from inoculum located at one side of the substrate, when compared to non-directional growth (inoculum mixed throughout the substrate). The maximum translocation distance was also greater (≥ 50 and 22 cm , respectively). In conclusion, ^{14}C -AIB translocation switches between vegetative growth and towards developing mushrooms, especially via cords and when source-sink relationships change.

Introduction

The white button mushroom *Agaricus bisporus* is a high-quality food that is rich in protein and fibre and contains useful vitamins, minerals, and anti-cancer polysaccharides. This fungus produces mushrooms after extensive colonisation of the substrate by a mycelial network. In the Netherlands, the substrate is typically a horse-manure-based compost. The industrial production process of this compost and subsequent growth of *A. bisporus* is characterised by four phases PI-PIV (Gerrits, 1988). In phase I (PI) thermophilic bacteria replace mesophilic bacteria, while the substrate temperature increases to $80 \text{ }^\circ\text{C}$ due to microbial metabolic activity. During the conditioning phase (PII) the released ammonia is sequestered by actinomycetes and thermophilic fungi, like *Scytalidium thermophilum*. Phase III (PIII) is initiated by introducing *A. bisporus* spawn to the PII compost. After 16 - 19 days incubation at $25 \text{ }^\circ\text{C}$, the colonised PIII compost is transported to the growers, where it is topped with a layer of casing soil. This initiates phase IV (PIV), during which mushrooms are produced in 2 - 3 flushes at weekly intervals.

The mycelium within the compost consists of a network of hyphae that provides the growing mushrooms with food and water. However, only about half of the total carbohydrates in the compost has been consumed after mushrooms have been harvested (Chen et al. 2000; Jurak, 2015; Iiyama et al. 1994). The availability of substrate degrading enzymes does not seem to be the limiting factor (Jurak et al. 2014, 2015b; Vos et al. 2017b, 2018). Therefore, efficient translocation from the mycelium to the fruiting bodies may constrain overall resource utilisation.

Work in other fungi has led to the hypothesis of tip-directed bulk flow supporting long distance translocation (Jennings, 1987). This translocation would be caused by small pressure differences along the hyphae, that typically result from differential uptake of osmotically active compounds like ions and nutrients (Lew, 2005), *de novo* synthesis of

osmolytes (Lew, 2011), external differential osmotic potentials (Muralidhar et al. 2016) or growth itself (Heaton et al. 2010). Bulk flow has been shown to exceed rates that would have been expected by diffusion alone or motor-driven movement of vesicles along the cytoskeleton. However, growth-induced bulk flow can deliver substances close to the tip, but additional mechanisms are required to cover the final distance to the apex (see Heaton et al. 2010 for a detailed explanation), such as diffusion, and cytoplasmic streaming / mixing (Bleichrodt et al. 2013; Lu et al. 2016; Pieuchot et al. 2015; Steinberg, 2014).

Many saprotrophic basidiomycetes form aggregates of individual hyphae called 'mycelial strands' (Jennings and Watkinson, 1982), 'linear organs' (Moore, 1998) or 'cords' (Tlalka et al. 2002). Cords develop predominantly on substrate with low nitrogen concentrations and high C / N ratios (Watkinson, 1975, 1979). Cords of *Serpula lacrymans* develop around vessel hyphae that become wider, thin walled, empty, and lose their septa (Helsby, 1976). Watkinson (1971, 1975) found that vessel hyphae may exude nitrogen by autolysis and stimulate aggregation of young hyphae to form strands. Branches of these hyphae do not diverge, but rather grow parallel to the vessel hyphae (Butler, 1957; 1958). This is accompanied by hyphal attachment and anastomosis (Moore, 1998), and the formation of an extracellular matrix (Jennings and Watkinson, 1982). Thick-walled fibre or tendril hyphae envelope the structure, resulting in a (sub-)millimetre wide insulated cord (Mathew, 1961; Nuss et al. 1991). Some vessel hyphae may lyse and form even wider spaces in the cord. Cords have been shown to transport phosphorous (Wells et al. 1990; Wells and Boddy, 1995), nitrogen (Arnebrant et al. 1993; Tlalka et al. 2002; Watkinson, 1984), carbon (Brownlee and Jennings, 1982a,b), and water (Jennings, 1984). When cords arrive at a new food source, individual hyphae spread out from the cord and start branching to colonise the resource (Watkinson, 1971). Probably, the cue for this is the nitrogen level within the cords that holds the individual hyphae bundled together under low nutrient conditions, but when nitrogen levels in the new food source exceed the internal cord levels, the cohesive growth is lost (Moore, 1998). Connections between the newly discovered source and the original source are consolidated, radial growth from the inoculum stops and the mycelial network that is not connected to a source regresses as resources are reallocated (reviewed by Boddy, 1999). Mycelial regression is believed to be mediated by autolysis or apoptosis (Umar and van Griensven, 1988; Watkinson, 1999).

It is not yet known which part of the mycelium contributes to the feeding of the mushrooms and how this depends on growth conditions. Therefore, we here studied resource translocation patterns during vegetative growth and mushroom development in *A. bisporus*. To this end, translocation of the ^{14}C -labeled amino acid analogue aminoisobutyric acid (^{14}C -AIB) was assessed in real time. We show that colonisation of the substrate by directional growth (one-sided inoculation) results in formation of more cords and a 5 fold higher translocation rate of nutrients over a longer distance, when compared to non-directional growth (mixed inoculation of the compost). Under laboratory growth conditions this was accompanied by a higher mushroom yield. However, this was not sustained in larger, semi-industrial growth conditions.

Material and Methods

Culturing

A. bisporus production strain A15 (Sylvan, Netherlands) was routinely grown on nutrient-pour casing soil or on PII horse-manure based compost (CNC Grondstoffen, Milsbeek, the Netherlands). For network fusion experiments on casing, 80 g casing soil was manually compressed in 12 x 12 cm square Petri dishes (Greiner, Kremsmünster, Austria) and inoculated with rye grains that had been colonised with *A. bisporus* A15. To test translocation following directional growth, 15 g PIII compost (12 x 3 cm) was placed next to 50 g PII compost (12 x 9 cm) in square Petri dishes (12 x 12 cm) as a 17 mm thick layer (Fig. 1A). For mushroom production, Halbschalen cultures were used by tilling square dishes (Eger, 1962). To this end, 10 g PIII compost (12 x 1 cm), 40 g PII compost (12 x 8 cm) and 20 g casing soil (12 x 2 cm) were placed as blocks next to each other in dishes (similar to Fig. 1B). This resulted in directional growth. For mushroom production following non-directional growth, 50 g PIII compost in a 12 x 9 cm area was abutted by a block of 20 g casing soil (12 x 2 cm) (similar to Fig. 1C). For long-range

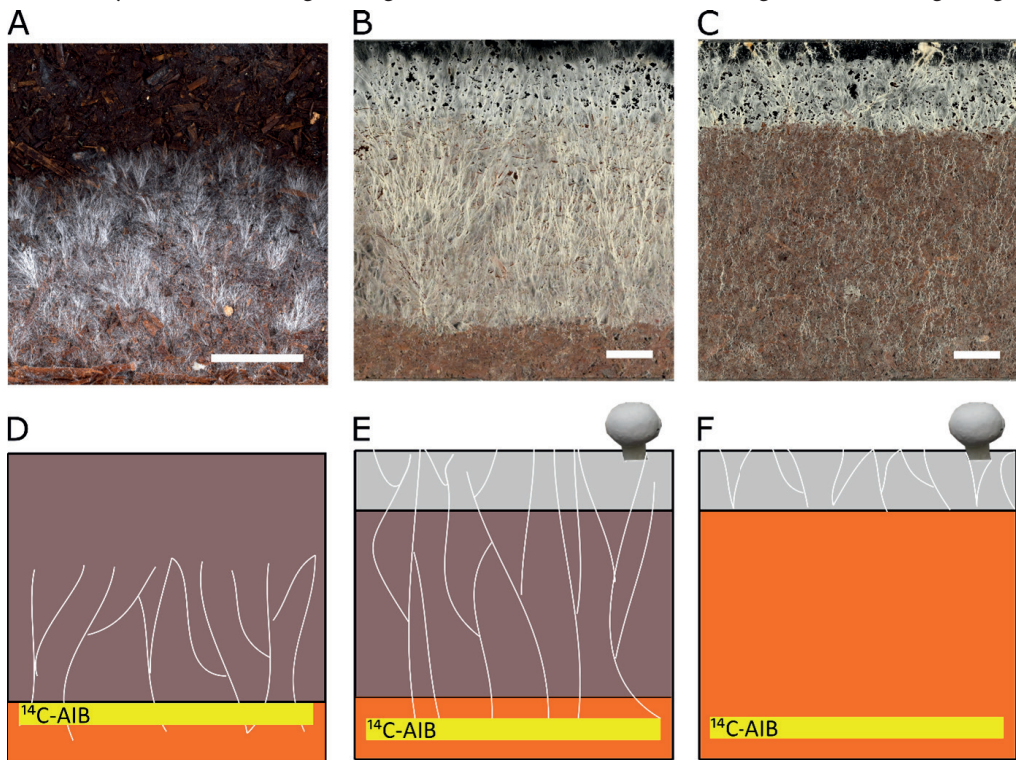


Figure 1. Experimental set up to determine translocation efficiency of $^{14}\text{C-AIB}$ within directionally grown vegetative mycelium (A, D), or to mushrooms in directionally- (B, E) or non-directionally (C, F) grown Halbschalen cultures. Bright field images (A - C) and schematic representations of these (D - F) are shown. The yellow rectangles indicate $^{14}\text{C-AIB}$ labelling zones. PIII compost (orange), PII compost (brown) and casing soil (gray) are indicated (D - F). Bars represent 3 cm (A - C).

translocation experiments, similar but larger cultures were set up in 24.5 x 24.5 cm dishes. For directional growth, 50 g PIII compost (24.5 x 3 cm), 225 g PII compost (24.5 x 13.5 cm) and 110 g casing soil (24.5 x 5.5 cm) were placed next to each other in a 25 mm thick layer (Fig. 1B). Likewise, for non-directional growth, 275 g PIII compost (24.5 x 16.5 cm) and 110 g casing soil (24.5 x 5.5 cm) were used (Fig. 1C). Cultures were incubated at 22 °C and 80 % RH for about ≥ 30 or 14 days for these directional and non-directional growth modes, respectively, unless stated otherwise. Mushroom formation was induced by venting at 18 °C at 80 % RH. To evaluate maximum translocation distance, 65 mm wide gutters of 0.5 or 1 m length were used. Gutters of 0.5 m length were filled with 45 g PIII compost, 350 g PII compost and 60 g casing soil for directional growth (Fig. 2A), or with 395 g PIII compost and 60 g casing soil for non-directional growth (Fig. 2B), at a compost density of 0.4 kg l⁻¹. Gutters of 1 m length were filled with 45 g PIII compost, 790 g PII compost and 60 g casing soil for directional growth (Fig. 2C), or with 835 g PIII compost and 60 g casing soil for non-directional growth (Fig. 2D). Generally, incubations for directional growth spanning 50 or 100 cm took over 2 or 4 months, respectively, while non-directional growth in 50 and 100 cm gutters took 1 month. ¹⁴C-AIB label was applied at one end of the gutter when >10 mm mushrooms had formed on the other end (Fig. 2). Mushrooms were allowed to mature over 3 days to circa 5 cm diameter before harvesting for liquid scintillation counting (LSC).

To determine mushroom yield, 500 g PIII compost was placed at the bottom of boxes (26 x 20 x 22 cm; Manutan, Gonesse, France) and 2 kg PII compost was placed on top for directional growth (similar to Fig. 1B, but now in 3 dimensions (3D)). For non-directional growth 500 g PIII and 2 kg PII compost were mixed (similar to Fig. 1C, but now in 3D and

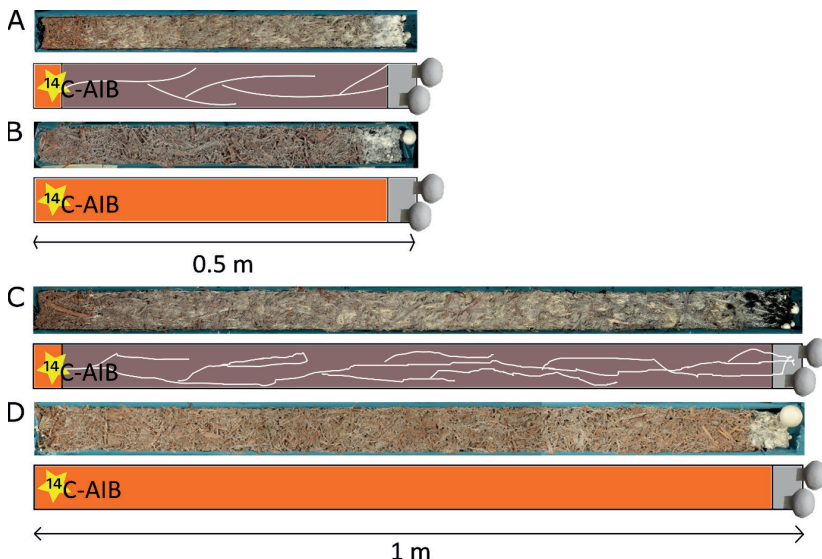


Figure 2. Directional (A, C) and non-directional (B, D) growth in gutters of 50 cm (A, B) and 100 cm (C, D), to determine maximum translocation distance of ¹⁴C-AIB to mushrooms. The yellow stars indicate the ¹⁴C-AIB labelling zones. PIII compost (orange), PII compost (brown) and casing soil (gray) are indicated. Bright field images are shown at time of labelling and schematic representations thereof. After 3 days, all cultures had developed mature mushrooms (circa 5 cm in diameter).

a mix of PIII and PII compost was used, instead of only PIII compost). Alternatively, 2.5 kg PIII compost was used for non-directional growth (similar to Fig. 1C, but now in 3D). Compost was topped with 1 kg casing soil after 12, 14 and 19 days for non-directional mixed, non-directional and directional growth, respectively. Mushrooms were harvested for up to 2 months after inoculation.

Liquid scintillation counting

Cultures were labelled with 2-10 μCi 2-amino[1- ^{14}C]isobutyric acid (^{14}C -AIB; 2.11 GBq / mmol aqueous solution in 2 % ethanol, Amersham, Buckinghamshire, UK) that was mixed with 1% Triton X-100 (Merck, New Jersey, USA) in 9 g / l NaCl solution and incubated for 3 days to allow mushroom formation. Mushrooms were weighed and cut in pieces that were then dissolved in 2 ml 98 % sulfuric acid (Sigma-Aldrich, Massachusetts, USA) g^{-1} wet weight mushroom. This was followed by adding 9 volumes CaCl_2 to precipitate sulphate, which would otherwise react with the scintillation cocktail. Samples were vortexed, centrifuged for 5 min at 10,000 g, and 100 μl supernatant was transferred to a LSC tube (Pony Vial 6 ml, Perkin Elmer, Massachusetts, USA), after which 5 ml Ultima Gold™ LSC Cocktail (Merck) was added. Samples were counted for 2 x 5 min (disintegrations per min (dpm)) using a Tri-Carb 2300TR liquid scintillation analyser (Packard Instrument Company, Massachusetts). Radioactivity was quantified using calibration curves in presence and absence of dissolved mushroom sample to correct for reduced counting efficiency in the presence of the organic material.

Imaging ^{14}C -AIB translocation using Photon Counting Scintillation Imaging

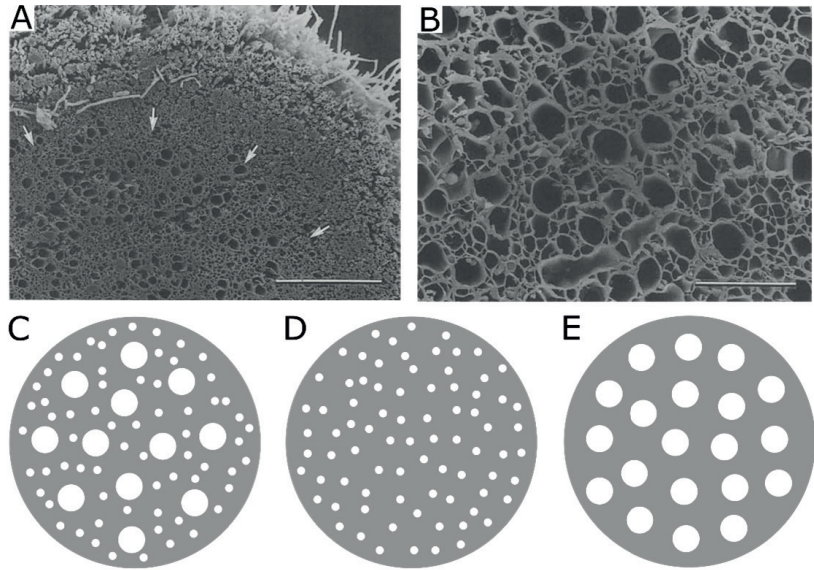
For compost and Halbschalen cultures, a 12 x 12 cm scintillation screen (Intensifying screens BioMax® Transcreen® LE, Merck) was placed at the bottom of the Petri dish, after which PII and / or PIII compost and / or casing soil was added. For casing soil cultures, the screen was placed on top, covering the entire colony but with a hole cut at the position of the rye grain inoculum. The phosphorous layer of the screen was facing the substrate. 2 μCi ^{14}C -AIB was typically mixed with 2 ml 1 % Triton X-100 (Merck) in 9 g / l NaCl solution and was applied to the cultures. Alternatively, pieces of Whatman® Filter Paper (Merck) were placed on the rye grain inoculum, to which 0.25-0.5 μCi undiluted label was added.

^{14}C -AIB translocation was imaged using a photon-counting system (HRPCS-3, Photek, St Leonards, UK) equipped with a three-stage multichannel plate (MCP) image intensifier that was mounted in a dark box (Tlalka et al. 2002). Signals were integrated over 1 h intervals and cultures were typically imaged for at least 72 h. Movies were imported into ImageJ, visualized using the Perceptually Uniform Colour LUT CET-D1A, and exported as AVI file with 5 frames s^{-1} . For some figures, the signal was integrated over the total time of the experiment (ImageJ summed intensity), or for intervals of several hours as indicated (using a bespoke ImageJ script, see online version <https://doi.org/10.1016/j.funbio.2020.09.002> for Script S1). Translocation velocities were determined as the time for the signal to increase over background in manually defined regions of interest (ROIs), at a given distance from the inoculum. To detect accumulation of ^{14}C -AIB in mushrooms, mushrooms were longitudinally cut in half. Slices (one half was cut in longitudinal slices; the other half was cross sectioned) were put on a scintillation screen. These samples, compost and Halbschalen cultures were imaged from below, while casing cultures were

imaged from above, by inverting the camera system.

Modelling translocation dynamics in hyphal cords, hyphal growth and mushroom expansion

We set out to analyse flow in cords using flow mechanics by representing their hyphae as pipes. An electron microscopy image from Cairney (1990), showing a cord cross section of *Agaricus carminescens* (Fig. 3A), was used to determine the total surface area of a cord. Individual hyphae within the cord (Fig. 3B) were segmented using ImageJ, since the



Volume Flowrate (ml h ⁻¹)	1.22E-5	7.15E-6	1.14E-4
Supports number of hyphae	7920	4660	74,600

Figure 3. Structure of cords and their volume flow rates according to three scenarios. (A) Internal structure of an *A. carminescens* cord. Arrows depict the boundary of the medulla. Bar represents 20 μm . (B) Magnification of the medulla showing many wide vessel hyphae. Bar represents 30 μm . (C) Scenario 1 is based on the naturally observed cord (as seen in A, B) composed of both thin and vessel hyphae. (D) Scenario 2 depicts a cord that is composed of only thin hyphae of $\text{\O} 3 \mu\text{m}$. (E) Scenario 3 is a cord that is exclusively composed of $\text{\O} 12 \mu\text{m}$ vessel hyphae. Volume flow rate calculations in a 5 cm long cord have been based on Poiseuille's Law (Eq. 2, Material and Methods) for laminar flow in pipes, ignoring the presence of septa and taking the cytoplasmic viscosity as water. The observed translocation velocity in cords of 3.5 mm h^{-1} implies a pressure difference of 2 Pa cm^{-1} (Eq. 1). The following parameters were thus used: pressure difference 10 Pa ($5 \text{ cm} \cdot 2 \text{ Pa cm}^{-1}$), viscosity of water (η) 8.98E-4 Pa s , cord length (L) 5 cm. Height differences, evaporation, exudation, or cell wall deformation have been assumed to be zero. The cord volume flow rate and the number of hyphae at the periphery of a colony that a cord can support with the water needed for their growth is indicated for each scenario. (A, B) Reprinted from 'Internal structure of mycelial cords of *Agaricus carminescens* from Heron Island, Great Barrier Reef', Vol 94/ edition number 1, Cairney JWG, Pages 117-119, Copyright (1990), with permission from Elsevier. [https://doi.org/10.1016/S0953-7562\(09\)81271-9](https://doi.org/10.1016/S0953-7562(09)81271-9)

resolution of Fig. 3A was too low to segment individual hyphae. To this end, thresholding was performed to generate a binary image and the particle analysis tool was used to segment the hyphae and determine their cross-sectional surface area. Individual hyphal radius r was calculated from the segmented cross-sectional area. Poiseuille's Law was used to calculate the pressure difference over a certain length (Pa m^{-1}) in such a pipe, required to cause the observed translocation velocity (Nobel, 1991; Brody et al. 1996), Eq. 1: $\frac{dP}{dx} = \frac{v \cdot 8\eta}{r^2}$, where v is the velocity (m s^{-1}), η is the viscosity of the fluid (Pa s), and r is the

radius of the pipe (m). The pressure difference per hyphal length (Pa m^{-1}) was calculated based on the mean observed translocation velocity in cords of 3.5 mm h^{-1} and taking the viscosity of water (0.00089 Pa s), since this is close to the viscosity of cytoplasm (Swaminathan et al. 1997). We calculated the volume flow rate for each hypha in the segmented cord using Poiseuille's Law, Eq. 2: $Q = \frac{(P_1 - P_2)r^4}{\frac{8}{\pi}\eta L}$, where Q = volume flow rate

($\text{m}^3 \text{ s}^{-1}$), $P_1 - P_2$ = pressure difference (Pa) as calculated from Eq. 1, r = pipe radius (m), η = viscosity (Pa s), L = pipe length (m) (Fig. 3B). Using the scale bars in Fig. 3A and 3B reproduced from Cairney (1990), we calculated the ratio of the total surface area of the cord and the part of the surface area of the cord that was represented by Fig. 3B. The total volume flow rate of the cord was then calculated by multiplying this ratio with the sum of the individual hyphae volume flow rates. This follows from the fact that the pressure difference in parallel pipes is equal, but the sum of the flow in the individual pipes is the total volume flow rate (Engineering ToolBox, 2011). Alternatively, volume flow rates were calculated from the same pressure difference in two hypothetical scenarios: (i) a $200 \mu\text{m}$ wide cord represented as a bundle of small individual hyphae each having a $3 \mu\text{m}$ diameter (Fig. 3D); (ii) or as a bundle of $12 \mu\text{m}$ diameter vessel hyphae (Fig. 3E).

We determined how many $3 \mu\text{m}$ wide growing hyphae can be supported by a cord. To this end, the cord total volume flow rate was divided by the volume of growth h^{-1} of a single hypha ($\pi \cdot r^2 \cdot h = \pi \cdot 1.5^2 \mu\text{m} \cdot 217 \mu\text{m h}^{-1}$ [growth rate]). The number of cords needed to support mushroom expansion was calculated as follows. Mushroom wet weight was multiplied by water content (90 %) to calculate how much water it contained. This number was then divided by Q (ml h^{-1}) of a single cord of 50 cm length and by the number of hours (72 h) it took to expand the mushroom. The maximum number of mushrooms that could be formed, was calculated by dividing the total cross sectional surface area of the culture by the cross-sectional surface area of the number of cords that was needed to support a single mushroom.

Statistical analysis

Means were compared using a two-tailed Student's t-test. Power was calculated using software 'PS: Power and Sample Size Calculation' version 3.1.6 (Dupont and Plummer, 1990).

Results

^{14}C -AIB translocates to actively growing zones of *Agaricus bisporus*

Fungal hyphae consist of ~90 % water and therefore growth needs a supply of water to fill the new growth volume. We assessed whether growth-induced bulk flow induces movement of water and nutrients to the growing periphery of the colony and what the speed of that movement was using photon counting scintillation imaging (PCSI, Tlalka et al. 2002, 2007). ^{14}C -AIB was loaded at the PIII-PII compost interface after 2 / 3 of the surface area of the PII compost had been directionally colonised from the PIII compost (Fig. 1D). ^{14}C -AIB predominantly moved in the direction of the growing periphery and hardly within the PIII compost inoculum. The signal moved at a speed of $6.55 \pm 1.38 \text{ mm h}^{-1}$ (mean \pm 95 % CI) to the periphery during the first 9 - 15 h (Movie S1), while the growth speed was 30 fold lower ($0.217 \pm 0.02 \text{ mm h}^{-1}$). The signal became more and more intense at the periphery after this initial phase (Fig. 4E), confirming that translocation was faster than growth. The travelling signal was not homogenously spatially distributed, but was concentrated in hyphal cords, indicated by the tubular localisation of the ^{14}C -AIB signal (Fig. 4F). However, once reaching the periphery, the signal became more diffuse (Fig. 4E), indicating that the label was redistributed in finely branched hyphae. From then onwards, the translocation rate followed the growth rate (Movie S1, see online version). We hypothesised that less cord formation would decrease translocation velocity. Radially symmetric growing colonies that had been inoculated from a single rye grain spawn, produced less predominant cords (Fig. 4G). ^{14}C -AIB was loaded on the rye grain inoculum and translocated with $3.68 \pm 0.31 \text{ mm h}^{-1}$ towards the colony margin (Fig. 4G-L, Movie S2, see online version). This was about half the speed observed during directional growth. In

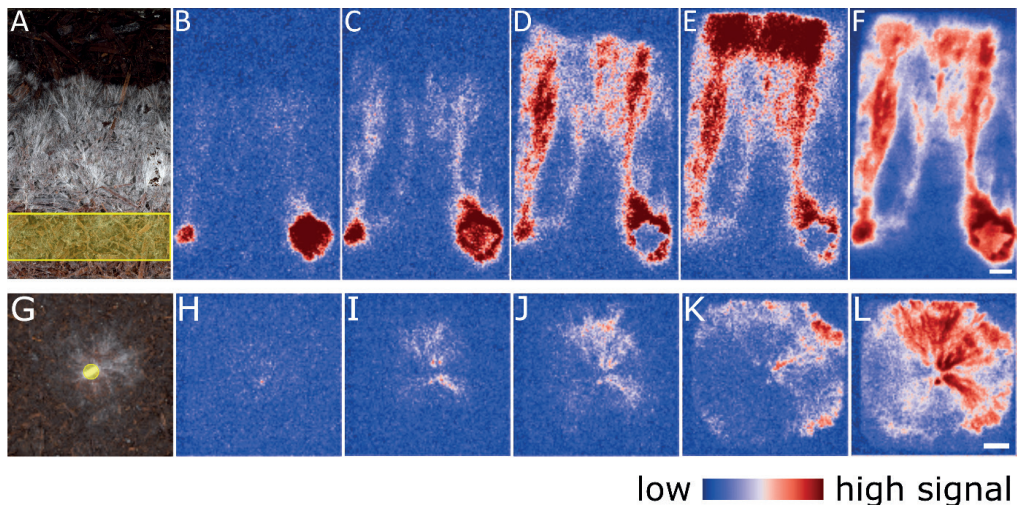


Figure 4. ^{14}C -AIB translocation during directional (A - F) and radial colonisation (G-L) of PII compost. (A, G) bright field images. Yellow regions represents labelling zones. Distribution of label after 9 or 3 h (B, H), 21 or 18 h (C, I), 42 or 36 h (D, J), and 72 h (E, K), with (F, L) representing time integration of the signal, respectively. Bars represent 1 or 2 cm (F, L), respectively.

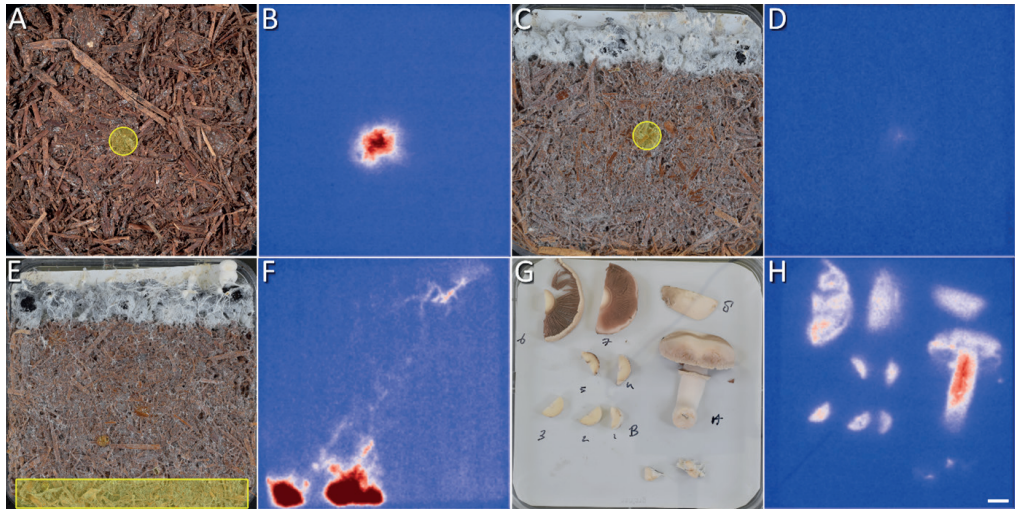


Figure 5. Translocation of ^{14}C -AIB in cultures reconnecting the mycelial network or producing mushrooms. Bright field images (A, C, E, G), yellow regions indicate labelling zones. PCSI time integrated signal images (B, D, F, H) for 132 h (B), 84 h (D), 96 h (F), and 72 h (H). When PIII compost had been broken and allowed to regenerate for 5 days (A), no clear translocation is present (B). ^{14}C -AIB was applied to PIII compost cultures with casing soil that had either developed only small resting pins (C) or an expanding mushroom (E). (D) No translocation was observed when only resting pins are present (D), while ^{14}C -AIB translocates diagonally from the compost, through the cords in the casing soil and towards the expanding mushroom (F). (G) Mushroom harvested from culture (E), showing accumulation of ^{14}C AIB (H). Bar represents 1 cm.

contrast, essentially no translocation was observed when label was added to cultures that had already been fully colonised (no growth; data not shown) or that consisted of PIII compost that had been manually broken to pieces and that had been allowed to reconnect for 5 days, effectively allowing a small amount of growth everywhere (Fig. 5B).

Maturing mushrooms pull ^{14}C -AIB from the compost

Mushroom expansion should generate a pull of water and nutrients from the substrate. To test this, Halbschalen cultures were used to assess transport in mushroom forming cultures (Fig. 5C). Halbschalen cultures were made by placing a layer of colonised compost (PIII) adjacent to a small layer of casing soil in square Petri dishes (similar to Fig. 1F). After colonisation of the casing layer and following formation of small pins (primordia), ^{14}C -AIB was added at the far side of the compost not in contact with the casing layer. When pins did not expand during the experiment, no translocation was observed through the hyphal cords in the casing layer supporting the pins (Fig. 5D). In contrast, translocation occurred through the compost to the hyphal cords in the casing layer (Fig. 5F, Movie S3, see online version) when pins developed into mushrooms (>10 mm diameter) (Fig. 5E; the mushroom is at the upper right corner of the dish). ^{14}C -AIB was detected by PCSI throughout the mushrooms after slicing these fruiting bodies (Fig. 5G and H). A translocation velocity of 5.6 mm h^{-1} was detected from the compost into the mushroom.

Directional growth promotes nutrient translocation to the mushrooms

We observed that directionally grown cultures (Fig. 1B) produced more and wider cords than non-directional growth (Fig. 1C), suggesting a better transport capacity. To test this, ^{14}C -AIB translocation to mushrooms was assessed in cultures with directional growth and non-directional growth (Fig. 1E and 1F, respectively). Mushrooms contained 5 fold more ($p = 0.027$, power = 0.89) ^{14}C -AIB g^{-1} in directionally growing cultures when compared to non-directionally grown cultures (347 ± 118 kdpm g^{-1} versus 70 ± 62 kdpm g^{-1} , mean \pm 95 % CI). We set out to test whether the enhanced transport observed for directional growth, would result in higher mushroom yield. Mushrooms were harvested from the same small-scale Halbschalen cultures (Fig. 1E and F), or from larger more industrially relevant setups in boxes (similar to Fig. 1E and F but now 3-dimensional). In Halbschalen cultures, directional growth gave 1.5 fold more yield than non-directional growth ($p = 0.027$, power = 0.9), whereas directional growth in boxes gave similar ($p = 0.63$, power = 0.06) or 1.3 fold lower ($p = 0.026$, power = 0.17) yields when compared to non-directional growth (PIII compost) and non-directional mixed growth (mix of PIII and PII compost at 1:4 ratio), respectively (Table 1).

Since directional growth provided better transport capacity for the mushrooms than non-directional growth, we hypothesised that directional growth might enable nutrient transport over a longer distance. To determine the maximum translocation distance for ^{14}C -AIB, gutters of 0.5 or 1 m were filled with compost and casing soil (Fig. 2). ^{14}C -AIB label was applied at one end of the gutter when >10 mm mushrooms had formed on the other end. Mushrooms were allowed to mature over 3 days. ^{14}C -AIB was detected in mushrooms harvested from 50 cm (Fig. 2A), but not 100 cm directional growth gutters (Fig. 2C), while no label was detected in mushrooms from non-directional growth (Fig. 2B and D). In the former case (Fig. 2A), the translocation speed was ≥ 6.9 mm h^{-1} .

^{14}C -AIB translocates to neighbouring colonies growing on casing soil

The standard industrial production of mushrooms uses phase III compost that requires the formation of an interconnected network to allow transport of resources from the vegetative mycelium to developing mushrooms. To test whether fusion and cord formation enabled colony wide translocation, *A. bisporus* was grown on compressed casing soil. The colony first produced a finely branched mycelium that eventually developed into hyphal cords with diameters ranging from 76 - 382 μm (186 ± 24 ; mean \pm 95 % CI). Cords were observed extending out from the rye spawn grain. These cords branched and occasionally formed loopy lateral cross-connections. The number of cords close to the inoculum was

Table 1. Mushroom yields for directional and non-directional (mixed) growth for three replicates.

Growth mode	Yield (mean g wet weight \pm 95 % CI*)	Culture type
Directional	82 \pm 5	Halbschalen
Non-directional (PIII compost)	50 \pm 7	Halbschalen
Directional	735 \pm 40	box
Non-directional (PIII compost)	766 \pm 106	box

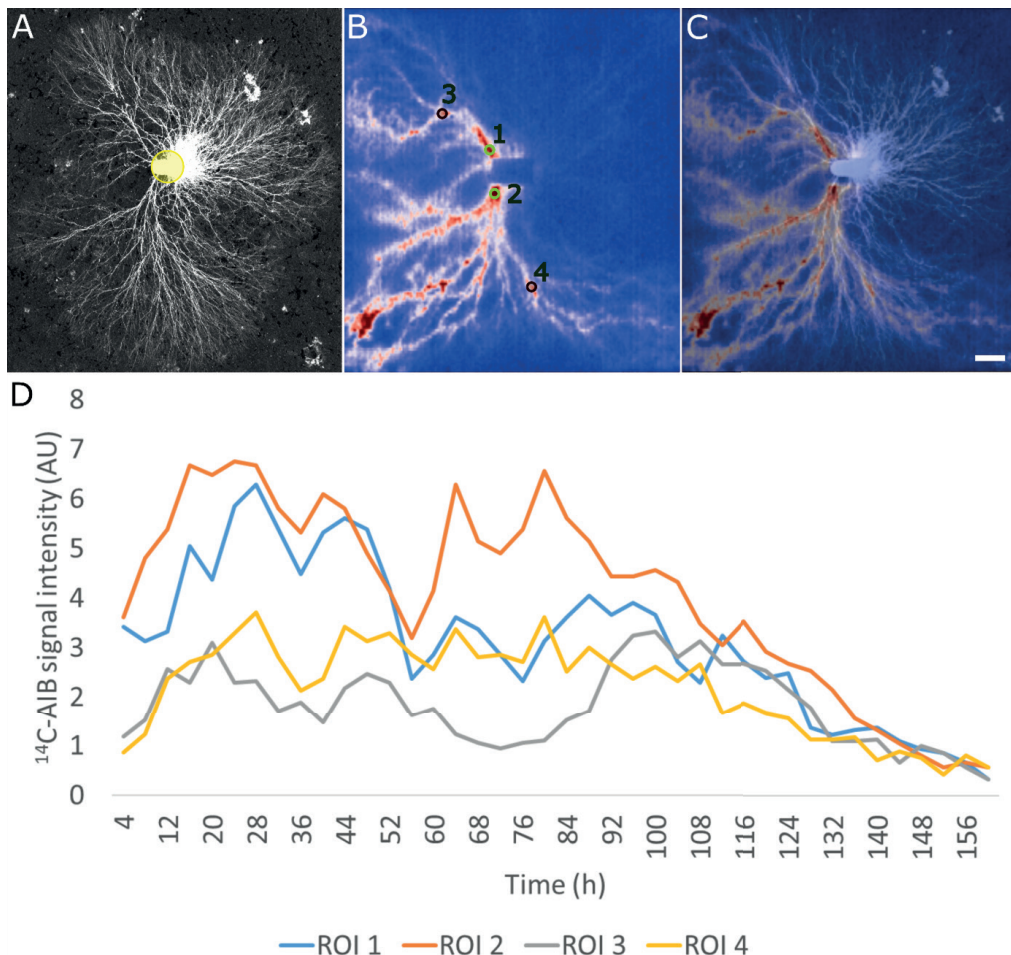


Figure 6. Translocation of ¹⁴C-AIB in a colony growing on casing soil. (A) bright field image with the ¹⁴C-AIB labelling zone indicated by a yellow circle. (B) PCSI 4 h interval time integrated signal over 156 h. (C) merge of (A) and (B). Bar represents 1 cm. (D) Time-lapse intensity profile of the ¹⁴C-AIB signal in regions of interest (ROI) drawn in panel (B). Accumulative signal over time was 126, 163, 73, 88 AU in the respective ROIs.

much smaller than the number of cords at the periphery of the colony (Fig. 6A), but the diameter of the former cords was 2x larger ($p = 0.00$, power = 1.00). This suggests that cords in older parts of the colony can fuse or that more hyphae fuse with existing cords over time. The thickest cords close to the inoculum translocated most of the ¹⁴C-AIB over time (Fig. 6, Movie S4, see online version); the label that had been applied to the rye grain in the centre of the colony moved outwards via these hyphal cords. The mean translocation velocity in cords on casing soil was $3.47 \pm 0.03 \text{ mm h}^{-1}$. Less translocation was observed in a cord connected to a relatively small mycelial zone when compared to a cord that was connected to a large mycelial zone (Fig. 6B and D).

We investigated whether neighbouring colonies could connect, thereby increasing

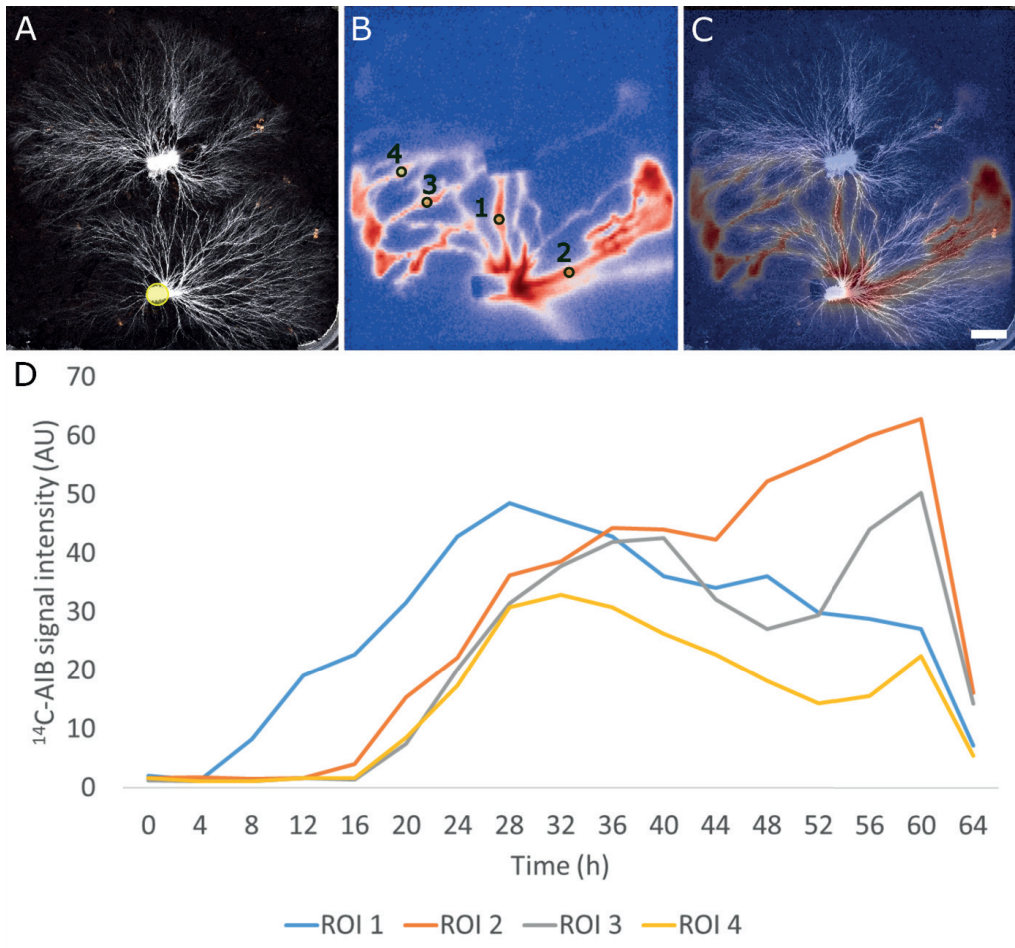


Figure 7. Translocation of ^{14}C -AIB within and between two colonies growing on casing soil. (A) Bright field image with the ^{14}C -AIB labelling zone indicated by a yellow circle. (B) PCSI 4 h interval time integrated signal over 65 h. Regions with high ^{14}C -AIB intensity can be observed at the colony periphery where mycelium cannot be seen. This is explained by the presence of fine branching hyphae that explore the substrate at the colony periphery and are thus hardly visible at the resolution of the image (A). (C) merge of (A) and (B). (C) Bar represents 1 cm. (D) Time-lapse intensity profile of the ^{14}C -AIB signal in regions of interest (ROI) drawn in panel (B). Accumulative signal over time was 460, 500, 385, and 252 AU in the respective ROIs.

the mycelial network from which the mushrooms could draw nutrients. When cords of neighbouring colonies met, they made functional transport connections through anastomosis as indicated by the translocation of ^{14}C -AIB between colonies through these connected cords (Fig. 7). When ^{14}C -AIB was added to the centre of one colony (Fig. 7B and D, Movie S5, see online version), and subsequently to the periphery in both colonies (Fig. 7B and D). When 3 colonies were grown in line and ^{14}C -AIB was added to the left one, it translocated both to the growth front, but also laterally to the neighbouring colony (Fig. 8B, Movie S6, see

online version). In the second colony a similar behaviour was observed, but higher levels of the tracer accumulated at the periphery (Fig. 8B). This colony also showed most growth of all three colonies (Fig. 8A). Eventually, the furthest right colony also received some ^{14}C -AIB (Fig. 8B and D). From the image analysis it was not clear whether the middle colony received label from the left colony via the lateral cord first or via periphery interactions or both at the same time (Fig. 8D).

Modelling flow in cords reveal why cords are translocation highways

We assessed the extent that cords provide enhanced transport capacity when compared to single hyphae due to their architecture. Cords in *A. bisporus* were found to have a diameter of $\sim 200\ \mu\text{m}$. EM imaging on *Agaricus carminescens* cords (Fig. 3A and B), which closely resemble those of *A. bisporus* (Mathew, 1961), shows that they are composed of thousands of individual hyphae (Cairney, 1990). Some of these hyphae, called vessel hyphae, have diameters of up to $14\ \mu\text{m}$. These hyphae usually have degraded septa and can thus be

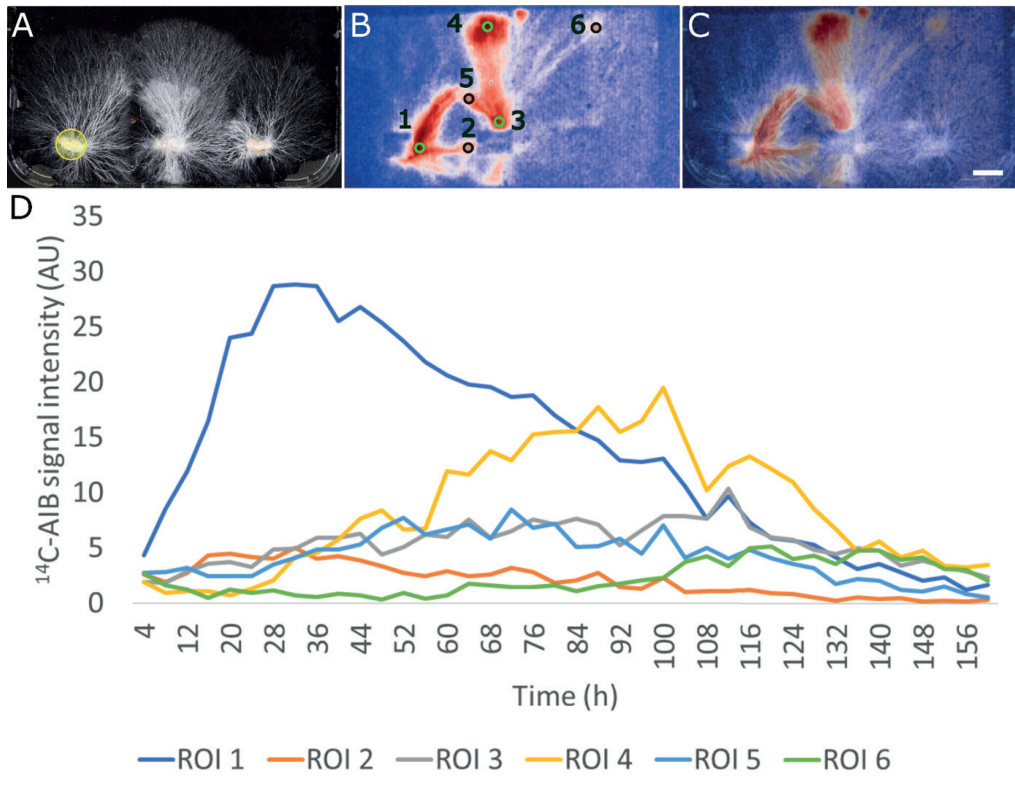


Figure 8. Translocation of ^{14}C -AIB translocation within and between three colonies growing on casing soil. (A) bright field image with the ^{14}C -AIB labelling zone indicated by a yellow circle. (B) PCSI 4 h interval time integrated signal over 160 h. (C) merge of (A) and (B). Bar represents 1 cm. (D) Time-lapse intensity profile of the ^{14}C -AIB signal in regions of interest (ROI) drawn in panel (B). Accumulative signal over time was 556, 85, 215, 337, 169, and 90 AU in the respective ROIs.

considered as pipes. Poiseuille's Law can be used to calculate the pressure difference over a certain length (Pa m^{-1}) in such a pipe, required to cause an observed translocation velocity (Brody et al. 1996; Nobel, 1991; see Material and Methods). We observed a translocation speed of 3.5 mm h^{-1} in cords on casing soil. In a typical $12 \text{ }\mu\text{m}$ wide vessel hypha, within such a cord, this would only require a pressure difference of 2 Pa cm^{-1} ($2\text{E-}5 \text{ bar cm}^{-1}$). For simplicity, we assumed that cytoplasm has a similar viscosity as water, that viscosity and hyphal diameter is constant throughout the network, and that hyphae do not branch or fuse. It is important to state that these assumptions may impact the modelled values.

To get an idea about the magnitude of this flow, we performed image analysis on Cairney's electron microscopy images (Cairney, 1990; see Fig. 3A and B) and segmented the cross section of each individual hypha in part of the cord. Using Poiseuille's Law for laminar flow of fluids in pipes, we calculated the volume flow rate (Q). A typical cord has a total volume flow rate of $1.22\text{E-}5 \text{ ml h}^{-1}$ (see Fig. 3A - C). The increase in volume for an individual hypha growing ($217 \text{ }\mu\text{m h}^{-1}$) in the periphery of the colony with diameter of $3 \text{ }\mu\text{m}$ is $1534 \text{ }\mu\text{m}^3 \text{ h}^{-1}$ ($\pi \cdot r^2 \cdot h = \pi \cdot 1.5^2 \text{ }\mu\text{m} \cdot 217 \text{ }\mu\text{m h}^{-1}$) = $1.53\text{E-}9 \text{ ml h}^{-1}$. Thus, a single cord with a length of 5 cm and $200 \text{ }\mu\text{m}$ in diameter, could theoretically support the growth of 7920 hyphae ($1.22\text{E-}5 \text{ ml h}^{-1} / 1.53\text{E-}9 \text{ ml h}^{-1}$). Now, if we compare this to a cord that would be composed of only thin hyphae of $\text{Ø } 3 \text{ }\mu\text{m}$ (Fig. 3D; cross section cord = $\pi \cdot r^2 = \pi \cdot 0.01^2 = 3.14\text{E-}4 \text{ cm}^2$; cross section hyphae = $\pi \cdot 1.5\text{E-}4^2 = 7.07\text{E-}8 \text{ cm}^2$; thus the cord consists of 4444 thin hyphae = $3.14\text{E-}4 / 7.07\text{E-}8$), a total volume flow rate of the cord of $7.15\text{E-}6 \text{ ml h}^{-1}$ is obtained ($4444 \cdot 1.61\text{E-}9 \text{ ml h}^{-1}$ ($Q_{\text{single hypha}}$)). This could only sustain the growth of 4660 hyphae ($7.15\text{E-}6 \text{ ml h}^{-1} / 1.53\text{E-}9 \text{ ml h}^{-1}$). On the other hand, if a cord would be exclusively composed of 278 ($3.14\text{E-}4 / (\pi \cdot 0.0006^2) \text{ cm}^2$) $\text{Ø } 12 \text{ }\mu\text{m}$ vessel hyphae (Fig. 3E), a pressure difference of 2 Pa cm^{-1} would generate a volume flow rate of $1.14\text{E-}4 \text{ ml h}^{-1}$ ($278 \cdot 4.12\text{E-}7 \text{ ml h}^{-1}$ ($Q_{\text{single hypha}}$)). This would be able to support growth of $74,600$ hyphae ($1.14\text{E-}4 \text{ ml h}^{-1} / 1.53\text{E-}9 \text{ ml h}^{-1}$) and is a factor of ~ 9 more than that of a typical cord.

Mushroom formation may be limited by network capacity

We investigated whether mushroom production could be limited by the supporting network architecture using the following calculation. The water content of a typical 30 g mushroom 3 days after initiation of swelling is about 27 ml . If all the water would be taken up at the inoculum and translocated over 50 cm to the mushroom with a pressure difference of 2 Pa cm^{-1} , this would require a volume flow rate of $1.21\text{E-}5 \text{ ml h}^{-1}$ in a single cord (Poiseuille's Law), and requires $30,865$ ($27 \text{ ml} / 1.21\text{E-}5 \text{ ml h}^{-1} / 72 \text{ h}$) typical $200 \text{ }\mu\text{m}$ wide cords transporting water to the mushroom over a 72 h period. This number of cords would occupy a surface area of ($\pi \cdot 1\text{E-}2^2 \text{ cm} \cdot 30,865 \text{ cords}$) 9.7 cm^2 , which is feasible within the 36 cm^2 cross section area in a gutter (see Fig. 2). This would also limit the maximum number of expanding mushrooms to 4 ($36 / 9.7 \text{ cm}^2$) in such a culture, but this ignores any spacing between cords or water evaporation by the mushrooms. If we allow spacing between the cords, then less cords would be present in the culture, thus less water transport capacity would be available to supply the mushrooms. If mushrooms evaporate water, even a higher volume of water transport would be needed than just the water content of the mushrooms to replenish the evaporated water as well. Thus, in both cases the number of mushrooms that could be supplied with water would be lower. Equally, we

have rarely seen more than 2 expanding mushrooms per culture, which matches these predictions.

Discussion

Tip directed ^{14}C -AIB translocation was only observed when vegetative cultures of *A. bisporus* were actively growing. This has also been reported for ^{14}C -glucose in *Morchella esculenta* (Amir et al. 1994), for ^{14}C -AIB in *Phanerochaete velutina* (Tlalka et al. 2002, 2003), and in *S. lacrymans* (Tlalka et al. 2008a). Translocation velocities of 3.68 ± 0.31 and 3.47 ± 0.03 mm h^{-1} were observed in radially grown mycelium on compost, and cords of radially grown mycelium on casing, respectively. These rates compare with the velocity of 3.7 ± 0.4 mm h^{-1} in radially grown *Phanerochaete velutina* colonies (Tlalka et al. 2008b). ^{14}C -AIB was translocated to the growing periphery at a faster rate of 6.55 ± 1.38 mm h^{-1} in directionally growing mycelium (Fig. 1D). The fact that translocation velocity in directionally grown cultures was almost two fold higher than in the other cultures may be related to the higher level of cord formation and cords having larger diameters than in the other conditions (Fig. 1A). ^{14}C -AIB was translocated to the mushrooms with 5.6 mm h^{-1} . The maximum detectable translocation distance of ^{14}C -AIB was between 50-99 cm in directional (Fig. 2A and C) and 22 - 49 cm in non-directional growth (Fig. 1F; Fig. 2B and D). Mushrooms developed on directionally grown cultures (Fig. 1E) contained 5 fold higher levels of ^{14}C -AIB than mushrooms from non-directionally grown cultures (Fig. 1F). Together, this indicates that directional growth promotes higher transport capacity over longer distances, likely due to the presence of cords as suggested by modelling (see below).

Oscillations of ^{14}C -AIB translocation have been reported in *P. velutina* and *Coniophora puteana* (Fricker et al. 2007). We also observed temporal changes in scintillation count in *A. bisporus*, which appeared to be pulsatile with fluctuations over 30 - 60 h (Fig. 6D, Fig. 7D and Movie S4, see online version). However, we were not able to determine the period accurately in these relatively short time courses. Translocation was not observed after colonies had fully colonised the substrate or during regeneration of the mechanically disrupted mycelial network of PIII compost. This is in line with mathematical modelling where the extent of nutrient flow through the mycelial network was related to the amount of growth at the periphery of the colony (Heaton et al. 2010). In the case of network regeneration in PIII compost, growth occurs everywhere to enable anastomosis and reconnection, so the vectors of growth would all add up to result in a flow of zero. Together, our data indicate that long-distance translocation only occurs when there is a distinct sink, such as occurs during directional growth.

Cords in *A. bisporus* were found to have a diameter of ~ 200 μm . We observed a translocation speed of 3.5 mm h^{-1} in cords. In a typical 12 μm wide vessel hypha, within such a cord, this would only require a pressure difference of 2 Pa cm^{-1} ($2\text{E-}5$ bar cm^{-1}). This is much lower than the estimated pressure difference of 100 Pa cm^{-1} in *Neurospora crassa* hyphae of similar diameter (Lew, 2005). Since *N. crassa* hyphae do not form cords, this points to cord function. Only a fraction of the pressure difference would be needed to drive the same volume flow rate in cords in *A. bisporus* compared to single hyphae in *N. crassa*. This follows from the fact that the pressure difference in parallel pipes is equal, but the sum of the flow in the individual pipes is the total volume flow rate (Engineering ToolBox, 2011). So, at a relatively lower differential cost of ion uptake or osmolyte

accumulation, cords would be able to create a hydrostatic pressure via osmotic uptake of water and drive substantial flows to sinks located elsewhere.

We found that a typical single cord (Fig. 3C), with a length of 5 cm and 200 μm in diameter, could theoretically support the growth of ~ 8000 hyphae. If we compare this to a cord that would be composed of only thin hyphae of $\text{\O} 3 \mu\text{m}$ (Fig. 3D), this could only sustain growth of ~ 5000 hyphae, thus the presence of wide vessel hyphae is key to a cord's transport capabilities. This is further exemplified by plotting volume flow rate versus hyphal length and comparing different hyphal diameters (Fig. 9). Since this generates a hyperbola, the length of a hypha is thus far less important than its diameter for determining its volume flow rate. After only a few microns of length the asymptote is already approached, thus hyphal length has a negligible effect on translocation over distances of millimeters to centimeters. On the other hand, if a cord were composed of only vessel hyphae (Fig. 3E), this would be able to support growth of 74,600 hyphae and is a factor of ~ 9 more than that of a typical cord.

^{14}C -AIB was translocated through the compost and casing layer to the developing mushrooms (Fig. 5F), but not to their earlier initials (Fig. 5D), the resting primordia (or 'pins') that did not expand. Mushrooms contain up to 50 % (dry weight) mannitol (Hammond and Nichols, 1979; Rast, 1965), but only low levels of trehalose and glucose. In contrast, the vegetative mycelium contains trehalose (16 %), mannitol (5 %), glucose (2 %) and sucrose (3 %) at the stage of casing the substrate (Hammond and Nichols, 1976a). High mannitol levels have also been observed in mushrooms of *Lentinula edodes*, *Boletus* sp. and *Cantharellus cibarius* (Kalač, 2016; Tan and Moore, 1994;). Thus, it may be that mannitol is the main osmolyte driving water translocation to mushrooms. Indeed, mannitol levels were positively correlated with yield, but for trehalose and glycogen the reverse was true (Hammond and Nichols, 1979).

Mushrooms evaporate water and even do so better than plants or human built solar

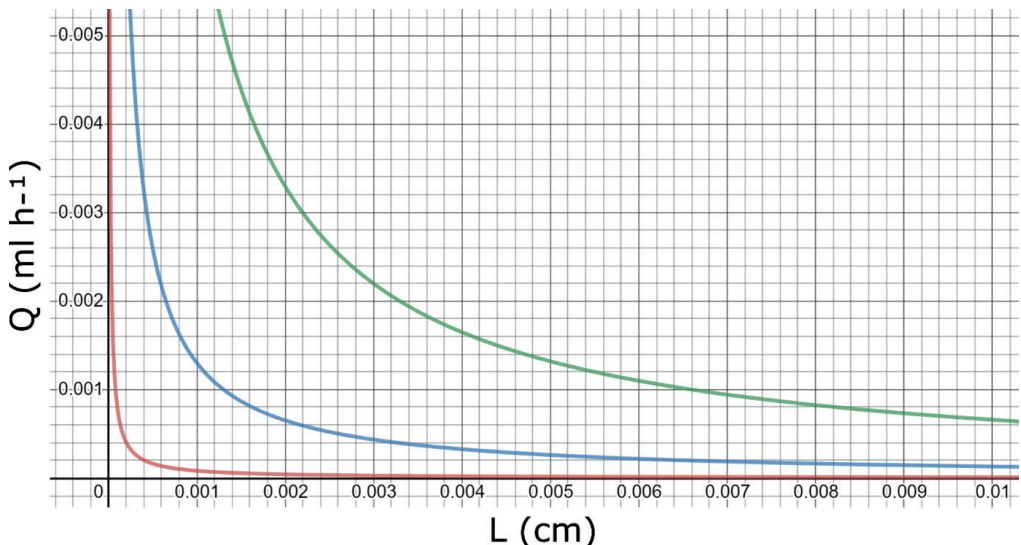


Figure 9. The influence of hyphal length L and diameter on volume flow rate Q , taking a pressure difference of 2 Pa and diameters of 4 (red), 8 (blue), and 12 μm (green line) according to Poiseuille's Law.

steam generators (Dressaire et al. 2016; Husher et al. 1999; Xu et al. 2017). Although this goes at the expense of expansion of the mushroom, it creates a flow of water from the mycelium. This is due to the under pressure that evaporation generates and will concentrate the already present osmolytes. This is analogous with evaporation through leaves driving translocation of nutrients through xylem in plants (Siebrecht et al. 2003). This flow of water also carries new solutes to the mushrooms thereby potentially creating a positive feedback loop by building up an osmotic potential, particularly during the day when evaporation is high. This in turn could explain the quick expansion of mushrooms due to their rapid swelling and may explain why they often appear overnight, when evaporation is lower.

Together, this indicates that mushroom expansion may involve the interplay of at least five components: (i) The mycelial network should provide sufficient transport potential; (ii) the mushrooms should exploit this by maximally pulling water via osmosis, by efficiently converting trehalose and glycogen to mannitol; (iii) resources should be optimally allocated to the former two; (iv) water should be readily available in the substrate; and (v) a diurnal cycle of evapotranspiration that establishes an osmotic ratchet by drawing osmolytes into the mushroom during the day by transpiration, but with no expansion, followed by swelling at night. We found contrasting results when comparing yields in Halbschalen and box cultures for directional and non-directional (mixed) growth (Table 1). Box cultures evaporated relatively much more water than Halbschalen cultures did (data not shown), most likely since the latter were closed until fruiting. The fact that the improved network architecture (many wide cords) in directional growth did not give higher yield in box cultures, was thus likely due to suboptimal water availability in the compost and / or casing soil, since more water would have been evaporated than in the non-directional growth cultures, due to a longer incubation time. Faster mushroom development may be obtained in the future if water availability and / or mannitol production rate could be augmented, network architecture can be optimised, or evaporation could be controlled.

Acknowledgements

This research was funded by NWO TTW grant ‘Traffic control’ [15493] and by a Microbiology Society research visit grant [GA000981].

4

Water requirements of *Agaricus bisporus* during growth and fructification

Koen C. Herman, Han A.B. Wösten, Robert-Jan Bleichrodt

Abstract

Agaricus bisporus is grown commercially on compost topped with a peat-based casing layer. Water is transported from the compost and the casing to enable formation of white button mushrooms by this species. Here, water transport from the casing and different parts of the compost into mushrooms was studied and linked to their water potential, osmotic potential, and matric potential. Water in the mushrooms mainly originated from the casing and to a lesser extent from the top and intermediate layers of the compost. Based on these results, alternative casing regimes were tested to increase mushroom production. This resulted in an increase in total yield up to 1.4 fold when a fresh layer of casing was added on top of the old casing or when the casing was replaced after harvesting the second flush. Data indicate that the difference in water potential can drive water transport from the casing to the first flush, but not the second flush of mushrooms. The water potential in the compost indicates that water cannot be translocated to the mushrooms at all. Therefore, other components of the water potential should drive this water flow. We hypothesize that this component is the turgor of the mycelium.

Introduction

Agaricus bisporus is commercially cultivated in the Netherlands on a composted mixture of horse manure (either or not supplemented with chicken manure), wheat straw, and gypsum, which has a water content of 65 - 67 %. Compost colonized by *A. bisporus* is transported to the grower, where it is applied as a 20 cm thick layer and topped with a 5 cm thick peat-based casing layer with a water content of 80 %. After colonisation of the casing layer, mushroom formation is induced by lowering the air temperature from 22 °C to 18 °C and by lowering CO₂ levels by ventilation. Mushrooms appear in at least two flushes at weekly intervals.

Water is transported from the compost and casing during development of mushrooms, which consist of >90 % water. Water in the substrate is commonly replenished during cultivation as this increases the yield (Flegg, 1974; Kalberer, 1990a). Watering is done at regular intervals starting directly after the application of the casing soil. Delaying the start of watering increases colonization of the casing with dense mycelium but decreases mushroom yield (Flegg, 1975). At a certain moment, watering is no longer effective because colonization of the compost and casing by *A. bisporus* is accompanied by increased hydrophobicity of the substrate. This is likely due to self-assembly of hydrophobins (Lugones et al., 1998) into amphipathic membranes that expose their hydrophobic side towards the air within air voids in the substrate (Wösten, 2001). As a result, the colonized compost and casing layers barely absorb added water (Amsing, 1990). This raises the question whether water is limiting during mushroom production. Although more than half of the water originally present at casing is still present in spent compost (Gerrits, 1994), it is unclear whether this water is available for uptake by the mycelium.

Movement of water depends on the water potential (Ψ), which is a measure of pressure (Pa). Water flows from high to low Ψ , if unobstructed. Ψ of pure water is zero; therefore, Ψ in a biological system is usually negative. Ψ consists of several components, including, but not limited to, the osmotic potential (Ψ_{osm}), matric potential (Ψ_{mat}), and pressure potential (Ψ_{π}) (For a more in-depth explanation see Herman and Bleichrodt, 2021; **Chapter**

1). Commonly, only Ψ and Ψ_{osm} are measured, while Ψ_{mat} or Ψ_{π} are calculated from the difference between both terms. This can be done by logically excluding the influence of other components. For example, Ψ_{π} (in this case the atmospheric pressure) can be assumed to be the same between different areas in soil. Therefore, the difference between Ψ and Ψ_{osm} would (mostly) be explained by Ψ_{mat} .

Fungi take up water via osmosis by creating a lower Ψ_{osm} than their environment (Lew, 2011). This is done by synthesizing low molecular weight compatible solutes from larger storage polysaccharides or by adjusting ion homeostasis (Lew et al., 2006). Mannitol and trehalose act as the main compatible solutes in *A. bisporus*. Their levels are as high as 14 and 38 mM in the mycelium and 302 and 18 mM in developing mushrooms, respectively. Fructose, glucose, and sucrose have also been detected but are only present in low concentrations (Hammond and Nichols, 1976a; Wannet et al., 2000). Uptake of water from the environment increases the intracellular Ψ_{π} , i.e. turgor, which can drive passive transport of intracellular water and nutrients within the mycelium. However, this only occurs if water moves into a new area by exudation, evaporation, or growth at the hyphal tips (Heaton et al., 2010).

Water content and Ψ of the compost and casing change over time during mushroom cultivation. The compost initially provides more water to the developing mushrooms than the 5 cm casing soil. However, mushrooms will take up gradually more water from the casing during development (Kalberer, 1983). Applying a thinner casing layer (3 cm) reduces the mushroom yield and relatively more water will be taken up from the compost than the casing (Kalberer, 1985). The water content in the compost decreases with each successive flush, with the top layer decreasing the most and the bottom layer decreasing the least (Kalberer, 1985).

Ψ_{osm} (although reported as Ψ) of the casing soil was -0.07 MPa at casing and -0.26 MPa after the 2nd flush when the cultures were watered in between the flushes (Kalberer, 1987). Ψ_{osm} of the top and middle layers of the compost decreased more, i.e. from -1.08 to -1.35 MPa and -1.08 to -1.47 MPa, respectively (Kalberer, 1987). These measurements were later repeated at a commercial mushroom farm, also including Ψ (Kalberer, 2006). Here it was shown that the middle layer had a significantly lower Ψ and Ψ_{osm} compared to the top and bottom layer. The Ψ and Ψ_{osm} were reported to decrease from -1.71 MPa and -1.62 MPa before the 1st flush to -2.30 MPa and -2.02 MPa after the 2nd flush, respectively. Again, the bottom layer decreased the least in water content, Ψ and Ψ_{osm} . Ψ_{mat} was calculated to be maximally -0.3 MPa, which indicates that the Ψ_{osm} is the primary component of Ψ in the substrate during cultivation (Kalberer, 2006). Unfortunately, data on the casing soil were not included and the watering regime was not described. Ψ_{osm} of fruiting bodies is in the range of -0.74 to -1.35 MPa. By assuming $\Psi_{\text{mat}} = 0$, the turgor within the mushrooms was determined to be 0.3 to 0.5 MPa (Kalberer, 2006). Whether mushrooms indeed do not have a Ψ_{mat} is not known.

In contrast to previous studies, we here systematically assessed water transport from the casing and different parts of the compost into mushrooms as well as Ψ and Ψ_{osm} in compost, casing, and mushrooms. To this end, we did not water the compost and casing during the flushes to exclude the effects of external water on cultivation of *A. bisporus*. Data show that the casing, and to a lesser extent the top and intermediate layers of the compost, mainly supply water to the mushrooms. Based on the results of this study and previous findings, we propose how water flows into first and second flush mushrooms and

tested alternative casing regimes to increase mushroom production. This resulted in an increase in total yield up to 1.4 fold when a fresh layer of casing was added on top of the old casing or when the casing was replaced after harvesting the second flush.

Material & Methods

Strains and culture conditions

Boxes (17 x 27 x 21,5 cm) were filled with 2.5 kg PIII compost (CNC Grondstoffen, Milsbeek, the Netherlands) (i.e. PII compost colonized with *A. bisporus* strain A15; Sylvan, Netherlands), overlaid with 1 kg casing soil (CNC Grondstoffen, Milsbeek, the Netherlands) and incubated at 22 °C at a relative humidity of 85 %. Cultures with colonized casing were transferred to 18 °C at a relative humidity of 90 % to induce mushroom formation. Experiments were performed using biological triplicates.

Alternative growth conditions

Mushrooms were grown as described above but with modifications. First, the old casing layer was replaced by a new layer of 1 kg casing soil after harvesting the second flush of mushrooms or a new layer of 1 kg casing soil was placed on top of the old casing soil. Alternatively, an extra layer of 1 kg casing soil was placed underneath the 2.5 kg PIII compost and the 1 kg casing soil from the start of the culture. Finally, cultures were directionally grown by filling boxes with 500 g of PIII compost as inoculum, topped with 2 kg PII compost and 1 kg casing soil. As a result of the modifications, clear distinctions between flushes were not always apparent. Mushrooms were therefore continuously harvested when they had a diameter of 40 – 60 mm until no more mushrooms appeared.

Water- and osmotic potential & water content measurements

Water content, Ψ and Ψ_{osm} of compost, casing layer, and 1st and 2nd flush fruiting bodies were determined during the cropping process of *A. bisporus*. To this end, the 2.5 kg PIII compost was divided in a top, middle, and bottom layer of equal volume with fiberglass meshes (1.5 x 2 mm mesh size). Samples were destructively taken at inoculation (0 d), venting (11 d), pinning (18 d), 1st flush (22 d), and 2nd flush (32 d). Fruiting bodies, casing and compost layers were sampled in triplicate to determine the water content (using 2 g samples), Ψ (using 2 g samples) and Ψ_{osm} (70 g samples). Ψ (MPa) was measured with a potentiometer (WP4-T, Decagon Devices, Pullman WA, USA). Water content (%) of samples was determined by weighing samples before and after drying for three days at 60 °C. Except at venting, all layers were weighed separately. Ψ_{osm} was determined by hydraulic pressing (120 - 150 kN) the samples to obtain residual water. Osmolality of the residual water was measured with an osmometer (Vaprotm 5520, Wescor, Logan UT, USA), after which Ψ_{osm} (MPa) was calculated from: $\Psi_{\text{osm}} = -\text{Osmolality} * \rho_{\text{water}} * R * T$, where the osmolality is expressed as milliosmoles kg⁻¹, ρ_{water} is the density of water at 22 °C (0.997 g cm⁻³), R is the ideal gas constant (8.314 10⁻³ L MPa K⁻¹ mol⁻¹), and T is the temperature in Kelvin (295.15 K).

Pressure generated by white button mushrooms

The force exerted by the mushrooms and their surface area were determined to calculate the pressure generated by these fruiting bodies. To this end, a custom frame was built

(34.9 x 24.9 cm) onto which a glass plate (29.5 x 19.5 cm) was fixed to an adjustable height (see Fig. 3). A custom scale was created by connecting a load cell (maximum load 5 kg) to a HX711 amplifier connected to a Wemos D1 Mini ESP8266. The weight data were pushed every 10 sec to a Blynk server via WiFi, where data could be monitored in real-time and downloaded. The load cell was inserted into a kitchen scale. During the experiment a timelapse camera (TLC200 Pro, Brinno, Taipei, Taiwan) was mounted above the glass plate to determine the area of contact of the mushrooms with the glass plate. This area was determined by using ImageJ (Schindelin et al., 2012). Boxes were filled completely (containing 3.0 kg PIII and 1.1 kg casing soil) ensuring that the mushrooms would make contact with the glass plate directly after their emergence.

Statistics

Statistical analysis was done using R (version 4.2.0). The effect of each stage of the cultivation process on the amount of water, Ψ and Ψ_{osm} of the casing was analysed using a one-way ANOVA with a Tukey HSD post-hoc test. A two-way ANOVA with subsequent Tukey HSD post-hoc test was used to test for differences between the top, middle, and bottom compost layers of each cultivation stage.

Results

Casing soil and the upper part of the compost are the main suppliers of water for mushrooms

Water content, Ψ and Ψ_{osm} of the casing layer and the bottom, intermediate and top layers of the compost were determined throughout the cropping process. During the whole process 1.07 kg of water (i.e. 52.5 %) was lost from the culture (Fig. 1A), of which 443 g between inoculation and pinning. Most of this 443 g originated from the casing layer (65 %), probably due to evaporation. An amount of 420 g was lost from the culture between pinning and the 1st flush, which equals the amount of 430 g of water found in the mushrooms of the 1st flush (Fig. 1B). Again, most of the water originated from the casing (48 %) with each following compost layer below contributing less. A total of 206 g was lost between the 1st flush and the 2nd flush, of which half was found back in the mushrooms of the 2nd flush. Although not significant, most water (i.e. 45.5 %) was lost from the casing ($p = 0.253$), while again the least amount (i.e. 16.5 %) was lost from the bottom layer ($p < 0.01$) of the compost. A significant interaction was found between the compost layers and the cropping stages ($p < 0.001$), which indicates that *A. bisporus* uses different amounts of water from each of the three compost layers. Indeed, the amount of water in the bottom layer (400 g) differed significantly ($p < 0.01$) compared to the top (289 g) and middle (317 g) layers after the 2nd flush.

In parallel, Ψ of the casing and the top, intermediate and bottom layers of the compost was determined (Fig. 2A). Ψ of the casing layer decreased the most (1.69 MPa) during the cropping process ($p < 0.01$), while that of the bottom layer of the compost decreased the least (0.42 MPa) (Fig. 2A). Again, a significant interaction was found between the Ψ of the layers of compost and the cropping stages ($p < 0.01$). Ψ of the bottom layer (-2.36 MPa) differed already significantly from the top (-2.94 MPa) and middle (-2.86 MPa) layers after the 1st flush ($p < 0.01$). No further effect on Ψ was observed in each of the compost layers between the 1st flush and 2nd flush ($p = 0.7$). This implies that the water in the bottom layer

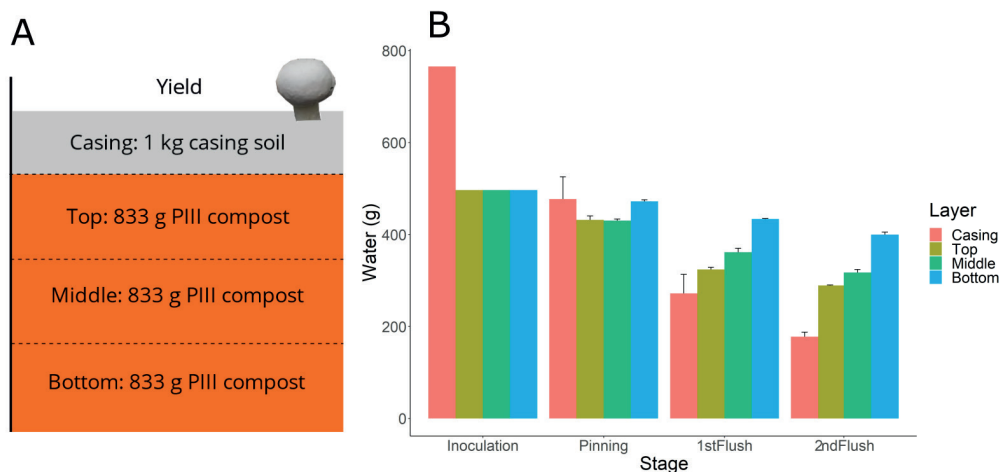


Figure 1. Culture setup (A) and amount of water in the casing and the top, intermediate and bottom layers of the compost at inoculation, venting, pinning, 1st flush, and 2nd flush (B). Yield of the first and second flush was 472.1 and 116.4 g, respectively. Error bars represent the standard error of the mean.

of spent substrate is the most accessible. However, it is used the least. Together, results show that casing together with the top and middle compost layers are the most important source of water for the fruiting bodies, whilst the bottom layer of the compost is the least important.

Within the same experiment, Ψ_{osm} was determined by measuring the osmolality of the residual water of the casing and the top, intermediate and bottom layers of the compost as well as that of the fruiting bodies. Data indicate that the 2nd flush fruiting bodies have a lower Ψ_{osm} than the 1st flush fruiting bodies. This effect is significant ($p < 0.05$, two-sample t test), but not after correcting for multiple comparisons. Ψ_{osm} almost fully explained Ψ of the casing and the three compost layers at inoculation and venting (Fig. 2B). The impact of Ψ_{osm} became increasingly reduced at successive time points. Most notably, Ψ_{osm} of the casing only explained 51 % and 31 % of Ψ during the 1st and 2nd flush, respectively (Fig. 2B). This likely has to do with increasing matrix potentials. A significant interaction was found between the Ψ_{osm} of the layers of compost and the stages of the cropping process ($p < 0.01$). Interestingly, Ψ_{osm} of the middle layer was lower when compared to both the top and bottom layer ($p < 0.01$), whilst the latter two did not differ from each other ($p = 0.07$). A lower Ψ_{osm} shows that more solutes are present. It is currently not known which solutes cause the lowered Ψ_{osm} in the middle layer.

The Ψ_{mat} was calculated as the difference between Ψ and Ψ_{osm} . Ψ_{mat} was a small component of the Ψ of compost and casing until venting, i.e. 0 MPa and -0.08 MPa respectively. However, Ψ_{mat} of the casing dropped significantly to -1.05 MPa from venting until after the 2nd flush ($p < 0.05$). No interaction was found between the stage of the cropping process and the compost layers ($p = 0.1$). Ψ_{mat} did decrease during subsequent stages in all compost layers but was never more negative than -0.5 MPa that was found after the 2nd flush in the top layer. Together, data indicate that Ψ_{osm} of the compost and casing layer determines the water potential in the beginning of cultivation, whilst the matric potential becomes increasingly important in later stages, most notably in the casing

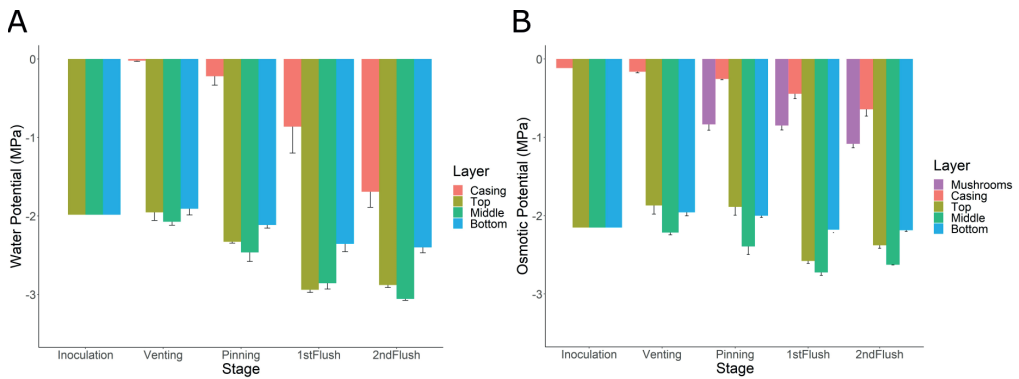


Figure 2. Water potential (A) and osmotic potential (B) of the casing and the top, intermediate and bottom layers of the compost at inoculation, venting, pinning, 1st flush, and 2nd flush (A, B), as well as the osmotic potential of the fruiting bodies (B). Error bars represent the standard error of the mean.

soil.

For water to flow into the mushrooms, Ψ of the fruiting bodies must be lower than that of the substrate. Assuming $\Psi_{\text{mat}} = 0$, Ψ would be $\Psi_{\text{osm}} + \Psi_{\pi}$, where values of Ψ_{π} are in the range of 0.3 to 0.5 MPa (Beecher et al., 2001; Kalberer, 2006). Ψ_{osm} of the first flush (-0.85 MPa) equalled the Ψ of the casing (-0.86 MPa) (Fig. 2). In contrast, Ψ_{osm} of the second flush was higher (-1.08 MPa) than that of Ψ of the casing and the compost layers (-1.69 MPa and -2.40 respectively), suggesting that fruiting bodies are not able to extract water from the casing after the 1st flush. This is however not the case as a 2nd flush did appear and water was still lost from this layer. This implies that other forces play a role such as the turgor pressure within the mycelium, or the Ψ_{mat} of the mushrooms.

Mushrooms generate a pressure of at least 31 kPa

Water can only be translocated by generating a pressure difference in a certain direction. This pressure difference can be estimated by creating a force in the opposite direction until the net movement of water is zero. Using this principle, the force generated by developing mushrooms was determined by measuring the weight increase of the box culture (3 kg PIII compost and 1.1 kg casing layer), resulting from the pressure exerted by the mushrooms on a fixed glass plate (Fig. 3). A time lapse camera monitored the surface area of mushrooms making contact with the glass plate (Fig. 3). The pressure generated by the mushrooms was calculated by dividing the force with the surface area. Developing mushrooms increased the weight linearly ($R^2 = 0.91$) with 129 g h^{-1} to a maximum additional weight of 2.49 kg (Fig. 4A). At this point three mushrooms had made contact with the glass surface with a combined surface area of 7.91 cm^2 (Fig. 4B), resulting in a pressure of 31 kPa exerted by the mushrooms. These data indicate that either the difference in Ψ between the casing layer and the developing fruiting bodies, or the difference in Ψ_{π} between the mushrooms and the mycelium is at least 31 kPa.

Redesigning culture conditions of the white button mushroom

Since the casing is a main supplier of water for the mushrooms, either the old casing layer was replaced with a new layer of casing or a new casing layer was added on top of the

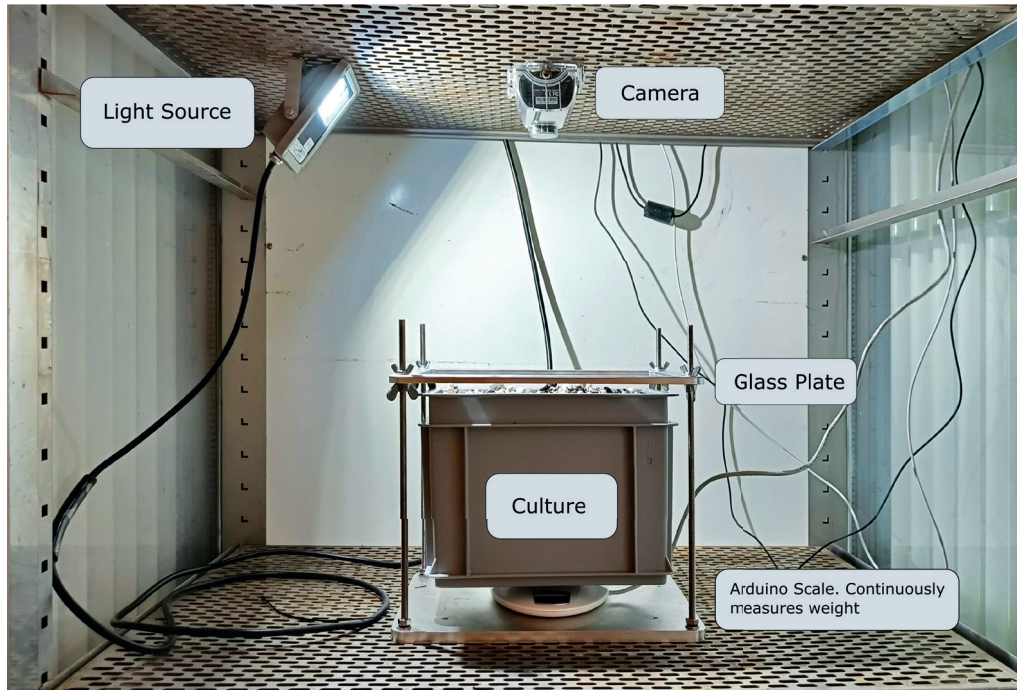


Figure 3. Experimental setup to measure the pressure exerted by fruiting bodies of *A. bisporus*. The glass plate fixed above the culture obstructed the elongation of the fruiting bodies, thereby the force generated by the mushrooms results in an apparent weight increase of the culture box. Weight increase is monitored by a custom datalogger scale.

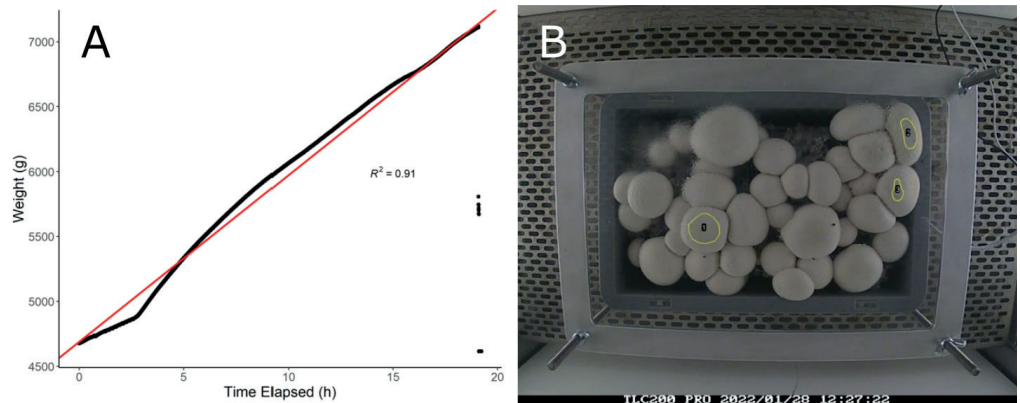


Figure 4. (A) Increase in weight (g) over time (h) during development of fruiting bodies. The moment the first fruiting body made contact with the glass plate was taken as $t = 0$. The red line indicates the fitted linear model ($R^2 = 0.91$). (B) Top view of the developing fruiting bodies. Yellow outlines show the contact area of the mushrooms with the glass plate at $t = 19$ h.

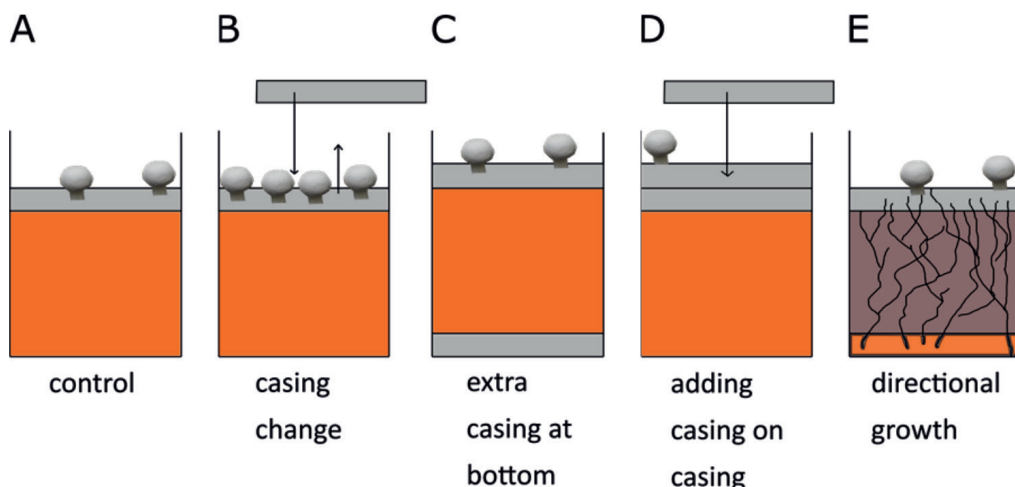


Figure 5. Different designs to grow white button mushrooms. Control condition with 2.5 kg of PIII compost (orange) and 1 kg casing layer (gray) (A). After harvesting two flushes of mushrooms, the old casing was removed and a new casing layer was placed on the compost (B) or a new layer of casing was placed on the old casing (D). Alternatively, a casing layer was placed beneath the compost from the start of the experiment (C). Also, PII compost (2.5 kg brown) was directionally colonised from a small layer of PIII compost at the bottom of the culture. Note that experiments B, D and E took longer to complete than A and C.

old casing layer after all mushrooms of the 2nd flush had been harvested. Alternatively, an extra casing layer was placed at the bottom of the culture from the start of the experiment. As a control, standard 3.5 kg box cultures (2.5 kg PIII compost + 1 kg casing layer) were used (Fig. 5A - D). The total yield of all conditions showed similar dry weight ($p > 0.106$) and contained similar water content ($p > 0.161$). The control group had an average total yield of 868 g (Table 1). The additional casing layer at the bottom did not increase the total yield ($p = 0.59$). By adding a new casing layer on top of the old one a 1.4-fold (i.e. 364 g more) increase in total yield compared to the control was observed ($p < 0.01$). Similarly, replacing the old casing layer with fresh casing resulted in 1.3-fold more yield (i.e. 295 g more) when compared to the control ($p < 0.05$). To assess the efficiency of the water usage of the alternative treatments and control we divided the total content of water (g) present in the compost and casing introduced during the experiment by the amount of water (g) found in the total yield. Similarly, this was done for the dry matter to calculate the efficiency of dry matter assimilation. The control had a water efficiency of 35 %, and a dry matter efficiency of 6 %. None of the alternative treatments differed significantly in water and dry matter efficiency from the control. This shows that the mushrooms resulting from the alternative casing strategies were as efficient as the control in using the available resources. However, mushrooms barely assimilate dry matter from the casing (data not shown), suggesting that the dry matter of the compost was used more efficiently in the treatment with added casing on top and the casing change treatment. Taken together, these data indicate that water is limiting for mushroom production, whilst the nutrients in the compost are not.

In the next set of experiments, PII compost was colonised directionally from a small PIII layer inoculum at the bottom of the culture (Fig. 5E). Compost colonized directionally

Table 1. Total yields of alternative growth strategies. Mushrooms were picked throughout the experiment, which lasted until no more mushrooms would form. Efficiencies are calculated by dividing the amount of water or dry matter in the mushrooms by their respective amounts in the used materials. Results are presented as average ($n = 3$) \pm 95 % confidence interval.

Treatment	Control	Adding extra casing	Additional casing layer at the bottom	Replacing the old casing layer
Experiment duration (d)	61	76	64	62
Yield (g)	868 \pm 220	1231 \pm 241	992 \pm 179	1162 \pm 157
Water translocation efficiency ($\text{g} \cdot \text{g}^{-1}$)	0.34 \pm 0.09	0.38 \pm 0.08	0.30 \pm 0.05	0.35 \pm 0.04
Dry matter assimilation efficiency ($\text{g} \cdot \text{g}^{-1}$)	0.078 \pm 0.016	0.098 \pm 0.013	0.087 \pm 0.025	0.093 \pm 0.029

shows 5-fold more transport of the amino acid analogue 14C-aminoisobutyric acid towards developing mushrooms (see Herman et al., 2022; **Chapter 3**). Therefore, we hypothesized that directional growth could support more yield. Contrarily, directional growth resulted in 1.3 fold less yield than the control ($p = 0.026$) and it took 7 more days to colonize the casing. Next, 2.5 kg of PII was inoculated either by mixing 11.7 g of spawn, or by placing a similar quantity underneath the compost. Colonization of the compost took 16 and 26 days, respectively, and yield was 1.2 fold less when compost was colonized directionally ($n = 2$). Together, data show that directional colonization of the substrate will take approximately 7 - 10 days longer than the traditional growing practice and does not increase mushroom yield.

Discussion

Water influx from the compost and the casing into developing mushrooms is key in the formation of *Agaricus bisporus* fruiting bodies. Here it was shown that water in the mushrooms mainly originates from the casing and to a lesser extent from the top and intermediate layer of the compost, while the bottom layer only plays a marginal role. These results are in line with the results of Kalberer (Kalberer, 2006, 1985, 1983) that showed that the casing is an important source of water and that lower compost layers contribute less water to the mushrooms in a system where water was applied to the casing during culturing. However, we report an increasingly lower Ψ for the casing during the cultivation, which could in part be because no watering was applied in our methods, but also because previous data on Ψ_{osm} were presented as Ψ (Kalberer, 1987). Our study indicates that Ψ_{mat} becomes increasingly negative throughout the cultivation when no watering is applied, most notably for the casing. Based on the results of this study, alternative casing regimes were tested to increase mushroom production. Replacing the casing after the second flush or adding a fresh layer on top of the old casing resulted in a 1.3 to 1.4 fold increased total yield, respectively, without affecting mushroom dry weight and water efficiency (i.e. the amount of water being translocated into mushrooms). Although this culture regime takes twice longer than a conventional setup, less compost is

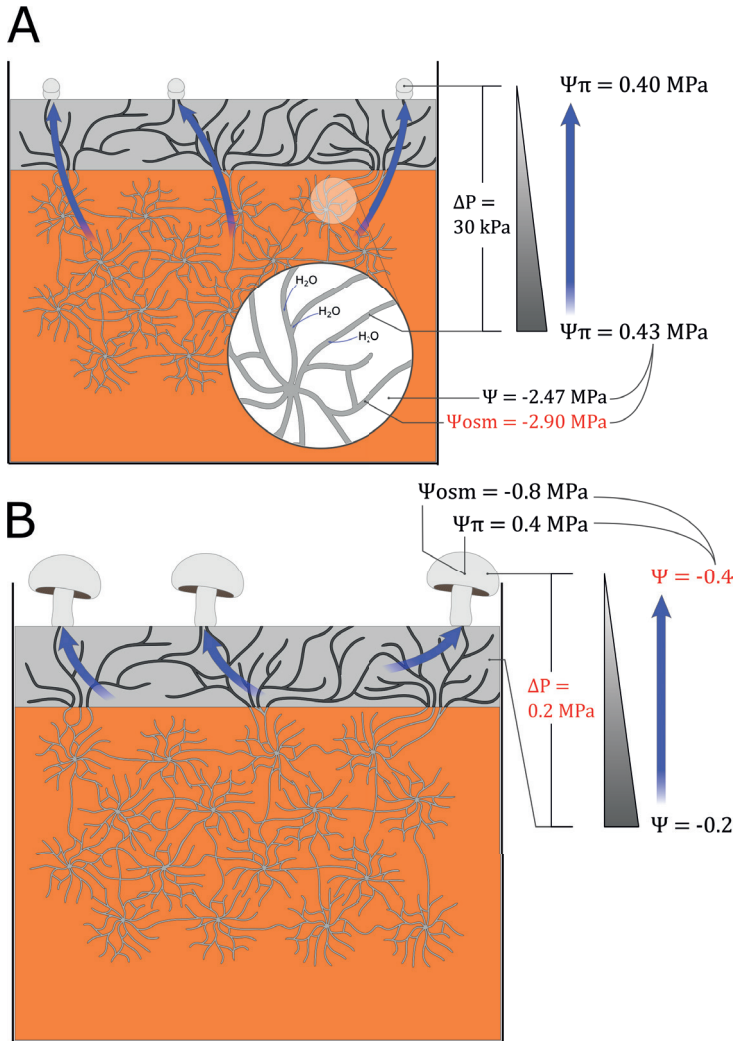


Figure 6. Schematic overview of possible water transport routes from the compost (A) and the casing (B) based on data on the water potential and its components from this study and previous literature. PIII compost (orange) is colonized by fine hyphae (grey), whilst the casing contains predominantly cords (dark grey). In transport route A, the fine hyphae must have a lower Ψ_{osm} than the compost to extract water from it. The water potential (Ψ) in the compost indicates that water cannot be translocated to the mushrooms at all. This discrepancy may be explained by a difference in turgor (Ψ_{π}) between the mycelium in the compost and the developing mushrooms. Our data suggests this pressure difference (ΔP) is minimally 31 kPa. Nutrients may be transported along with flow of water towards the mushrooms in this transport route. Alternatively in transport route B, mushrooms can extract water directly from the casing in the 1st flush, because their estimated Ψ is lower. However, this is no longer the case in the 2nd flush. This suggests more water is then translocated from the compost. As the casing does not provide any nutrients, transport route B only supplies water. It is possible that both transport routes act simultaneously during the different developmental stages of the mushroom. Numbers presented in red are either assumed or do not have data available on them. Blue arrows indicate the expected flow of water.

needed. We calculated that this setup is not cost effective at the current prices for compost (0,135 € kg⁻¹), casing (0.065 € kg⁻¹), and mushrooms (1.9 € kg⁻¹), and only will be cost effective if the price for compost goes up whilst the price for mushrooms go down.

Water is translocated rapidly to the developing mushrooms as they expand exponentially in size (Straatsma et al., 2013). This means that a difference in Ψ is maintained between the substrate and the developing fruiting bodies or that a difference in Ψ_{π} is maintained between the mycelium and the fruiting bodies. Our data indicate that this difference is at least 31 kPa. This finding is in agreement with previous studies that reported pressures differences of 70 kPa in *Coprinus sterquilinus* (Buller, 1931) and 59 kPa in *Coprinopsis cinerea* (Money and Ravishankar, 2005). These differences in pressure are up to 100 times smaller compared to the Ψ values in compost observed in this study. More accurate measurements on Ψ and its components are therefore crucial to advance our understanding on how these forces drive water translocation.

Data of this study also indicate that the differences in water potential cannot drive water from the compost towards the mushrooms but can drive water transport from the casing to the first flush mushrooms. This implies that other components of the water potential drive water transport from the compost to the mushrooms (all flushes) and from the casing to the 2nd flush mushrooms. We propose that water is translocated towards the developing mushrooms by different mechanisms (Fig. 6). Currently, measurements on Ψ_{π} (i.e. turgor) in the mycelium in compost have not been reported for *A. bisporus* and are a crucial component in understanding the flow of water towards mushrooms. A pressure gradient from the mycelium (higher Ψ_{π}) towards the mushrooms (lower Ψ_{π}) could explain the flow of water and nutrients despite the opposing Ψ gradient between the casing and the compost. This can only be the case if the mycelial cords found in the casing are highly impermeable for extracellular water (Eamus and Jennings, 1986; Kalberer, 1987), since

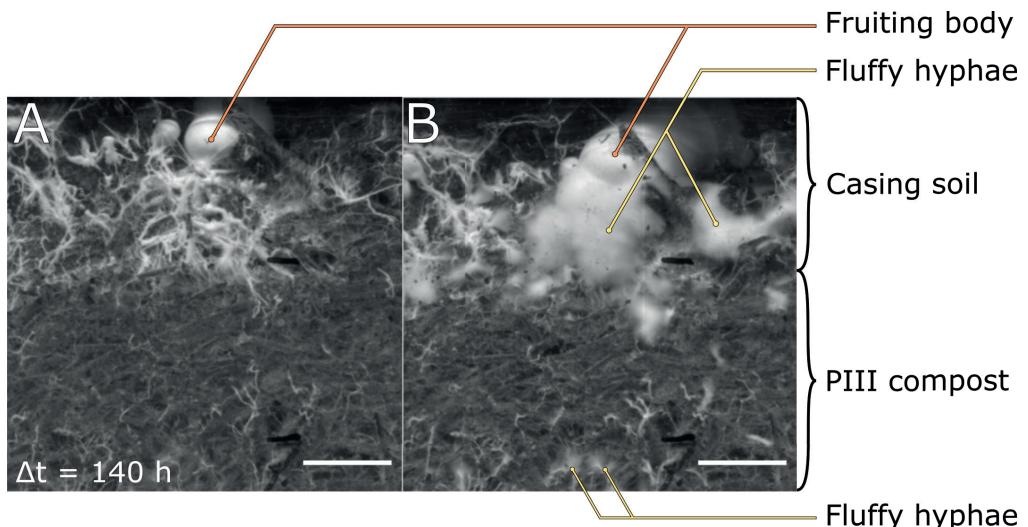


Figure 7. Bottom view of a developing fruiting body in a 12 x 12 plate filled with PIII compost and casing. (A) A developing fruiting body immediately prior to the onset of the emergence of 'fluffy hyphae'. (B) A mature fruiting body having formed a dense cluster of 'fluffy hyphae' around the base of the stem as well as along the length of existing cords. The time interval (Δt) between panel A and B is 140 hours. Scale bar = 1 cm.

water uptake by cords in casing would short circuit water transport from the compost to the mushrooms (see also Herman and Bleichrodt, 2021; **Chapter 1**). As an example, turgor in the mushrooms has been reported in the range of 0.3 to 0.5 MPa (Beecher et al., 2001; Kalberer, 2006). If the mycelium of *A. bisporus* generates the observed pressure difference of 31 kPa towards the mushrooms, the mycelium would need to maintain a Ψ_{π} of at least 0.33 to 0.53 MPa. This is realistic, as turgor in *Neurospora crassa* is in the range of 0.4 to 0.5 MPa under normal conditions (Lew, 2005) and *A. bisporus* can generate similar turgor *in vitro* (Molloy, 2004). To maintain this turgor, *A. bisporus* mycelium would need to achieve an intracellular Ψ_{osm} between -2.8 and -3.0 MPa for the 1st flush and between -3.2 and -3.4 for the 2nd flush based on the Ψ of the compost at these stages. This is again feasible as similar values for Ψ_{osm} have been found in other basidiomycetous fungi (Eamus and Jennings, 1986, 1984). These observations suggest that water translocation from the compost is possible under these conditions. Interestingly, the predicted Ψ_{osm} of the mycelium is substantially more negative than the observed Ψ_{osm} of -0.8 MPa and -1.2 MPa in the fruiting bodies during the 1st and 2nd flush respectively. Mushrooms should have roughly the same Ψ_{osm} as the Ψ_{osm} of the water they receive from the mycelium in the compost. This suggests that mushrooms either metabolise solutes into larger storage carbohydrates or acquire additional water from the casing via a different route. The former is deemed unlikely as the breakdown of glycogen has been reported in mushrooms (Hammond and Nichols, 1979). Another finding that supports the view of multiple transport routes for water to the mushrooms is that the total amount of dry matter in the yield is not influenced by the water potential of the casing soil. Lowering the osmotic potential of the casing by adding salt (NaCl) reduces the uptake of water from the casing soil, and consequently the total wet weight of the yield. Yet, the total amount of dry matter of the combined 1st and 2nd flush did not change in all treatments (Kalberer, 1990b). This indicates that transport of nutrients is mostly unaffected by the osmotic potential of the casing soil, whilst water transport is affected.

The casing soil has a Ψ of -0.2 MPa at the pinning stage. Mushrooms can extract water from it as their estimated Ψ is between -0.3 and -0.5 MPa, based on the measured Ψ_{osm} of 1st flush mushrooms (-0.8 MPa) and the previously found turgor values (Beecher et al., 2001; Kalberer, 2006) (Fig. 6B). This difference in Ψ (minimally 0.1 MPa) is sufficient to account for the measured 31 kPa the mushrooms can generate. In the 2nd flush however, the estimated Ψ of the fruiting bodies is higher than the measured Ψ of the casing. This suggests that mushrooms cannot take up water from the casing in the 2nd flush. If mushrooms extract water directly from the casing, they likely do so in the vicinity of the base of the stem. The casing would lose water locally, leaving patches of more easily extractable water for a 2nd flush. This would account for the higher variation found in the measurements on the casing. We have routinely observed clusters of dense hyphae forming around the base of the stem and along the length of cords (Fig. 7). These hyphae may facilitate water uptake directly from the casing. Alternatively, when less water is available in the casing, more water is taken up from the compost (Kalberer, 1985, 1983). Mushrooms could increase this water uptake from the compost by increasing evaporation. This would create a pathway for water transport analogous to the soil-plant-atmosphere continuum (Taiz and Zeiger, 2014). This is substantiated by our finding that only half of the lost water in the 2nd flush was accounted for by the water in the mushrooms. Yet, we cannot exclude that the missing water had evaporated in the period after the first

and before the second flush. If mushrooms extract more water from the compost, more nutrients are translocated as well, possibly further lowering the Ψ_{osm} when these are catabolised into compatible solutes. This is in accordance with our data as 2nd flush mushrooms have a lower Ψ_{osm} than 1st flush mushrooms. We expect that evaporation plays a more important role when conditions in the casing are drier, as is the case during the 2nd flush. If so, 2nd flush mushrooms should be more impaired in their development by preventing evaporation compared to 1st flush mushrooms.

Acknowledgements

This research was funded by NWO TTW grant ‘Traffic control’ [15493].

5

Colonisation of compost by wild type and commercial *Agaricus bisporus* strains assessed by a scanning imaging method

Koen C. Herman, Robert-Jan Bleichrodt, Johan J.P. Baars, Han A.B. Wösten

Abstract

The quality of the feeding compost is a critical factor in the production of mushrooms of *Agaricus bisporus*. Here, a scanning method is presented that can be used to assess this quality by quantifying the colonization of the substrate. This non-destructive method also showed that colonization of the compost is positively correlated with mushroom yield in wild type *A. bisporus* strains. Moreover, it was shown that the commercial strain A15 had the highest colonisation rate out of nine tested strains. All 9 strains except MES 01808 had evenly colonized the compost. Wild type strain MES 01808 also had colonized the substrate significantly higher when compared to the other strains, which was explained by intense local growth. Colonization of the substrate by the commercial strains MES 03828, 901, and A15 was less when compared to the wildtype strain MES 01808 but higher when compared to five other natural strains. Together, the scanning method can be used to monitor compost quality and to screen for productive strains.

Introduction

Agaricus bisporus, commonly known as the white button mushroom, is an important commercial crop. It is a high-quality food that is rich in protein and that contains beneficial polysaccharides. White button mushrooms are produced indoors at controlled temperature on agricultural waste streams. This makes their production independent of climate and arable land, while the use of waste streams contributes to a circular economy. *A. bisporus* is commercially grown in the Netherlands on a composted substrate of horse manure, wheat straw, gypsum, and water, which is either or not supplemented with chicken manure. Spontaneous fermentation of the mixture of these components is termed phase I (PI). This process, which is accompanied by a rise in temperature to as high as 80 °C, previously took place outdoors, but is now carried out in controlled tunnel like environments. PI is followed by a pasteurization and conditioning phase, called phase II (PII), carried out at 60 °C for two days and 45 °C for 3 days. Phase III is initiated by inoculating PII compost with spawn of *A. bisporus*. The mycelium colonizes the compost in 16 – 19 days at 25 °C. The product resulting from PIII is either or not supplemented with nitrogen rich compounds (Gerrits, 1988) and shipped to mushroom growers. Phase IV starts by adding a peat and lime-based casing on top of the PIII compost, which is colonized by *A. bisporus* from the latter substrate. The casing is essential for fruiting body formation as it is a source of water and scavenges self-inhibitory compounds produced by the mycelium (Eastwood et al., 2013). After colonization, fruiting is induced by lowering the temperature to 18 °C, while maintaining humidity (80 - 90 % RH). Mushrooms appear in 2 to 3 flushes with weekly intervals until the compost is considered spent.

The production of high-quality compost is a critical factor in the production of *A. bisporus* mushrooms. This compost should enable optimal growth of *A. bisporus* whilst excluding microbial competitors (Straatsma et al., 1989, 1994b). Although these conditions are generally met, variation in compost quality exists between batches. PII and PIII compost quality is defined by the resulting yield of mushrooms (Gerrits, 1972), commonly expressed as kg per kg compost or as kg per m² cropping surface. Consequently, the quality of the compost can only be assessed at the end of the cropping process (i.e., a few weeks after its production). This prevents making timely adjustments

during the production of the compost or even leads to batches not shipped to growers. Therefore, it is of utmost importance to be able to quantitatively assess the quality of the compost at the end of its production. This would also enable the optimization of the production parameters (e.g., temperature, humidity, and O₂ concentration).

It is generally assumed that thoroughly colonized compost is required for optimal fruiting body production. However, this has not yet been shown. Also, if the compost is not colonized sufficiently in a timely manner, the risk of infections increases (Seaby, 1996). Therefore, there is a high interest in monitoring the development of *A. bisporus* biomass in the compost during PIII. Several indicators of biomass have been proposed previously, all with their limitations. Common methods of estimating biomass are for example laccase activity (Matcham et al., 1985; Wood, 1980, 1979), colorimetric determination of chitin and chitosan derived hexosamine content (Sharma et al., 1977; Vos et al., 2017a; Whipps and Lewis, 1980), and determining the content of fungal specific cell membrane constituents, such as ergosterol (Ekblad et al., 1998; Wallander et al., 2013, 1997) and certain phospholipid fatty acids (PLFA) (Frostegård et al., 1991; Vos et al., 2017a). Data from a chitin assay are generally not in agreement with ergosterol and PLFA measurements on the same sample. It was proposed that the estimated biomass, as measured by the chitin assay, represents active, inactive, and dead biomass, while ergosterol and PLFA measurements would quantify active biomass only. This would imply that certain parts of a mycelium are inactive or dead (Ekblad et al., 1998; Vos et al., 2017a).

Here we present a scanning method to quantify the colonization of compost of 6 wild type and 3 commercial *A. bisporus* strains. In contrast to the other methods, the scanning method is non-destructive. Using the scanning method, we show that colonization is positively correlated with mushroom yield and that strains use different colonization strategies. The method described can not only be used for strain screening but also to monitor compost quality during PIII.

Material & Methods

Strains & culture conditions

A. bisporus strains 901, MES 01537, MES 01620, MES 01651, MES 01717, MES 01808, MES 01919, and MES 03828 were used in this study. Strain A15 was provided by Sylvan (Sylvan, Horst, Netherlands). Strains were routinely grown on malt extract agar (MEA) or PII compost (CNC Grondstoffen, Milsbeek, the Netherlands). Spawn was prepared by adding a quarter of a 14-day old colony to a sterilized mix of 50 g of rye grains, 2.1 g CaCO₃, and 1.0 g CaSO₄, except for strain A15, where commercial rye-based spawn was used.

Growth profiling

Square plates (12 cm x 12 cm) were filled in triplicate with 70 g PII and inoculated with 9 pre-colonized spawn grains in an evenly spaced 3 x 3 grid. The plates were placed on an Epson V300 / V370 document scanner (Seiko Epson Corporation, Tokyo, Japan) and incubated at 23 °C and 85 % RH for 39 days. Plates were imaged every 4 h with a resolution of 1200 dpi. The white mycelium contrasts with the dark compost, therefore the average gray value of each frame was taken as a marker for biomass with ImageJ. The resulting growth profiles were fitted with nonlinear quantile regression (Koenker and Park,

1996) using R with the package “quantreg” to a logistic model, where a is the maximum colonisation (i.e., the carrying capacity), b is the colonisation rate and x_0 is the value of x at the inflection point. To assess whether data were uni- or multi-modally distributed, an averaged histogram of all pixel values of a single frame was analysed by performing the Hartigans & Hartigans dip test (Hartigan and Hartigan, 1985) by using the R package “dipTest” (Maechler, 2013). Histograms had 512 bins with a fixed bin width of 128.

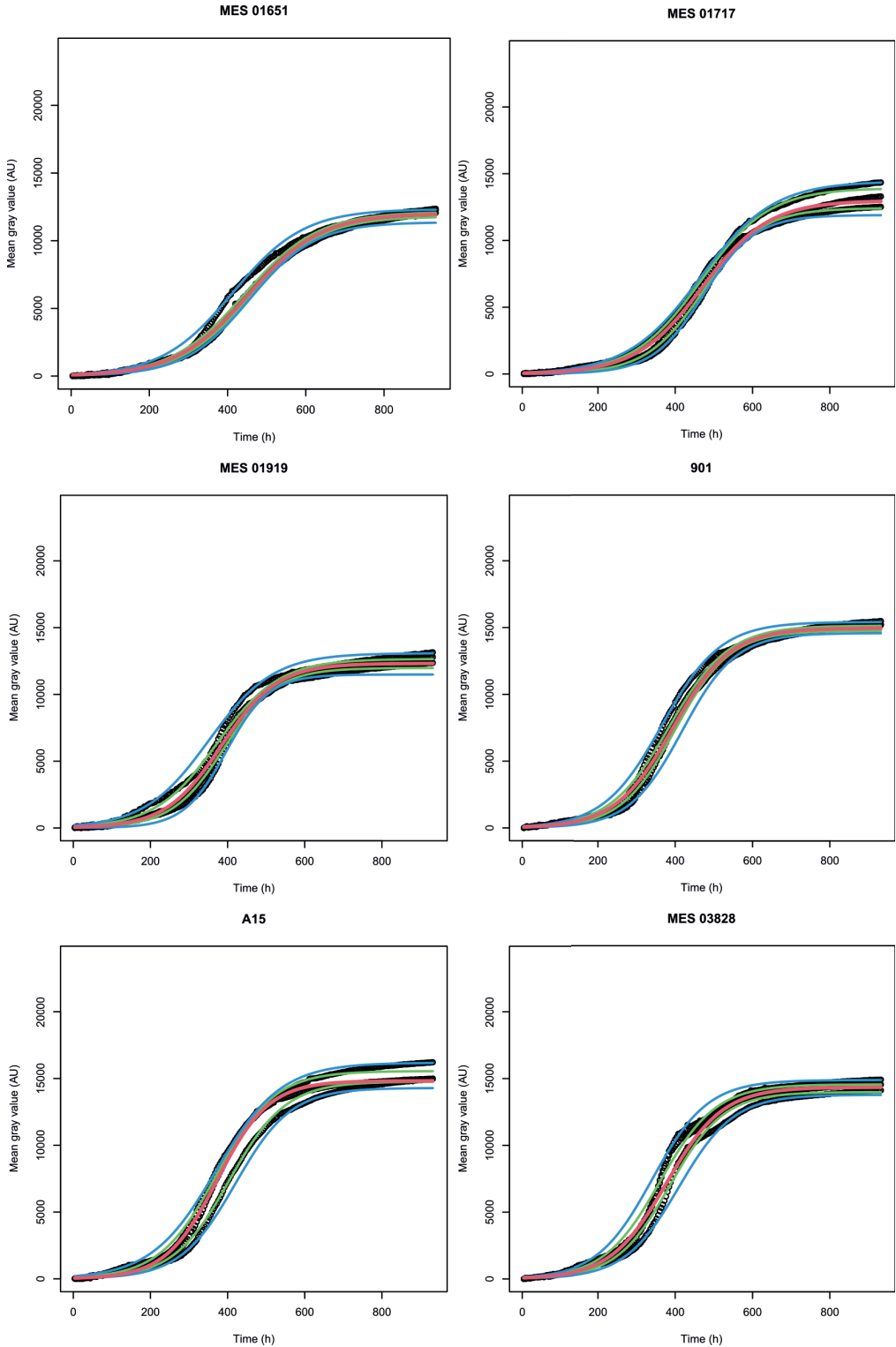
Yield of A. bisporus wild type strains

The yield of wild type *A. bisporus* strains was assessed. Briefly, boxes filled with 8 kg of PII compost were inoculated with spawn using biological triplicates. After 16 days the colonised compost was topped with a 5 cm layer of casing soil. The cultures were vented after the mycelium had colonized the casing soil for 11 days. The casing layer was ruffled 3 days prior to venting. The 1st and 2nd flush were harvested between day 8 and 14, and between day 15 and 28 after venting, respectively.

Results & Discussion

A scanning method was used to assess the growth of the commercial strains A15, 901, and MES 03828, as well as six wild type *A. bisporus* strains. To this end, the bottom of the cultures was scanned with a flatbed scanner. The whiteness of the whole image, measured as the average gray value, was taken as an indicator for mycelial colonisation at each timepoint during a 39-day growth period. A logistic model was used to describe the growth of the strains, even though not all followed logistic growth. Colonization of strains MES 01651, MES 01717, MES 01919, 901, and A15 did follow a logistic growth profile (Fig. 1). This type of growth is characterized by an even colonisation in all areas throughout the growth experiment. Growth of strains MES 03828 and MES 01620 did not show logistic growth, but showed an exponential phase, which was followed by a phase in which colonisation increased linearly until the maximum colonisation (i.e., the carrying capacity) was reached (Fig. 1). Consequently, this also resulted in an even colonisation in all areas. The timing of the transition from an exponential to a linear increase in colonisation was not visibly detectable in the timelapse. Strains MES 01537 & MES 01808 also did not show logistic growth but showed multiple colonization phases (Fig. 1). Initially, mycelium grew thin until the colony peripheries met after approximately 200 h. Next, colonization continued by filling up spaces in some areas of the colonized plate, whilst colonisation continued normally in other areas. In addition, hyphal cords developed. This resulted in an even colonisation in the case of strain MES 01537 but not in the case of strain MES 01808. After 39 days, MES 01808 had colonized the substrate significantly denser when compared to the other strains (Fig. 2A). Of the other strains, MES 03828, 901, and A15 showed a higher colonization rate when compared to the other strains. A15, but not MES 01808, showed the highest maximum colonisation rate (Fig. 2B).

MES 01808 did not colonize the total area uniformly, in contrast to the other strains (Fig. 3). The higher colonisation of MES 01808 (see above) can be explained by a local higher density of the mycelium, while the other regions showed a colonization similar to the other strains. The distribution of pixel values of MES 01808 was at least bimodal ($P < 0.001$), whereas all other strains showed a unimodal distribution (Table 1). A unimodal



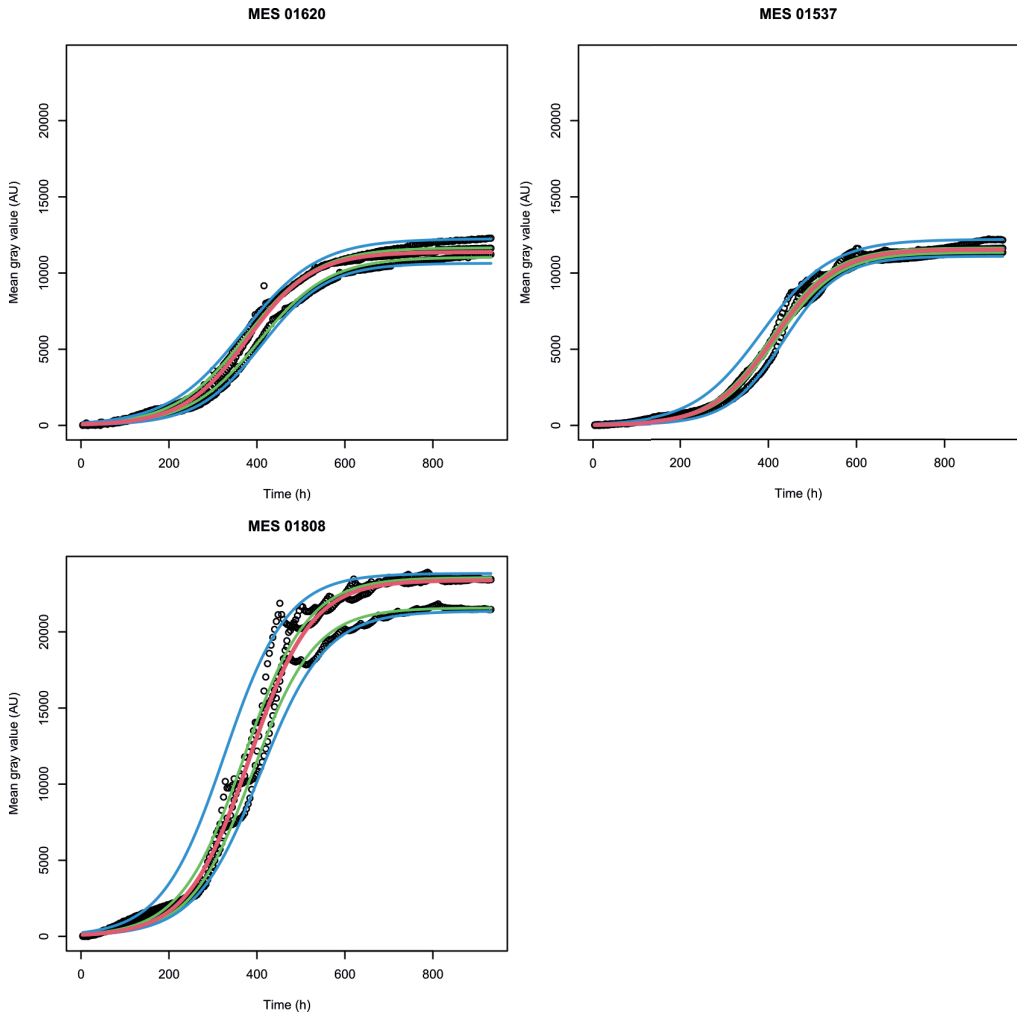


Figure 1. Growth profiles of *A. bisporus* strains in arbitrary units (AU) of grayscale. The data were fitted by nonlinear quantile regression to a logistic model. The area between the fitted blue and green lines contains 95 % and 50 % of the data, respectively. The fitted red line represents the median of the data.

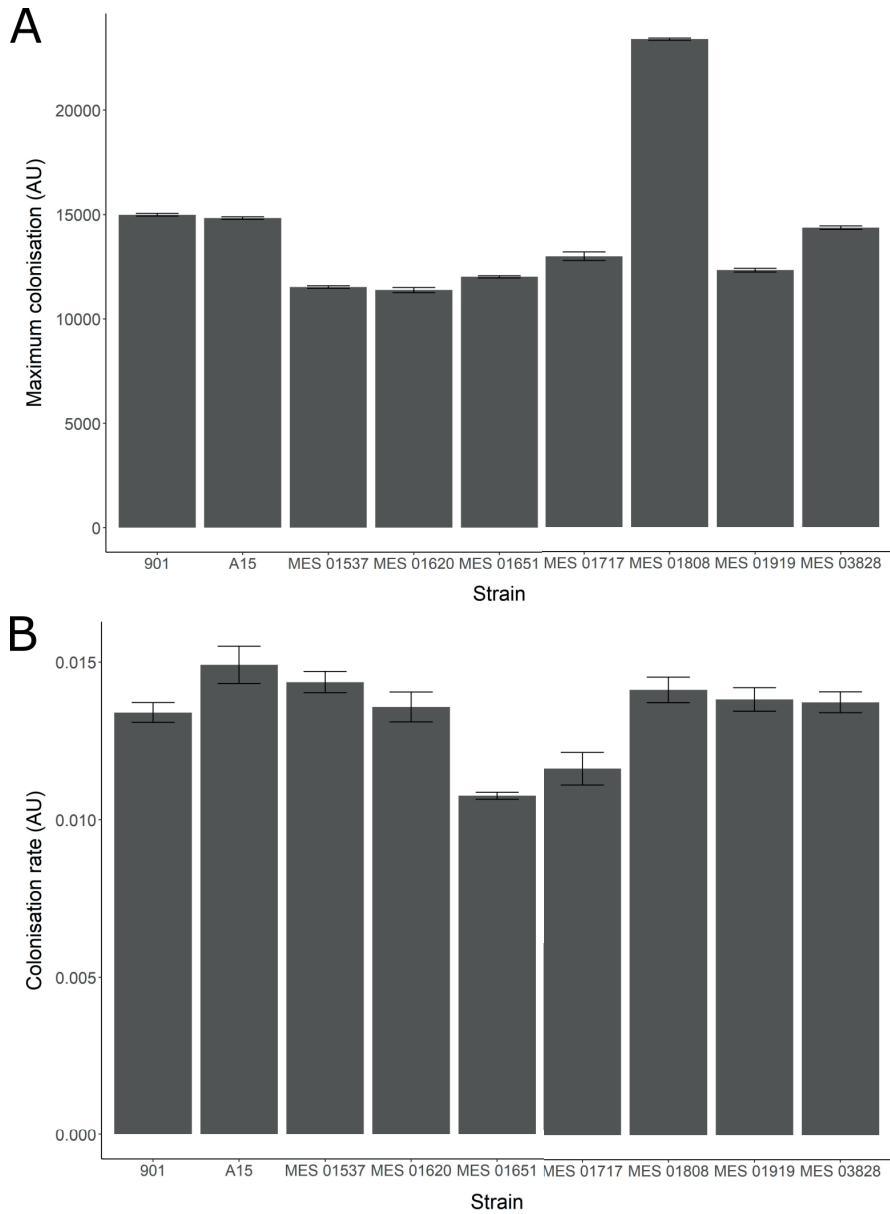


Figure 2. The maximum colonisation (i.e., carrying capacity) (A) and maximum colonisation rate (B) of the *A. bisporus* strains after 39 days of growth. The parameters were estimated by nonlinear regression and is interpreted as fully colonized compost at the end of the experiment (A). Results are an average of three replicates. Error bars represent $2.6 * SE$.

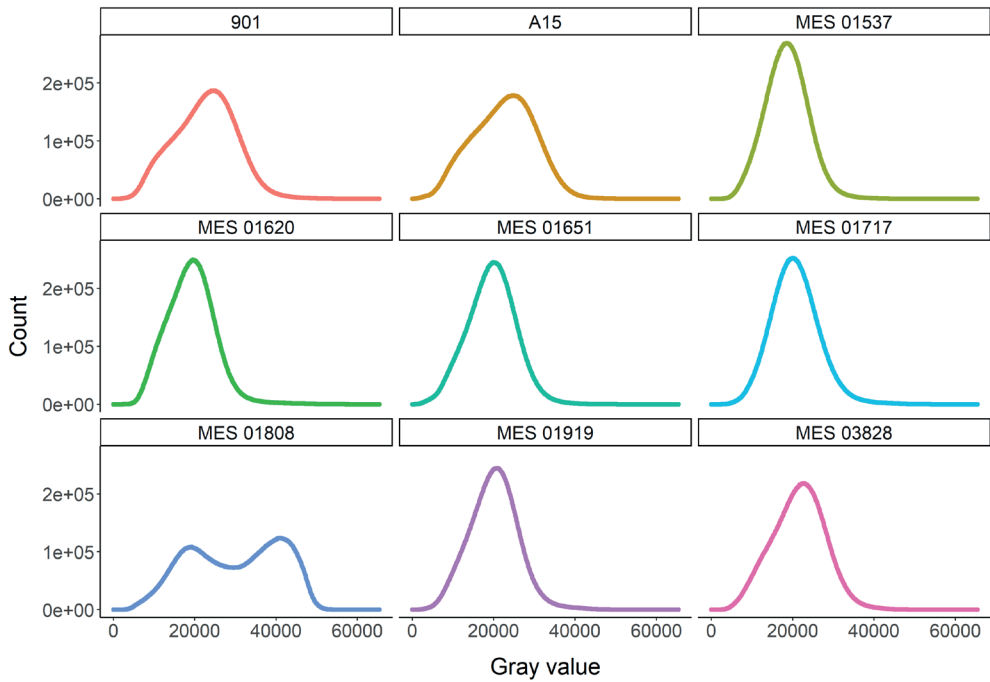


Figure 3. Distribution of gray scale of pixels after 39 days of colonization of the compost by *A. bisporus* strains. All strains except MES 01808 show a unimodal distribution of gray values. Each curve is an average of three replicates. Histograms had 512 bins with a fixed bin width of 128.

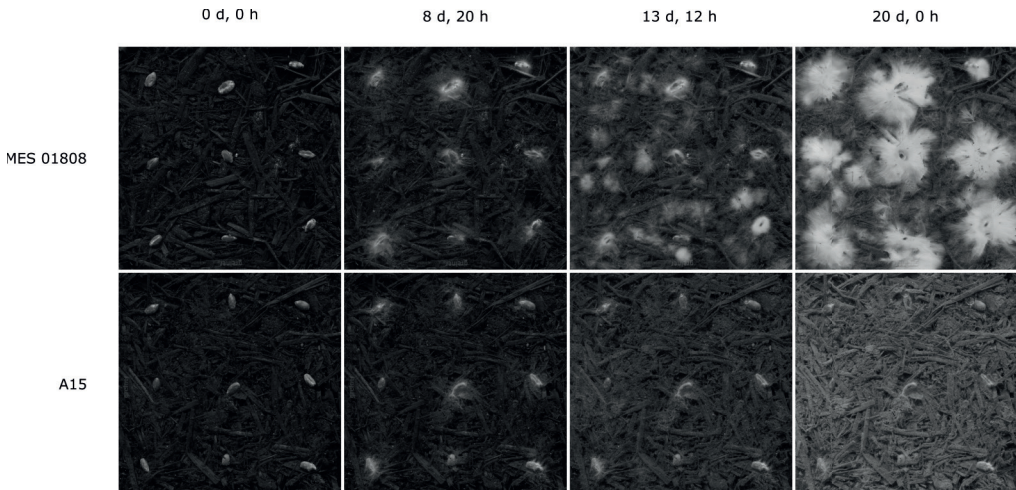


Figure 4. Still frames taken at different time points during colonisation of MES 01808 and A15. Colonies of these strains had colonised the complete compost area after 8 d and 20 h. Further colonisation occurred evenly (A15), or more intensely regionally (MES 01808).

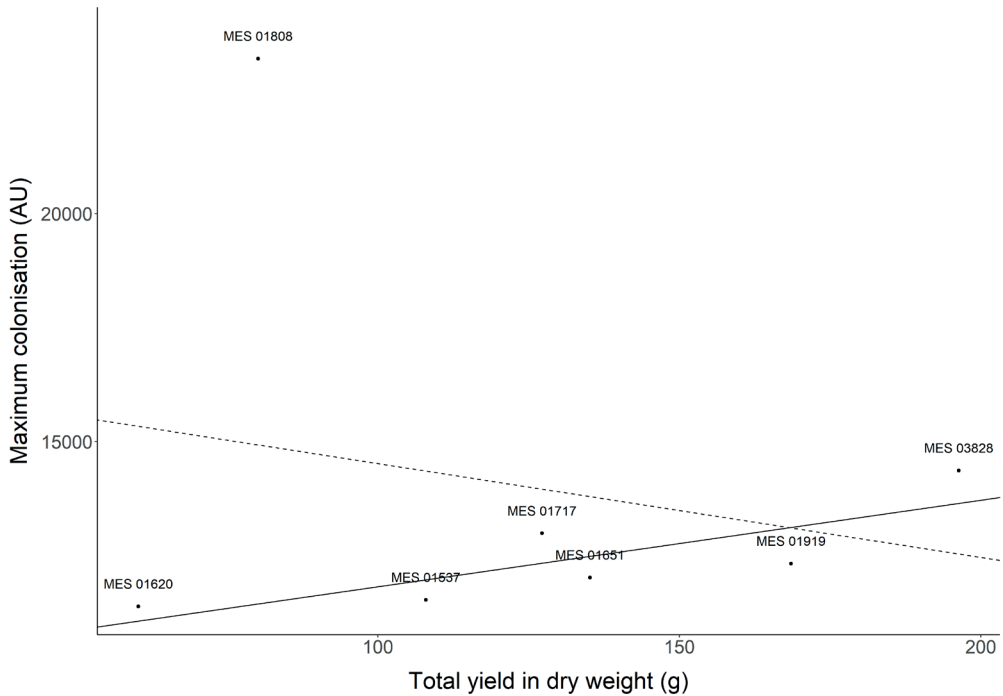


Figure 5. Correlation between the yield and the maximum colonisation of wild type *A. bisporus* strains and the commercial strain MES 03828. The dashed and solid lines show the correlation when MES 01808 was ($r^2 = -0.1$, $p = 0.6$) or was not ($r^2 = 0.6$, $p < 0.05$) included in the linear model.

distribution would be exemplary of a colonising strategy where every available space is initially colonised sparsely (e.g., A15). A bimodal distribution indicates a colonising strategy where available space is first colonised followed by regional intense and less intense colonisation (e.g., MES 01808) (Fig. 4).

Scanning A15 colonization of compost with 1 h intervals showed peaks in gray value that coincided with temperature peaks (Chapter 2; Vos et al., 2020). The peaks in gray value were the result of condensation of water following temperature changes in the compost. These peaks in gray value therefore did not correlate with peaks in colonization. In this Chapter, condensation peaks were not observed in the case of A15 because here an interval time between images of 4 hours was used. Despite this, condensation peaks were observed during growth of MES 01808 (Fig. 1), which took place after a phase of increased colonisation. Together, results indicate that temperature peaks can be accompanied by an increased growth rate in MES 01808 but not in A15.

Better colonisation is generally assumed to be indicative of a higher yield. This assumption was tested by comparing the maximum colonisation of the six wild type strains of *A. bisporus* and the commercial strain MES 03828 (Fig. 2A) with their yields under semi-commercial conditions. No correlation was observed between the average maximum colonisation and the total harvested dry weight ($p = 0.6$). However, a positive correlation was found when the MES 01808 data were treated as an outlier ($r^2 = 0.6$, p

< 0.05). This strain showed a very high colonization but a very low yield. Although not significant, a similar positive correlation was found between colonization of the compost and the averaged total fresh weight of the harvest ($r^2 = 0.6$, $p = 0.063$) (Fig. 5). Taken together, data indicate that *A. bisporus* strains that show better compost colonisation have higher yields. Additionally, it is suggested that growth resulting in a bimodal distribution of colonisation (such as that of MES 01808) is an undesirable trait in a strain selected for commercial use.

Acknowledgements

This research was funded by NWO TTW grant ‘Traffic control’ [15493].

6

Summary & General Discussion

Koen C. Herman

Introduction

Fungi are important drivers of both woody and non-woody litter decomposition in temperate forests (Hättenschwiler et al., 2005; Steffen et al., 2007), thereby contributing to global carbon recycling. The litter degrading saprobic agaricomycete *Agaricus bisporus* is adapted to partially decomposed humic rich environments and is commonly found in forest floors and grasslands (Kerrigan et al., 2013; Morin et al., 2012). Fungal biodiversity is relatively low in humic rich soils (Lindahl et al., 2007), where nutrients are not readily available. The ability of *A. bisporus* to acquire nutrients from humic substances by using extracellular ligninolytic enzymes and proteases would provide an advantage over other saprobic agaricomycetes in this unique niche (Heneghan et al., 2016; Morin et al., 2012). Next to this ecological role, *A. bisporus* is cultivated for its white button mushrooms (“champignons”) representing a global multibillion dollar industry. Most of these mushrooms are produced in Asia, followed by Europe. The Netherlands was the market leader in the EU with a production of 323000 tonnes in 2013. However, since 2013 mushroom production has dropped in the Netherlands to ~ 260.000 tonnes in 2020 (representing an EU market share of 18.4 %). Consequently, the Netherlands was recently succeeded by Poland as the largest producer of mushrooms in the EU (Fig. 1).

In the Netherlands, *A. bisporus* is produced on a composted mixture of wheat straw, horse manure, gypsum, and water, which is either or not supplemented with chicken manure. The compost is produced in a two-step process. Phase I (PI) is started by mixing the components. Metabolic activity of the thermophilic microbial community results

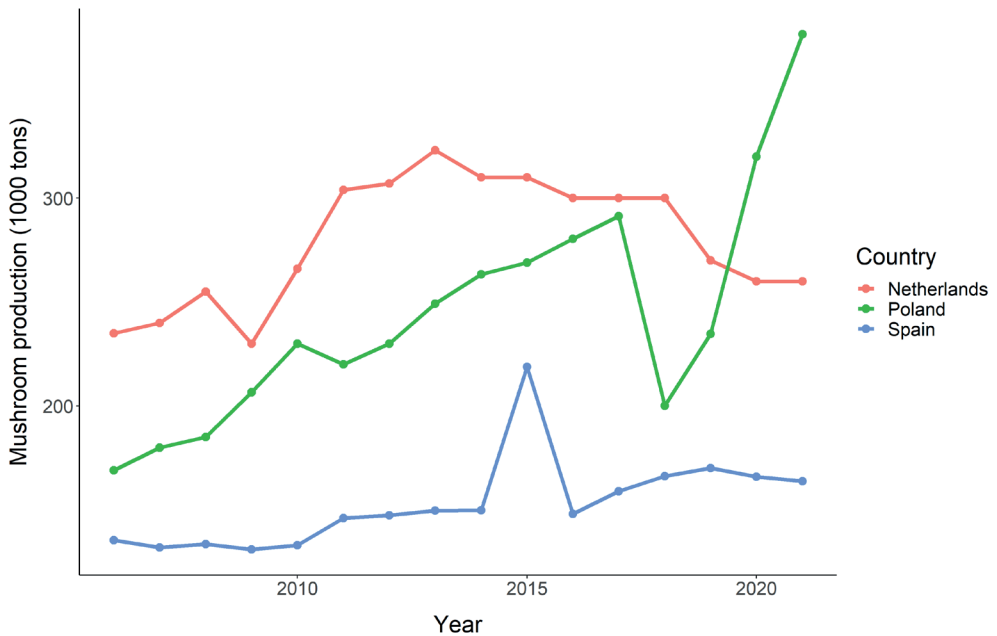


Figure 1. Production of Mushrooms in the three largest producing EU countries from 2006 to 2021 (Source: www.fao.org).

in an increase in temperature up to 80 °C. PI takes 3 – 6 days, during which bacteria degrade proteins and (hemi)cellulose and produce ammonia. This process is carried out indoors to control temperature and humidity. In Phase II (PII) the composted mixture is further pasteurised at 50 °C, and subsequently at 60 °C for 2 days. Finally, during a 3 day conditioning period at 45 °C air is circulated through the compost. Consequently, a specific microbial community develops in the compost (McGee, 2018; Zhang et al., 2014). Within this community, *Mycothermus thermophilus* (Syn. *Scytalidium thermophilum* / *Humicola insolens*) has been shown to be beneficial for the growth of *A. bisporus*, while Gram-negative bacteria serve as a food source for *A. bisporus* (Straatsma et al., 1991, 1994b; Straatsma and Samson, 1993; Vos et al., 2017a). The compost is colonized by *A. bisporus* during phase III (PIII). To this end, the substrate is mixed with pre-colonised rye-based spawn grains. A ratio of 4.7 g spawn kg⁻¹ compost (representing a volume of 2.5 litre) ensures that the mycelium originating from each spawn grain (0.05 g) should only extend ~ 2 cm in any direction before it encounters the mycelium of another grain. The inoculated PIII compost is placed in large tunnels. Air is circulated through the substrate to ensure an optimal growth temperature of 25 °C. The compost is fully colonised in 16 – 19 days and transported to mushroom growers. Phase IV (PIV) is started after a casing layer of peat mixed with lime is added on top of the substrate. The casing layer is colonised for 7 days, after which formation of mushrooms is induced. This is done by lowering the temperature to 18 °C, and by lowering the CO₂ concentration by venting whilst maintaining a high humidity (i.e. up to 90 % RH). Two to three flushes of mushrooms appear in weekly (7 – 8 days) intervals.

Lignin and polysaccharides in the substrate are only partially degraded during PI-PIV (Jurak et al., 2015a, 2015b; Kabel et al., 2017; Patyshakuliyeva et al., 2015, 2013). For example, recalcitrant xylan accumulates and only 45 % of the lignin is degraded during colonisation by *A. bisporus*. Yet, increasing enzyme activity by overexpressing α -1,3-l-arabinofuranosidase, active on substituted xylan, and manganese peroxidase, involved in lignin degradation and modification, has not resulted in a higher degree of compost degradation and a subsequent higher yield (Vos et al., 2018, 2017b). Additionally, the dynamics of the microbial community in compost and the microbial diet of *A. bisporus* have recently received attention. Bacterial biomass, in particular Gram-negative bacteria, decreases by 73 % after 26 days of growth by *A. bisporus* (Mcgee et al., 2018; McGee, 2017; Vos et al., 2017a). This has provided a clearer picture of the nutrients that are available to *A. bisporus* in the compost. Nutrients acquired by the mycelium of *A. bisporus* need to be transported towards mushrooms. This process is not yet fully understood and could pose another bottleneck in the optimal development of mushrooms. The aim of this Thesis was to study colonization of the compost by *A. bisporus* as well as the transport of water and nutrients within the vegetative mycelium and to the developing mushrooms. Understanding how mushrooms acquire the necessary food and water via their supporting mycelial network during their development should provide leads for a more efficient mushroom production.

Colonisation of the compost by *A. bisporus*

Good colonisation of compost by *A. bisporus* is generally assumed to be indicative of a higher mushroom yield. Colonisation starts once spawn grains are mixed with PII compost. The hyphae of *A. bisporus* that expand from the spawn grow by apical extension. When the apical compartment of the hypha exceeds a certain length, a cross wall is formed. As a result, hyphae consist of compartments that are separated by these septa. These hyphae can branch subapically, which gives rise to new hyphal tips. The increase in biomass of a mycelium thus depends on the extension rate of a tip and the number of tips. It has been observed in other fungi that after a brief lag period, the total length of hyphae and the number of tips both increase exponentially (Trinci, 1974, 1973). However, assessing the degree of colonisation within compost is not straightforward. Current methods of measuring the biomass in the compost (i.e. laccase activity, and measuring chitin, ergosterol, and phospholipid fatty acids (PLFA) content) rely on destructive sampling. We used a scanning imaging technique to monitor colonization of *A. bisporus* in the compost (**Chapters 2,5**). The white mycelium of *A. bisporus* contrasts against the dark background of the compost. Therefore, the increase in the average gray value of an image can be taken as a marker for colonisation. This scanning technique showed that the commercial *A. bisporus* strain A15 colonized a 12 x 12 x 1 cm compost volume in about 8 days with exploratory hyphae. This was followed by increased colonization of the substrate by filling in the gaps between the established network (**Chapter 5**). The wild-type strain MES 01808 had the highest maximum colonisation, followed by strains 901 and A15. All nine tested strains colonised the substrate evenly except for MES 01808, which showed a bimodal distribution of colonisation. The higher colonisation of MES 01808 can be explained by areas which are dense with mycelium whilst other areas were similarly colonised as in other strains, such as A15. Previous work showed a logistic profile for colonisation of compost by the former commercial *A. bisporus* strain Horst U1 (Straatsma et al., 1991). This was assessed by determining the percentage of sampled compost particles that showed growth when used as inoculum on a fresh agar plate. Using the scanning method, we showed that the wild type strains MES 01651, MES 01717, MES 01919 and the commercial *A. bisporus* strains A15 and 901 also follow a logistic growth profile. In contrast, growth of the commercial strain MES 03828 and wild-type MES 01620 could be described with an exponential phase followed by a linear phase before maximum colonisation was reached, while wild-type strains MES 01537 & MES 01808 showed multiple colonisation phases (**Chapter 5**).

A positive correlation ($r^2 = 0.6$, $p < 0.05$) was found between the maximum colonisation and the average yield of each strain if strain MES 01808, which showed the lowest yield, was not included. Thus, our data indicate that colonisation is a predictor for mushroom yield. Additionally, we suggest that growth resulting in a bimodal distribution of colonisation would be an undesirable trait for a commercial strain.

Production of CO₂, consumption of O₂, and temperature were measured during the growth of *A. bisporus* in compost (**Chapter 2**). Notably, bursts of respiratory activity were observed with a length of 2.5-5 h and intermediate periods varying from as low as 13 h (early colonization) to as high as 90 h (late colonization). A temperature increase of the compost up to 2 °C was detected 30 min after the start of a respiratory burst, peaked 45–90 min later, and took 2–8 h to normalize to pre-peak temperature. Thus, respiratory

and temperature bursts coincide. In fact, the temperature increase can be fully explained by the O₂ consumption (**Chapter 2**). Using the scanning method and a temperature sensor we observed that the respiratory and temperature bursts did not correlate with increased growth in the case of A15. Temperature bursts are distinguished as a peak in gray value. This was caused by condensation and subsequent evaporation of water. With this in mind, we suggest that the temporal increase in gray value can be associated with an increase in growth in other *A. bisporus* strains, such as MES 01808 (**Chapter 5**).

By using an infrared camera, it was observed that the temperature peaks travel through the mycelium with a velocity of 1 mm min⁻¹ (data not shown). Yet, the bursts of *A. bisporus* became increasingly synchronized over a distance of at least 50 cm. This was shown by placing temperature sensors at different positions in the compost. Evidence indicates that synchronization is the result of anastomosis of hyphae from the different mycelia of each spawn grain (**Chapter 2**). For instance, bursts synchronized when two portions of compost colonized by A15 were placed next to each other. In contrast, this did not occur when the incompatible strains A15 and Bispo15 were used.

RNA sequencing showed that *A. bisporus* genes encoding ligninolytic enzymes are most active before and during the respiratory bursts. (hemi-)cellulolytic genes and genes involved in degradation of microbial biomass were upregulated during and after the bursts, while genes encoding sugar and amino acid transporters were most active after a burst. From these results it was concluded that ligninolytic activity is separated in time with other activities such as degradation of cellulose and microbial biomass. This temporal separation may protect enzymes such as cellulases and those involved in degradation of bacterial biomass from the extracellular reactive oxygen species that are produced during ligninolytic activity in *A. bisporus*. Brown rot fungi would use a similar strategy by spatial separation of the production of ligninolytic and (hemi-)cellulolytic enzymes (Castaño et al., 2018; Presley and Schilling, 2017; Zhang et al., 2019, 2016). The temporal cycling in ligninolytic and cellulolytic activities as occurs in *A. bisporus* may be more efficient than the spatial separation since the same substrate molecules are exposed to different cycles of ligninolytic and (hemi-)cellulolytic activities.

Transport of water and nutrients through the mycelium and towards the fruiting bodies

In terrestrial environments, nutrients are often patchily distributed, both in space and time (Boddy et al., 2009). Therefore, nutrients such as sugars, sugar alcohols, amino acids, and phosphate are translocated through the mycelium towards areas of demand, such as growing hyphal tips or fruiting bodies (Fricker et al., 2017; Woolston et al., 2011). Filamentous fungi maintain turgor for optimal growth, but also small differences in turgor pressure exist in a fungal colony. These pressure differences can drive translocation via mass flow (Eamus and Jennings, 1984). A fundamental understanding on how mass flow is regulated is lacking. We studied the translocation capacities and directionality of the mycelial network of *A. bisporus* by using photon counting scintillation imaging of the radioactive amino acid analogue ¹⁴C-aminoisobutyric acid (¹⁴C-AIB) (**Chapter 3**; Herman et al., 2020). We showed that the translocation speed of ¹⁴C-AIB was 3.68 and 3.47 mm * h⁻¹ in *A. bisporus* mycelium grown on compost and casing, respectively. Similar

translocation velocities are observed in radially grown *P. velutina* colonies (Tlalka et al., 2008b). Notably, a 1.8-fold faster translocation to the growing *A. bisporus* periphery was observed when the mycelium was grown directionally in compost. This coincided with a five-fold higher ^{14}C -AIB content in the mushrooms when compared to mixed growth. Moreover, the translocation distance increased when the mycelium was grown directionally, which results in the formation of more cords. We showed that Poiseuille's Law supports the view of hyphal cords as translocation highways. Using electron microscopy images of *Agaricus carminescens* cords (Cairney, 1990) we calculated that a single cord can theoretically support up to nine-fold more hyphae by employing only 12 μm wide vessel hyphae instead of 3 μm wide fine hyphae. This shows that the vessel hyphae that are found in cords are key to their high transport capacity.

Tip directed ^{14}C -AIB translocation was only observed when vegetative cultures of *A. bisporus* were actively growing, indicating that growth induced mass flow is the main driver of translocation (Chapter 3; Herman et al., 2020). Whilst active growth and translocation are coupled in *A. bisporus*, the former is slower (typically $\sim 0.33 \text{ mm}$ versus $3.68 \text{ mm} \cdot \text{h}^{-1}$). This can be explained by hyphal branching. This effectively doubles the surface area through which the cytoplasm is transported from the upstream parent hypha. According to Poiseuille's Law, the flow speed will halve after the branching point to maintain a similar volumetric flow rate if the pressure difference remains constant before and after the branching point. This principle holds for every subsequent downstream branch point. Therefore, the flow speed drops by $\frac{1}{2^n}$, where v is the flow speed, a is the initial flow speed, and n is the number of branching points. Mass flow is much more efficient if water is taken up centrally in the mycelial colony and subsequently transported outward to the growing periphery. Alternatively, if all the water would be taken up by the tips in the colony margin, mass flow would not be able to sufficiently reach all the parts of the mycelium. With this in mind, transportation efficiency through the mycelium would be increased by reducing the number of branches close to the location of water uptake and increasing branching close to the periphery. This behaviour has been observed in *A. bisporus* growing on casing (data not shown) by bundling hyphae (i.e. cord formation) behind the periphery. It has been shown that nutrient rich patches increase the number of branching events in an area where food is patchily distributed (Boddy, 1999). If additional tips rapidly form in this area, mass flow would be drawn towards this area.

Considering that desiccation is common in upper soil, additional water might be needed for optimal enzyme activity to break down the substrate. If water is drawn from the hyphal tips, mass flow of water towards this area would be increased. Indeed, *A. bisporus* can redistribute water towards desiccated areas to increase enzyme activity (Gühr et al., 2015). Mass flow could therefore facilitate efficient colonisation of newly discovered resources in adverse environmental conditions. Taken together, this indicates that fungi can adapt the structure of their mycelium to ensure efficient translocation of nutrients in a heterogeneous environment.

Oscillations in transport direction have been observed in several filamentous fungi (Lindahl et al., 2001; Olsson and Gray, 1998; Schmieder et al., 2019; Tlalka et al., 2007, 2002). What drives these oscillations is currently not known and is key to understand the complex transport patterns within a mycelium. This observation challenges the view that mass flow transport is directed from source to sink, e.g. from the centre of the colony to the periphery. However, pressure driven mass flow and oscillatory translocation

behaviour could occur simultaneously in certain circumstances. For example, the septal cross walls could play a role in regulating the direction of transport (Schmieder et al., 2019). Septa can open and close dynamically in both ascomycetous (Bleichrodt et al., 2012) and basidiomycetous (van Peer et al., 2009) fungi. When hyphae anastomose, circular transport routes can be created. Depending on which septa are opened or closed, the direction of transport could be redirected to use an alternative route between the same sink and source. These findings may imply that a filamentous fungus that does not anastomose with its own hyphae should not be able to oscillate the direction of mass flow transport by opening or closing its septa. Oscillations in the direction of mass flow could also be explained by growth behind the mycelial periphery. When the periphery of a colony encounters a barrier and cannot continue growing, colonisation continues in such other areas of the mycelium (**Chapter 5**). This would lead to pressure driven mass flow that is directed towards the area where colonisation is most extensive.

A function of the mycelium is to provide an efficient flow of water and nutrients towards developing mushrooms. **Chapter 4** studied the contribution of the casing layer and different layers of the compost in providing the developing mushrooms with water. The casing was shown to be the most important source of water, whilst the upper, middle, and lower compost layer each contribute increasingly less. Next, the water potential (Ψ) and the osmotic potential (Ψ_{osm}) were determined in the casing, the compost layers, and the fruiting bodies throughout the cropping process. Water flows from high to low Ψ , if unobstructed. Several components make up Ψ , including, but not limited to, the osmotic potential (Ψ_{osm}), matric potential (Ψ_{mat}), and pressure potential (Ψ_{π}). Assuming other factors of Ψ are small, Ψ_{mat} may be inferred from the difference between Ψ and Ψ_{osm} . Ψ decreased during the cropping process in the casing and all compost layers. Like the water content, Ψ decreased the most in the casing layer, whilst the bottom compost layer decreased the least. Our data indicate that Ψ_{osm} of the compost and casing layer determines the water potential in the beginning of cultivation, whilst Ψ_{mat} becomes increasingly important in later stages, particularly in the casing soil. Most notably, the Ψ of the casing was almost completely explained by the Ψ_{osm} at inoculation and venting. In contrast, the Ψ_{osm} of the casing only explained 51 % and 31 % of Ψ during the 1st and 2nd flush, respectively.

Ψ cannot explain the flow of water from the compost towards the mushrooms (**Chapter 4**; Kalberer, 2006, 1990, 1987). Water flows from high to low water potential areas. However, Ψ of compost is generally lower than that of the mushrooms. This would imply that mushrooms cannot extract water from the compost, but this is not in line with the observed water loss in the compost during fruiting (**Chapter 4**; Kalberer, 1985, 1983). We point to the absence of data on turgor in the mycelium during fruiting as a gap in our understanding of the translocation of water towards the mushrooms. To translocate water towards mushrooms, a difference in Ψ between the substrate and the developing fruiting bodies or a difference in Ψ_{π} between the mycelium and the fruiting bodies is required. Using a pressure plate, our data indicate that this difference is at least 31 kPa. We provide a new hypothesis where multiple routes of water uptake work synergistically (**Chapter 4**). To test this hypothesis, future research should be directed at assessing the transport function of the cords present in the casing and the cluster of fluffy hyphae around the base of the mushroom stem. Understanding how and where water is taken up by *A. bisporus* is important in understanding the flow of water towards mushrooms.

Based on the findings in **Chapter 4**, new casing regimes (based on addition of extra water) were assessed to increase mushroom yield. Replacement of the casing layer or adding a fresh layer on top of the old casing after the second flush resulted in a 1.3 to 1.4-fold increased total yield. Yet, these new casing regimes are not cost effective. Relative mushroom dry weight and water efficiency (i.e. the amount of water being translocated into mushrooms) were not affected. **Chapter 4** showed that the amount of dry matter present in the substrate is not limiting for the formation of mushrooms. I therefore propose the water efficiency as an additional parameter to assess cultivation efficiency, i.e. how much of the total amount of water ends up in the mushrooms. This includes water present in the substrate from the start and water that is added by the watering regime. The added benefit of this parameter is that the influence of both the compost and the casing layer is considered.

Appendix

References

- Abadeh, A., Lew, R.R., 2013. Mass flow and velocity profiles in *Neurospora* hyphae: partial plug flow dominates intrahyphal transport. *Microbiology* 159, 2386–2394.
- Albertyn, J., Hohmann, S., Thevelein, J.M., Prior, B.A., 1994. GPD1, which encodes glycerol-3-phosphate dehydrogenase, is essential for growth under osmotic stress in *Saccharomyces cerevisiae*, and its expression is regulated by the high-osmolarity glycerol response pathway. *Mol. Cell. Biol.* 14, 4135–4144.
- Alexander, N.J., McCormick, S.P., Hohn, T.M., 1999. TRI12, a trichothecene efflux pump from *Fusarium sporotrichioides*: gene isolation and expression in yeast. *Mol. Gen. Genet.* 261, 977–984.
- Amir, R., Levanon, D., Hadar, Y., Chet, I., 1994. The role of source-sink relationships in translocation during sclerotial formation by *Morchella esculenta*. *Mycol. Res.* 98, 1409–1414.
- Amir, R., Steudle, E., Levanon, D., Hadar, Y., Chet, I., 1995. Turgor changes in *Morchella esculenta* during translocation and sclerotial formation. *Exp. Mycol.* 19, 129–136.
- Amsing, J.G.M., 1990. De waterhuishouding van een champignonbed. Invloed van watergeven en plastic folie onder de compost. *De Champignoncultuur* 34, 251–259.
- Arantes, V., Jellison, J., Goodell, B., 2012. Peculiarities of brown-rot fungi and biochemical Fenton reaction with regard to their potential as a model for bioprocessing biomass. *Appl. Microbiol. Biotechnol.* 94, 323–338.
- Arnebrant, K., Ek, H., Finlay, R.D., Söderström, B., 1993. Nitrogen translocation between *Alnus glutinosa* (L.) Gaertn. seedlings inoculated with *Frankia* sp. and *Pinus contorta* Dougl, ex Loud seedlings connected by a common ectomycorrhizal mycelium. *New Phytol.* 124, 231–242.
- Arnoldi, M., Fritz, M., Bäuerlein, E., Radmacher, M., Sackmann, E., Boulbitch, A., 2000. Bacterial turgor pressure can be measured by atomic force microscopy. *Phys. Rev. E. Stat. Phys. Plasmas Fluids Relat. Interdiscip. Topics* 62, 1034–1044.
- Atkey, P.T., Wood, D.A., 1983. An electron microscope study of wheat straw composted as a substrate for the cultivation of the edible mushroom (*Agaricus bisporus*). *J. Appl. Bacteriol.* 55, 293–304.
- Bahn, Y.S., Kojima, K., Cox, G.M., Heitman, J., 2006. A Unique Fungal Two-Component System Regulates Stress Responses, Drug Sensitivity, Sexual Development, and Virulence of *Cryptococcus neoformans*. *Mol. Biol. Cell* 17, 3122–3135.
- Bahn, Y.S., Xue, C., Idnurm, A., Rutherford, J.C., Heitman, J., Cardenas, M.E., 2007. Sensing the environment: Lessons from fungi. *Nat. Rev. Microbiol.* 5, 57–69.
- Beauzamy, L., Nakayama, N., Boudaoud, A., 2014. Flowers under pressure: ins and outs of turgor regulation in development. *Ann. Bot.* 114, 1517–1533.
- Beecher, T.M., Magan, N., Burton, K.S., 2001. Water potentials and soluble carbohydrate concentrations in tissues of freshly harvested and stored mushrooms (*Agaricus bisporus*). *Postharvest Biol. Technol.* 22, 121–131.
- Bleichrodt, R.J., van Velu, G.J., Recter, B., Maruyama, J.I., Kitamoto, K., Wösten, H.A.B., 2012. Hyphal heterogeneity in *Aspergillus oryzae* is the result of dynamic closure of septa by Woronin bodies. *Mol. Microbiol.* 86, 1334–1344.
- Bleichrodt, R., Vinck, A., Krijgheld, P., van Leeuwen, M.R., Dijksterhuis, J., Wösten, H.A.B., 2013. Cytosolic streaming in vegetative mycelium and aerial structures of *Aspergillus niger*. *Stud. Mycol.* 74, 31–46.
- Boddy, L., 1999. Saprotrophic cord-forming fungi: Meeting the challenge of heterogeneous environments. *Mycologia* 91, 13–32.
- Boddy, L., Hynes, J., Bebbler, D.P., Fricker, M.D., 2009. Saprotrophic cord systems: Dispersal mechanisms in space and time. *Mycoscience* 50, 9–19.
- Bonnen, A.M., Anton, L.H., Orth, A.B., 1994. Lignin-degrading enzymes of the commercial button mushroom, *Agaricus bisporus*. *Appl. Environ. Microbiol.* 60, 960–965.
- Bovio, S., Long, Y., Monéger, F., 2019 Use of atomic force microscopy to measure mechanical properties and turgor pressure of plant cells and plant tissues. *J. Vis. Exp.* 149, e59674.

- Boyer, J. S., 1995. Measuring the water status of plants and soils. Academic Press, Inc. pp. 49 – 102.
- Brody, J.P., Yager, P., Goldstein, R.E., Austin, R.H., 1996. Biotechnology at low Reynolds number. *Biophys. J.* 71, 3430-3441.
- Brownlee, C., Jennings, D.H., 1982a. Pathway of translocation in *Serpula lacrimans*. *Trans. Br. Mycol. Soc.* 79, 401-407.
- Brownlee, C., Jennings, D.H., 1982b. Long distance translocation in *Serpula lacrimans*: Velocity estimates and the continuous monitoring of induced perturbations. *Trans. Br. Mycol. Soc.* 79: 143-148.
- Buller, A.H.R. (1931) *Researches on Fungi*. Vol. 4. Longmans Green, London.
- Burton, K., Partis, M., Wood, D., Thurston, C., 1997. Accumulation of serine proteinase in senescent sporophores of the cultivated mushroom, *Agaricus bisporus*. *Mycol. Res.* 101, 146–152.
- Butler, G.M., 1958. The development and behaviour of mycelial strands in *Merulius lacrymans* (Wulf.) Fr.: II. Hyphal behaviour during strand formation. *Ann. Bot.* 22, 219-236.
- Cairney, J.W.G., 1990. Internal structure of mycelial cords of *Agaricus carminescens* from Heron Island, Great Barrier Reef. *Mycol. Res.* 94, 117-199.
- Carrasco, J., García-Delgado, C., Lavega, R., Tello, M.L., De Toro, M., Barba-Vicente, V., Rodríguez-Cruz, M.S., Sánchez-Martín, M.J., Pérez, M., Preston, G.M., 2020. Holistic assessment of the microbiome dynamics in the substrates used for commercial champignon (*Agaricus bisporus*) cultivation. *Microb. Biotechnol.* 13, 1933–1947.
- Castaño, J.D., Zhang, J., Anderson, C.E., Schilling, J.S., 2018. Oxidative damage control during decay of wood by brown rot fungus using oxygen radicals. *Appl. Environ. Microbiol.* 84, e01937-18.
- Chanter, D.O., Thornley, J.H.M., 1978. Mycelial growth and the initiation and growth of sporophores in the mushroom crop: a mathematical model. *J. Gen. Microbiol.* 106, 55–65.
- Chanter, D.O., 1979. Harvesting the mushroom crop: a mathematical model. *Microbiology* 115, 79-87.
- Chen, Y., Chefetz, B., Rosario, R., van Heemst, J.D.H., Romaine, P.C., Hatcher, P.G., 2000. Chemical nature and composition of compost during mushroom growth. *Compost Sci. Util.* 8: 347-359.
- Clarke, R.W., Jennings, D.H., Coggins, C.R., 1980. Growth of *Serpula lacrimans* in relation to water potential of substrate. *Trans. Br. Mycol. Soc.* 75, 271–280.
- Damaschke, K., Becker, G., 1966. Rhythmen des sauerstoffverbrauchs von basidiomyceten. *Mater. Org.* 1, 275–290.
- Dietz, S., von Bülow, J., Beitz, E., Nehls, U., 2011. The aquaporin gene family of the ectomycorrhizal fungus *Laccaria bicolor*: Lessons for symbiotic functions. *New Phytol.* 190, 927–940.
- Dressaire, E., Yamada, L., Song, B., Roper, M., 2016. Mushrooms use convectively created airflows to disperse their spores. *Proc. Natl. Acad. Sci. USA* 113, 2833–2838.
- Dupont, W.D., Plummer, W.D., 1990. Power and sample size calculations: A review and computer program. *Control. Clin. Trials* 11, 116-128.
- Eamus, D., Jennings, D.H., 1984. Determination of water, solute and turgor potentials of mycelium of various basidiomycete fungi causing wood decay. *J. Exp. Bot.* 35, 1782–1786.
- Eamus, D., Jennings, D.H., 1986. Turgor and fungal growth: Studies on water relations of mycelia of *Serpula lacrimans* and *Phallus impudicus*. *Trans. Br. Mycol. Soc.* 86, 527–535.
- Eastwood, D.C., Herman, B., Noble, R., Dobrovin-Pennington, A., Sreenivasaprasad, S., Burton, K.S., 2013. Environmental regulation of reproductive phase change in *Agaricus bisporus* by 1-octen-3-ol, temperature and CO₂. *Fungal Genet. Biol.* 55, 54–66.
- Eger, G., 1962. The “Halbschalentest” - a simple method for testing casing materials. *MGA Bull.* 148, 159-168.
- Ekblad, A.L.F., Wallander, H., Näsholm, T., 1998. Chitin and ergosterol combined to measure total and living fungal biomass in ectomycorrhizas. *New Phytol.* 138, 143–149.
- Engineering ToolBox, 2011. Pipes - in Series or Parallel. [online] Available at: https://www.engineeringtoolbox.com/pipes-series-parallel-d_1787.html

- van Erven, G., Hilgers, R., de Waard, P., Gladbeek, E.J., van Berkel, W.J.H., Kabel, M.A., 2019. Elucidation of in situ ligninolysis mechanisms of the selective white-rot fungus *Ceriporiopsis subvermispora*. *ACS Sustain. Chem. Eng.* 7, 16757-16764.
- Finn, R.D., Coggill, P., Eberhardt, R.Y., Eddy, S.R., Mistry, J., Mitchell, A.L., Potter, S.C., Punta, M., Qureshi, M., Sangrador-Vegas, A., Salazar, G.A., 2016. The Pfam protein families database: Towards a more sustainable future. *Nucleic. Acids. Res.* 44, D279–D285.
- Fischer, G., Kosinska-Eriksson, U., Aponte-Santamaría, C., Palmgren, M., Geijer, C., Hedfalk, K., Hohmann, S., De Groot, B.L., Neutze, R., Lindkvist-Petersson, K., 2009. Crystal structure of a yeast aquaporin at 1.15 Å reveals a novel gating mechanism. *PLoS Biol.* 7, e1000130.
- Flegg, P.B., 1962. The development of mycelial strands in relation to fruiting of the cultivated mushroom (*Agaricus bisporus*). *Mushr. Sci.* 5, 300-313.
- Flegg, P.B., 1974. The water requirement of the mushroom crop. *Sci. Hortic.* 2, 237-247.
- Flegg, P.B., 1975. The response of the mushroom crop to the pattern of watering. *Sci. Hortic.* 3, 137–142.
- Flegg, P.B., 1981. How do your mushrooms grow? *Mushroom J.* 108, 401-409.
- Floudas, D., Bentzer, J., Ahrén, D., Johansson, T., Persson, P., Tunlid, A., 2020. Uncovering the hidden diversity of litter-decomposition mechanisms in mushroom-forming fungi. *ISME J.* 14, 2046-2059.
- Fricker, M.D., Tlalka, M., Bebbler, D., Takagi, S., Watkinson, S.C., Darrah, P.R., 2007. Fourier-based spatial mapping of oscillatory phenomena in fungi. *Fungal Genet. Biol.* 44, 1077-1084.
- Fricker, M.D., Heaton, L.L.M., Jones, N.S., Boddy, L., 2017. The mycelium as a network. *Microbiol. Spectr.* 5, 1–32.
- Frostegård, Å., Tunlid, A., Bååth, E., 1991. Microbial biomass measured as total lipid phosphate in soils of different organic content. *J. Microbiol. Meth.* 14, 151–163.
- Furukawa, K., Hoshi, Y., Maeda, T., Nakajima, T., Abe, K., 2005. *Aspergillus nidulans* HOG pathway is activated only by two-component signalling pathway in response to osmotic stress. *Mol. Microbiol.* 56, 1246–1261.
- Gerrits, J.P.G., 1968. Organic compost constituents and water utilised by the cultivated mushroom during spawn run and cropping. *Mushroom Sci.* 7, 111-126.
- Gerrits, J.P.G., 1971. The influence of water in the preparation of mushroom compost and its control. *Mushroom Sci.* 8, 43-57.
- Gerrits, J.P.G., 1972. The influence of water in mushroom compost. *Mushroom Sci.* 8, 43–57.
- Gerrits, J.P.G., 1988. Nutrition and compost. In: van Griensven, L.J.L.D. (Ed.), *The cultivation of mushrooms*. Darlington Mushroom Laboratories Ltd, Darlington, pp. 29–72.
- Gerrits, J.P.G., 1994. Composition, use and legislation of spent mushroom substrate in The Netherlands. *Compost Sci. Util.* 2, 24–30.
- Goff, L., Trapnell, C., Kelley, D., 2013. *CummeRbund*: analysis, exploration, manipulation, and visualization of Cufflinks high-throughput sequencing data. R package version 2, 2013.
- Granlund, H.I., Jennings, D.H., Thompson, W., 1985. Translocation of solutes along rhizomorphs of *Armillaria mellea*. *Trans. Br. Mycol. Soc.* 84, 111–119.
- Grigoriev, I.V., Nikitin, R., Haridas, S., Kuo, A., Ohm, R., Otilar, R., Riley, R., Salamov, A., Zhao, X., Korzeniewski, F., Smirnova, T., 2014. MycoCosm portal: Gearing up for 1000 fungal genomes. *Nucl. Acids. Res.* 42: D699–D706.
- Grimm, D., Wösten, H.A.B., 2018. Mushroom cultivation in the circular economy. *Appl. Microbiol. Biotechnol.* 102, 7795–7803.
- Guhr, A., Borken, W., Spohn, M., Matzner, E., 2015. Redistribution of soil water by a saprotrophic fungus enhances carbon mineralization. *Proc. Natl. Acad. Sci. USA* 112, 14647–14651.
- Hammel, K.E., Kapich, A.N., Jensen, K.A., Ryan, Z.C., 2015. Reactive oxygen species as agents of wood decay by fungi. *Enzyme. Microb. Technol.* 30, 445–453.
- Hammond, J.B.W., Nichols, R., 1976a. Carbohydrate metabolism in *Agaricus bisporus* (Lange) Sing: changes in soluble carbohydrates during growth of mycelium and sporophore. *J. Gen. Microbiol.* 93, 309–320.

- Hammond, J.B.W., Nichols, R., 1976b. Glycogen in *Agaricus bisporus*. Trans. Brit. Mycol. Soc. 66, 325-327.
- Hammond, J.B.W., 1979. The role of non-structural carbohydrates in the life-cycle of *Agaricus bisporus*. Mushroom Sci. 10, 391-400.
- Hammond, J.B.W., Nichols, R., 1979. Carbohydrate metabolism in *Agaricus bisporus*: changes in non-structural carbohydrates during periodic fruiting (flushing). New Phytol. 83, 723-730.
- Hammond, J.B.W., 1981. Variations in enzyme activity during periodic fruiting of *Agaricus bisporus*. New Phytol. 89, 419-428.
- Hansen, L.D., MacFarlane, C., McKinnon, N., Smith, B.N., Criddle, R.S., 2004. Use of calorespirometric ratios, heat per CO₂ and heat per O₂, to quantify metabolic paths and energetics of growing cells. Thermochim. Acta. 422, 55-61.
- Hättenschwiler, S., Tiunov, A. V, Scheu, S., 2005. Biodiversity and litter decomposition in terrestrial ecosystems. Annu. Rev. Ecol. Evol. Syst. 36, 191-218.
- ten Have, R., Teunissen, P.J., 2001. Oxidative mechanisms involved in lignin degradation by white-rot fungi. Chem. Rev. 101, 3397-413.
- ten Have, R., Wijngaard, H., Ariës-Kronenburg, N.A., Straatsma, G., Schaap, P.J., 2003. Lignin degradation by *Agaricus bisporus* accounts for a 30% increase in bioavailable holocellulose during cultivation on compost. J. Agric. Food Chem. 51, 2242-5.
- Heaton, L.L.M., López, E., Maini, P.K., Fricker, M.D., Jones, N.S., 2010. Growth-induced mass flows in fungal networks. Proc. R. Soc. B Biol. Sci. 277, 3265-3274.
- Heleno, S. A., Barros, L., Martins, A., Queiroz, M. J., Santos-Buelga, C., Ferreira, I. C., 2012. Phenolic, polysaccharidic, and lipidic fractions of mushrooms from northeastern Portugal: chemical compounds with antioxidant properties. J. Agr. Food Chem. 60, 4634-4640.
- Heleno, S.A., Barros, L., Sousa, M.J., Martins, A., Ferreira, I.C.F.R., 2009. Study and characterization of selected nutrients in wild mushrooms from Portugal by gas chromatography and high performance liquid chromatography. Microchem. J. 93, 195-199.
- Heller, K.B., Lin, E.C., Wilson, T.H., 1980. Substrate specificity and transport properties of the glycerol facilitator of *Escherichia coli*. J. Bacteriol. 144, 274-278.
- Helsby, L., 1976. Structural development of mycelium of *Serpula lacrymans*. PhD thesis, University of Oxford.
- Heneghan, M.N., Burns, C., Costa, A.M.S.B., Burton, K.S., Challen, M.P., Bailey, A.M., Foster, G.D. (2016) Functional analysis of *Agaricus bisporus* serine proteinase 1 reveals roles in utilization of humic rich substrates and adaptation to the leaf-litter ecological niche. Environ. Microbiol. 18, 4687-4696.
- Herman, K.C., Wösten, H.A.B., Fricker, M.D., Bleichrodt, R.J., 2020. Growth induced translocation effectively directs an amino acid analogue to developing zones in *Agaricus bisporus*. Fungal Biol. 124, 1013-1023
- Herman, K.C., Wösten, H.A.B., Fricker, M.D., Bleichrodt, R.J., 2020. Growth induced translocation effectively directs an amino acid analogue to developing zones in *Agaricus bisporus*. Fungal Biol. 124, 1013-1023.
- Herman, K.C., Bleichrodt, R., 2021. Go with the flow: mechanisms driving water transport during vegetative growth and fruiting. Fungal Biol. Rev. 41, 10-23.
- Hofrichter, M., 2002 Review: lignin conversion by manganese peroxidase (MnP). Enzyme Microb. Technol. 30, 454-466.
- Hohmann, S., 2002. Osmotic stress signaling and osmoadaptation in yeasts. Microbiol. Mol. Biol. Rev. 66, 300-372.
- Hohmann, S., Krantz, M., Nordlander, B., 2007. Yeast osmoregulation. Meth. Enzymol. 428, 29-45.
- Hohmann, S., 2009. Control of high osmolarity signalling in the yeast *Saccharomyces cerevisiae*. FEBS Lett. 583, 4025-4029
- Hong, J.-S., Kim, T.-Y., 1988. Contents of free-sugars & free-sugaralcohols in *Pleurotus ostreatus*, *Lentinula edodes* & *Agaricus bisporus*. Korean J. Food Sci. Technol. 20, 459-462.
- Hunter, S., Apweiler, R., Attwood, T.K., Bairoch, A., Bateman, A., Binns, D., Bork, P., Das, U., Daugherty, L., Duquenne, L., Finn, R.D., 2009. InterPro: The integrative protein signature database. Nucleic Acids. Res. 37, 211-215.

- Husher, J., Cesarov, S., Davis, C.M., Fletcher, T.S., Mbutia, K., Richey, L., Sparks, R., Turpin, L.A., Money, N.P., 1999. Evaporative cooling of mushrooms. *Mycologia* 91, 351-352.
- Iiyama, K., Stone, B.A., Macauley, B.J., 1994. Compositional changes in compost during composting and growth of *Agaricus bisporus*. *Appl. Environ. Microbiol* 60, 1538-1546.
- Jennings, L., Watkinson, S.C., 1982. Structure and development of mycelial strands in *Serpula lacrimans*. *Trans. Br. Mycol. Soc.* 78, 465-474.
- Jennings, D.H., 1984. Water flow through mycelia. In: Jennings DH, Rayner ADM (eds), *The Ecology and Physiology of the Fungal Mycelium*. Cambridge University Press, Cambridge, UK, pp. 55-79.
- Jennings, D.H., 1987. Translocation of solutes in fungi. *Biol. Rev.* 62: 215-243.
- Jurak, E., 2015. How mushrooms feed on compost: conversion of carbohydrates and lignin in industrial wheat straw based compost enabling the growth of *Agaricus bisporus*. Dissertation, Wageningen University.
- Jurak, E., Kabel, M.A., Gruppen, H., 2014. Carbohydrate composition of compost during composting and mycelium growth of *Agaricus bisporus*. *Carbohydr. Polym.* 101, 281-288.
- Jurak, E., Patyshakuliyeva, A., Kapsokalyvas, D., Xing, L., Van Zandvoort, M.A.M.J., de Vries, R.P., Gruppen, H., Kabel, M.A., 2015a. Accumulation of recalcitrant xylan in mushroom-compost is due to a lack of xylan substituent removing enzyme activities of *Agaricus bisporus*. *Carbohydr. Polym.* 132, 359-368.
- Jurak, E., Punt, A.M., Arts, W., Kabel, M.A., Gruppen, H., 2015b. Fate of carbohydrates and lignin during composting and mycelium growth of *Agaricus bisporus* on wheat straw based compost. *PLoS One* 10, e0138909.
- Kabel, M.A., Jurak, E., Mäkelä, M.R., de Vries, R.P., 2017. Occurrence and function of enzymes for lignocellulose degradation in commercial *Agaricus bisporus* cultivation. *Appl. Microbiol. Biotechnol.* 101, 4363-4369.
- Kalač, P., 2016. Carbohydrates and dietary fiber. In: Bandeira N, Leme MK, Garcia ACA (eds), *Edible Mushrooms: Chemical Composition and Nutritional Value*. Academic Press, Elsevier, USA, pp. 32-45.
- Kalberer, P.P., 1983. Influence of the depth of the casing layer and the harvesting time on changes of the water content of the casing layer and the substrate caused by the first flush of mushrooms. *Sci. Hortic.* 21, 9-18.
- Kalberer, P.P., 1985. Influence of the depth of the casing layer on the water extraction from casing soil and substrate by the sporophores, on the yield and on the dry matter content of the fruit bodies of the first three flushes of the cultivated mushroom, *Agaricus bisporus*. *Sci. Hortic.* 27, 33-43.
- Kalberer, P.P., 1987. Water potentials of casing and substrate and osmotic potentials of fruit bodies of *Agaricus bisporus*. *Sci. Hortic.* 32, 175-182.
- Kalberer, P.P., 1990a. Influence of the water potential of the casing soil on crop yield and on dry-matter content, osmotic potential and mannitol content of the fruit bodies of *Agaricus bisporus*. *J. Hortic. Sci.* 65, 573-581.
- Kalberer, P.P., 1990b. Water relations of the mushroom culture *Agaricus bisporus*: Study of a single break. *Sci. Hortic.* 41, 277-283.
- Kalberer, P.P., 2006. Availability of water in the substrate of *Agaricus bisporus*. *Eur. J. Hortic. Sci.* 71, 207-211.
- Kathiara, M., Wood, D.A., Evans, C.S., 2000. Detection and partial characterization of oxalate decarboxylase from *Agaricus bisporus*. *Mycol. Res.* 104, 345-350.
- Kerrigan, R.W., Challen, M.P., Burton, K.S., 2013. *Agaricus bisporus* genome sequence: a commentary. *Fungal Genet. Biol.* 55, 2-5.
- Kersten, P.J., Kirk, T.K., 1987. Involvement of a new enzyme, glyoxal oxidase, in extracellular H₂O₂ production by *Phanerochaete chrysosporium*. *J. Bacteriol.* 169, 2195-2201.
- Kim, D., Langmead, B., Salzberg, S.L., 2015. HISAT: A fast spliced aligner with low memory requirements. *Nat. Methods.* 12, 357-360.
- Korripally, P., Hunt, C.G., Houtman, C.J., Jones, D.C., Kitin, P.J., Cullen, D., Hammel, K.E., 2015. Regulation of gene expression during the onset of ligninolytic oxidation by *Phanerochaete chrysosporium* on spruce wood. *Appl. Environ. Microbiol.* 81, 7802-7812.

- Krantz, M., Becit, E., Hohmann, S., 2006a. Comparative analysis of HOG pathway proteins to generate hypotheses for functional analysis. *Curr. Genet.* 49, 152–165.
- Krantz, M., Becit, E., Hohmann, S., 2006b. Comparative genomics of the HOG-signaling system in fungi. *Curr. Genet.* 49, 137–151.
- Krijgsheld, P., Nitsche, B.M., Post, H., Levin, A.M., Muller, W.H., Heck, A.J., Ram, A.F., Altelaar, A.M., Wösten, H.A.B., 2013. Deletion of *flbA* results in increased secretome complexity and reduced secretion heterogeneity in colonies of *Aspergillus niger*. *J. Proteome Res.* 12, 1808–1819.
- Krogh, A., Larsson, B., Von Heijne, G., Sonnhammer, E.L., 2001. Predicting transmembrane protein topology with a hidden Markov model: Application to complete genomes. *J. Mol. Biol.* 305, 567–580.
- Lavín, J.L., Ramírez, L., Ussery, D.W., Pisabarro, A.G., Oguiza, J.A., 2010. Genomic analysis of two-component signal transduction proteins in basidiomycetes. *J. Mol. Microbiol. Biotechnol.* 18, 63–73.
- Lavín, J.L., García-Yoldi, A., Ramírez, L., Pisabarro, A.G., Oguiza, J.A., 2013. Two-component signal transduction in *Agaricus bisporus*: A comparative genomic analysis with other basidiomycetes through the web-based tool BASID2CS. *Fungal Genet. Biol.* 55, 77–84.
- Lawrence, C.L., Botting, C.H., Antrobus, R., Coote, P.J., 2004. Evidence of a new role for the high-osmolarity glycerol mitogen-activated protein kinase pathway in yeast: regulating adaptation to citric acid stress. *Mol. Cell. Biol.* 24, 3307–3323.
- Lee, J., Reiter, W., Dohnal, I., Gregori, C., Beese-Sims, S., Kuchler, K., Ammerer, G., Levin, D.E., 2013. MAPK Hog1 closes the *S. cerevisiae* glycerol channel Fps1 by phosphorylating and displacing its positive regulators. *Genes Dev.* 27, 2590–2601.
- Levin, J.Z., Yassour, M., Adiconis, X., Nusbaum, C., Thompson, D.A., Friedman, N., Gnirke, A., Regev, A., 2010. Comprehensive comparative analysis of strand-specific RNA sequencing methods. *Nat. Methods.* 7, 709–715.
- Lew, R.R., 2005. Mass flow and pressure-driven hyphal extension in *Neurospora crassa*. *Microbiology* 151, 2685–2692.
- Lew, R.R., Levina, N.N., Shabala, L., Anderca, M.I., Shabala, S.N., 2006. Role of a mitogen-activated protein kinase cascade in ion flux-mediated turgor regulation in fungi. *Eukaryot. Cell* 5, 480–487.
- Lew, R.R., 2011. How does a hypha grow? the biophysics of pressurized growth in fungi. *Nat. Rev. Microbiol.* 9, 509–518.
- Leyh, R., Blok, C., 2017. Input/Output: hoeveelheid en volume compost in de champignonweek. Rapport GTB 1437, 1–42.
- Lindahl, B., Finlay, R., Olsson, S., 2001. Simultaneous, bidirectional translocation of ³²P and ³³P between wood blocks connected by mycelial cords of *Hypholoma fasciculare*. *New Phytol.* 150, 189–194.
- Lindahl, B.D., Ihrmark, K., Boberg, J., Trumbore, S.E., Höglberg, P., Stenlid, J., Finlay, R.D., 2007. Spatial separation of litter decomposition and mycorrhizal nitrogen uptake in a boreal forest. *New Phytol.* 173, 611–620.
- Liu, X. Bin, Xia, E.H., Li, M., Cui, Y.Y., Wang, P.M., Zhang, J.X., Xie, B.G., Xu, J.P., Yan, J.J., Li, J., Nagy, L.G., Yang, Z.L., 2020. Transcriptome data reveal conserved patterns of fruiting body development and response to heat stress in the mushroom forming fungus *Flammulina filiformis*. *PLoS One* 15, 1–18.
- Lu, W., Winding, M., Lakonishok, M., Wildonger, J., Gelfand, V.I., 2016. Microtubule-microtubule sliding by kinesin-1 is essential for normal cytoplasmic streaming in *Drosophila* oocytes. *Proc. Natl. Acad. Sci. U.S.A.* 113, E4995–5004.
- Luard, E.J., Griffin, D.M., 1981. Effect of water potential on fungal growth and turgor. *Trans. Br. Mycol. Soc.* 76, 33–40.
- Luard, E.J., 1982a. Effect of osmotic shock on some intracellular solutes in two filamentous fungi. *J. Gen. Microbiol.* 128, 2575–2581.
- Luard, E.J., 1982b. Accumulation of intracellular solutes by two filamentous fungi in response to growth at low steady state osmotic potential. *J. Gen. Microbiol.* 128, 2563–2574.
- Lugones, L.G., Wösten, H.A.B., Wessels, J.G.H., 1998. A hydrophobin (ABH3) specifically secreted by vegetatively growing hyphae of *Agaricus bisporus* (common white button mushroom). *Microbiology* 144, 2345–2353.

- Mader, E.O., 1943. Some factors inhibiting the fructification and production of the cultivated mushroom, *Agaricus campestris* L. *Phytopathology* 33, 1134-1145.
- Maeda, T., Takekawa, M., Saito, H., 1995. Activation of yeast PBS2 MAPKK by MAPKKs or by binding of an SH3-containing osmosensor. *Science* 269, 554-558.
- Matcham, S.E., Jordan, B.R., Wood, D.A., 1985. Estimation of fungal biomass in a solid substrate by three independent methods. *Appl. Microbiol. Biotechnol.* 21, 108-112.
- Mathew, K.T., 1961. Morphogenesis of mycelial strands in the cultivated mushroom, *Agaricus bisporus*, *Trans. Br. Mycol. Soc.* 44, 285-290.
- McGee, C.F., Byrne, H., Irvine, A., Wilson, J., 2017. Diversity and dynamics of the DNA and cDNA-derived bacterial compost communities throughout the *Agaricus bisporus* mushroom cropping process. *Ann. Microbiol.* 67, 751-761.
- McGee, C.F., 2018. Microbial ecology of the *Agaricus bisporus* mushroom cropping process. *Appl. Microbiol. Biotechnol.* 102, 1075-1083.
- Molloy, S., 2004. Sugar transport and water relations of *Agaricus bisporus*, Ph.D Thesis, Chapter 3. Cranfield University.
- Money, N.P., Ravishankar, J.P., 2005. Biomechanics of stipe elongation in the basidiomycete *Coprinopsis cinerea*. *Mycol. Res.* 109, 627-634.
- Moore, D., 1998. Development of form. In: *Fungal Morphogenesis*. Cambridge University Press, Cambridge, UK, pp. 249-287.
- Morin, E., Kohler, A., Baker, A.R., Foulongne-Oriol, M., Lombard, V., Nagy, L.G., Ohm, R.A., Patyshakuliyeva, A., Brun, A., Aerts, A.L., Bailey, A.M., Billette, C., Coutinho, P.M., Deakin, G., Doddapaneni, H., Floudas, D., Grimwood, J., Hildén, K., Kües, U., Labutti, K.M., Lapidus, A., Lindquist, E.A., Lucas, S.M., Murat, C., Riley, R.W., Salamov, A.A., Schmutz, J., Subramanian, V., Wösten, H. a B., Xu, J., Eastwood, D.C., Foster, G.D., Sonnenberg, A.S.M., Cullen, D., de Vries, R.P., Lundell, T., Hibbett, D.S., Henrissat, B., Burton, K.S., Kerrigan, R.W., Challen, M.P., Grigoriev, I. V., Martin, F., Nagye, L.G., Ohm, R.A., Patyshakuliyeva, A., Brun, A., Aerts, A.L., Bailey, A.M., Billette, C., Coutinho, P.M., Deakin, G., Doddapaneni, H., Floudas, D., Grimwood, J., Hilden, K., Kues, U., Labutti, K.M., Lapidus, A., Lindquist, E.A., Lucas, S.M., Murat, C., Riley, R.W., Salamov, A.A., Schmutz, J., Subramanian, V., Wosten, H.A.B., Xu, J., Eastwood, D.C., Foster, G.D., Sonnenberg, A.S.M., Cullen, D., de Vries, R.P., Lundell, T., Hibbett, D.S., Henrissat, B., Burton, K.S., Kerrigan, R.W., Challen, M.P., Grigoriev, I.V., Martin, F., 2012. Genome sequence of the button mushroom *Agaricus bisporus* reveals mechanisms governing adaptation to a humic-rich ecological niche. *Proc. Natl. Acad. Sci. USA* 109, 17501-17506.
- Moukha, S.M., Wosten, H.A.B., Asther, M., Wessels, J.G.H., 1993. In situ localization of the secretion of lignin peroxidases in colonies of *Phanerochaete chrysosporium* using a sandwiched mode of culture. *J. Gen. Microbiol.* 139, 969-978
- Mounir, A., Messnaoui, B., Dinane, A., Samaouli, A., 2020. Determination of water activity, osmotic coefficient, activity coefficient, solubility, excess Gibbs energy and transfer Gibbs energy of KCl-D-sucrose-water mixture at 298.15 K. *J. Chem. Thermodyn.* 142, 105962.
- Muralidhar, A., Swadel, E., Spiekerman, M., Sui, S., Fraser, M., Ingerfeld, M., Tayagui, A.B., Garrill, A., 2016. A pressure gradient facilitates mass flow in the oomycete *Achlya bisexualis*. *Microbiology* 162, 206-213.
- Nehls, U., Dietz, S., 2014. Fungal aquaporins: cellular functions and ecophysiological perspectives. *Appl. Microbiol. Biotechnol.* 98, 8835-8851.
- Nobel, P.S., 1991. Plants and fluxes. In: *Physicochemical and Environmental Plant Physiology*. San Diego Academic Press, San Diego, USA, pp. 508-513.
- Noble, R., Dobrovin-Pennington, A., Evered, C., Mead, A., 1999. Properties of peat-based casing soils and their influence on the water relations and growth of the mushroom (*Agaricus bisporus*). *Plant Soil* 207, 1-13.
- Nuss, I., Jennings, D.H., Weltkamp, C.J., 1991. Morphology of *Serpula lacrymans*. In: Jennings DH, Bravery AF (eds), *Serpula lacrymans: Fundamental Biology and Control Strategies*. John Wiley & Sons, Chichester, UK, pp. 9-38.

- O'Connor, E., Owens, R.A., Doyle, S., Amini, A., Grogan, H., Fitzpatrick, D.A., 2020. Proteomic investigation of interhyphal interactions between strains of *Agaricus bisporus*. *Fungal Biol.* 124, 579–591.
- O'Rourke, S.M., Herskowitz, I., O'Shea, E.K., 2002. Yeast go the whole HOG for the hyperosmotic response. *Trends Genet.* 18, 405–412.
- Olsson, S., Gray, S.N., 1998. Patterns and dynamics of ³²P-phosphate and labelled 2-aminoisobutyric acid (¹⁴C-AIB) translocation in intact basidiomycete mycelia. *FEMS Microbiol. Ecol.* 26, 109–120.
- Osono, T., 2007. Ecology of ligninolytic fungi associated with leaf litter decomposition. *Ecol. Res.* 22, 955–974.
- Panadero, J., Pallotti, C., Rodríguez-Vargas, S., Rande-Gil, F., Prieto, J.A., 2006. A downshift in temperature activates the high osmolarity glycerol (HOG) pathway, which determines freeze tolerance in *Saccharomyces cerevisiae*. *J. Biol. Chem.* 281, 4638–4645.
- Parkhomchuk, D., Borodina, T., Amstislavskiy, V., Banaru, M., Hallen, L., Krobitch, S., Lehrach, H., Soldatov, A., 2009. Transcriptome analysis by strand-specific sequencing of complementary DNA. *Nucleic Acids Res.* 37, e123.
- Patyshakuliyeva, A., Jurak, E., Kohler, A., Baker, A., Battaglia, E., de Bruijn, W., Burton, K.S., Challen, M.P., Coutinho, P.M., Eastwood, D.C., Gruben, B.S., Mäkelä, M.R., Martin, F., Nadal, M., van den Brink, J., Wiebenga, A., Zhou, M., Henrissat, B., Kabel, M., Gruppen, H., de Vries, R.P., 2013. Carbohydrate utilization and metabolism is highly differentiated in *Agaricus bisporus*. *BMC Genomics* 14, 663.
- Patyshakuliyeva, A., Mäkelä, M.R., Sietiö, O.M., de Vries, R.P., Hildén, K.S., 2014. An improved and reproducible protocol for the extraction of high quality fungal RNA from plant biomass substrates. *Fungal Genet. Biol.* 72, 201–206.
- Patyshakuliyeva, A., Post, H., Zhou, M., Jurak, E., Heck, A.J.R., Hildén, K.S., Kabel, M.A., Mäkelä, M.R., Altelaar, M.A.F., de Vries, R.P., 2015. Uncovering the abilities of *Agaricus bisporus* to degrade plant biomass throughout its life cycle. *Environ. Microbiol.* 17, 3098–3109.
- van Peer, A.F., Müller, W.H., Boekhout, T., Lugones, L.G., Wösten, H.A.B., 2009. Cytoplasmic continuity revisited: Closure of septa of the filamentous fungus *Schizophyllum commune* in response to environmental conditions. *PLoS One* 4, e5977.
- Petersen, T.N., Brunak, S., von Heijne, G., Nielsen, H., 2011. SignalP 4.0: discriminating signal peptides from transmembrane regions. *Nat. Methods* 8, 785–786.
- Pieuchot, L., Lai, J., Loh, R.A., Leong, F.Y., Chiam, K.H., Stajich, J., Jedd, G., 2015. Cellular subcompartments through cytoplasmic streaming. *Dev. Cell* 34, 410–420.
- Presley, G.N., Panisko, E., Purvine, S.O., Schilling, J.S., 2018. Coupling Secretomics with enzyme activities to compare the temporal processes of wood metabolism among white and brown rot fungi. *Appl. Environ. Microbiol.* 84, e00159–18.
- Presley, G.N., Schilling, J.S., 2017. Distinct growth and secretome strategies for two taxonomically divergent brown rot fungi. *Appl. Environ. Microbiol.* 83, e02987–16.
- Proft, M., Struhl, K., 2004. MAP kinase-mediated stress relief that precedes and regulates the timing of transcriptional induction. *Cell* 118, 351–361.
- Ramirez, M.L., Chulze, S.N., Magan, N., 2004. Impact of osmotic and matric water stress on germination, growth, mycelial water potentials and endogenous accumulation of sugars and sugar alcohols in *Fusarium graminearum*. *Mycologia* 96, 470–478.
- Rast, D., 1965. Zur stoffwechselphysiologischen bedeutung van Mannit und Trehalose in *Agaricus bisporus*. *Planta* 64, 81–93.
- Rawlings, N.D., Barrett, A.J., Finn, R., 2016. Twenty years of the MEROPS database of proteolytic enzymes, their substrates, and inhibitors. *Nucleic Acids Res.* 44, D343–D350.
- Reis, F.S., Barros, L., Martins, A., Ferreira, I.C., 2012. Chemical composition and nutritional value of the most widely appreciated cultivated mushrooms: an inter-species comparative study. *Food Chem. Toxicol.* 50, 191–197.

- Reiser, V., Raitt, D.C., Saito, H., 2003. Yeast osmosensor Sln1 and plant cytokinin receptor Cre1 respond to changes in turgor pressure. *J. Cell Biol.* 161, 1035–1040.
- Riber Rasmussen, C., 1959. Controlled air movement and its effect on cropping yields. *Mushroom Sci.* 5, 222–234.
- Riley, R., Salamov, A.A., Brown, D.W., Nagy, L.G., Floudas, D., Held, B.W., Lvasseur, A., Lombard, V., Morin, E., Otilar, R., Lindquist, E.A., Sun, H., LaButti, K.M., Schmutz, J., Jabbour, D., Luo, H., Baker, S.E., Pisabarro, A.G., Walton, J.D., Blanchette, R.A., Henrissat, B., Martin, F., Cullen, D., Hibbett, D.S., Grigoriev, I. V., 2014. Extensive sampling of basidiomycete genomes demonstrates inadequacy of the white-rot/brown-rot paradigm for wood decay fungi. *Proc. Natl. Acad. Sci. U. S. A.* 111, 9923–9928.
- Roberts, A., Trapnell, C., Donaghey, J., Rinn, J.L., Pachter, L., 2011. Improving RNA-Seq expression estimates by correcting for fragment bias. *Genome Biol.* 12, 1–14.
- Ross, R.C., Harris, P.J., 1983. The significance of thermophilic fungi in mushroom compost preparation. *Sci. Hortic.* 20, 61–70.
- Saito, H., Posas, F., 2012. Response to hyperosmotic stress. *Genetics* 192, 289–318.
- San Antonio, J., Flegg, P., 1964. Transpiration from the sporophore of *Agaricus bisporus* 'White'. *Am. J. Bot.* 51, 1129–1132.
- Savoie, J.M., Salmones, D., Mata, G., 2007. Hydrogen peroxide concentration measured in cultivation substrates during growth and fruiting of the mushrooms *Agaricus bisporus* and *Pleurotus* spp. *J. Sci. Food Agric.* 87, 1337–1344.
- Schaber, J., Adrover, M.À., Eriksson, E., Pelet, S., Petelenz-Kurdziel, E., Klein, D., Posas, F., Goksör, M., Peter, M., Hohmann, S., Klipp, E., 2010. Biophysical properties of *Saccharomyces cerevisiae* and their relationship with HOG pathway activation. *Eur. Biophys. J.* 39, 1547–1556.
- Schilling, J.S., Kaffenberger, J.T., Liew, F.J., Song, Z., 2015. Signature wood modifications reveal decomposer community history. *PLoS One* 10, 120679.
- Schindelin, J., Arganda-Carreras, I., Frise, E., Kaynig, V., Longair, M., Pietzsch, T., Preibisch, S., Rueden, C., Saalfeld, S., Schmid, B., Tinevez, J.Y., White, D.J., Hartenstein, V., Eliceiri, K., Tomancak, P., Cardona, A., 2012. Fiji: an open-source platform for biological-image analysis. *Nat. Methods* 9, 676–682.
- Schmieder, S.S., Stanley, C.E., Rzepiela, A., van Swaay, D., Sabotič, J., Nørrelykke, S.F., deMello, A.J., Aebi, M., Künzler, M., 2019. Bidirectional propagation of signals and nutrients in fungal networks via specialized hyphae. *Curr. Biol.* 217–228.
- Seaby, D.A., 1996. Investigation of the epidemiology of green mould of mushroom (*Agaricus bisporus*) compost caused by *Trichoderma harzianum*. *Plant Pathol.* 45, 913–923.
- Sharma, P.D., Fisher, P.J., Webster, J., 1977. Critique of the chitin assay technique for estimation of fungal biomass. *Trans. Br. Mycol. Soc.* 69, 479–483.
- Siebrecht, S., Herdel, K., Schurr, U., Tischner, R., 2003. Nutrient translocation in the xylem of poplar--diurnal variations and spatial distribution along the shoot axis. *Planta* 217, 783–793.
- Smith, R.S., 1973. Continuous automatic measurement of rhythms in fungal respiration using a gas chromatograph. *Can. J. Bot.* 51, 701–710.
- Sonnenberg, A.S.M., Sedaghat-Telgerd, N., Lavrijssen, B., Ohm, R.A., Hendrickx, P.M., Scholtmeijer, K., Baars, J.J.P., van Peer, A., 2020. Telomere-to-telomere assembled and centromere annotated genomes of the two main subspecies of the button mushroom *Agaricus bisporus* reveal especially polymorphic chromosome ends. *Sci. Rep.* 10, 1–15.
- Soveral, G., Madeira, A., Loureiro-Dias, M.C., Moura, T.F., 2008. Membrane tension regulates water transport in yeast. *Biochim. Biophys. Acta - Biomembr.* 1778, 2573–2579.
- Steffen, K.T., Cajthaml, T., Šnajdr, J., Baldrian, P., 2007. Differential degradation of oak (*Quercus petraea*) leaf litter by litter-decomposing basidiomycetes. *Res. Microbiol.* 158, 447–455.
- Steinberg, G., 2014. Endocytosis and early endosome motility in filamentous fungi. *Curr. Opin. Microbiol.* 20, 10–18.

- Stoop, J. M. H., Mooibroek, H., 1998. Cloning and characterization of NADP- mannitol dehydrogenase cDNA from the button mushroom, *Agaricus bisporus*, and its expression in response to NaCl stress. *Appl. Environ. Microbiol.* 64, 4689-4696.
- Stouthamer, A.H., 1973. A theoretical study on the amount of ATP required for synthesis of microbial cell material. *Antonie Van Leeuwenhoek* 39, 545-565.
- Straatsma, G., Gerrits, J.P., Augustijn, M.P., op den Camp, H.J.O., Vogels, G.D., van Griensven, L.J.L.D., 1989. Population dynamics of *Scytalidium thermophilum* in mushroom compost and stimulatory effects on growth rate and yield of *Agaricus bisporus*. *Microbiology* 135, 751-759.
- Straatsma, G., Gerrits, J.P.G., Gerrits, T.M., op den Camp, H.J.M., van Griensven, L.J.L.D., 1991. Growth kinetics of *Agaricus bisporus* mycelium on solid substrate (mushroom compost). *J. Gen. Microbiol.* 137, 1471-1477.
- Straatsma, G., Samson, R.A., 1993. Taxonomy of *Scytalidium thermophilum*, an important thermophilic fungus in mushroom compost. *Mycol. Res.* 97, 321-328.
- Straatsma, G., Olijnsma, T.W., Gerrits, J.P., Amsing, J.G., op den Camp, H.J.O., van Griensven, L.J.L.D., 1994a. Inoculation of *Scytalidium thermophilum* in button mushroom compost and its effect on yield. *Appl. Environ. Microbiol.* 60, 3049-3054.
- Straatsma, G., Samson, R.A., Olijnsma, T.W., Op den Camp, H.J.M., Gerrits, J.P.G., van Griensven, L.J.L.D., 1994b. Ecology of thermophilic fungi in mushroom compost, with emphasis on *Scytalidium thermophilum* and growth stimulation of *Agaricus bisporus* mycelium. *Appl. Environ. Microbiol.* 60, 454-458.
- Straatsma, G., Sonnenberg, A.S., van Griensven, L.J.L.D., 2013. Development and growth of fruit bodies and crops of the button mushroom, *Agaricus bisporus*. *Fungal Biol.* 117, 697-707.
- Straatsma, G., Sonnenberg, A.S.M., van Griensven, L.J.L.D., 2013. Development and growth of fruit bodies and crops of the button mushroom, *Agaricus bisporus*. *Fungal Biol.* 117, 697-707.
- Swaminathan, R., Hoang, C.P., Verkman, A.S., 1997. Photobleaching recovery and anisotropy decay of green fluorescent protein GFP-S65T in solution and cells: cytoplasmic viscosity probed by green fluorescent protein translational and rotational diffusion. *Biophys. J.* 72, 1900-1907.
- Szeto, C.Y.Y., Wong, Q.W.L., Leung, G.S., Kwan, H.S., 2008. Isolation and transcript analysis of two-component histidine kinase gene *Le.nik1* in Shiitake mushroom, *Lentinula edodes*. *Mycol. Res.* 112, 108-116.
- Taiz, L., Zeiger, E., Max Moller, I., Murphy, A., 2014. *Plant Physiology and Development*, Sixth Edition. Sinauer Associates.
- Tamás, M.J., Luyten, K., Sutherland, F.C.W., Hernandez, A., Albertyn, J., Valadi, H., Li, H., Prior, B.A., Kilian, S.G., Ramos, J., Gustafsson, L., Thevelein, J.M., Hohmann, S., 1999. Fps1p controls the accumulation and release of the compatible solute glycerol in yeast osmoregulation. *Mol. Microbiol.* 31, 1087-1104.
- Tan, Y.H., Moore, D., 1994. High concentrations of mannitol in the shiitake mushroom *Lentinula edodes*. *Microbios* 79, 31-35.
- Tegelaar, M., Wösten, H.A.B., 2017. Functional distinction of hyphal compartments. *Sci. Rep.* 7, 6039.
- Tegelaar, M., van der Lans, G.P.A., Wösten, H.A.B., 2020. Apical but not sub-apical hyphal compartments are self-sustaining in growth. *Antonie van Leeuwenhoek* 113, 697-706.
- Thompson, W., Eamus, D., Jennings, D.H., 1985. Water flux through mycelium of *Serpula lacrimans*. *Trans. Brit. Mycol. Soc.* 84, 601-608.
- Thornton, W.M., 1917. The relation of oxygen to the heat of combustion of organic compounds. London, Edinburgh, Dublin *Philos. Mag. J. Sci.* 33, 196-203.
- Tlalka, M., Watkinson, S.C., Darrah, P.R., Fricker, M.D., 2002. Continuous imaging of amino-acid translocation in intact mycelia of *Phanerochaete velutina* reveals rapid, pulsatile fluxes. *New Phytol.* 153, 173-184.
- Tlalka, M., Hensman, D., Darrah, P.R., Watkinson, S.C., Fricker, M.D., 2003. Noncircadian oscillations in amino acid transport have complementary profiles in assimilatory and foraging hyphae of *Phanerochaete velutina*. *New Phytol.* 158, 325-335.

- Tlalka, M., Bebber, D.P., Darrah, P.R., Watkinson, S.C., Fricker, M.D., 2007. Emergence of self-organised oscillatory domains in fungal mycelia. *Fungal Genet. Biol.* 44, 1085–1095.
- Tlalka, M., Fricker, M., Watkinson, S., 2008a. Imaging of long-distance alpha-aminoisobutyric acid translocation dynamics during resource capture by *Serpula lacrymans*. *Appl. Environ. Microbiol.* 74, 2700–2708.
- Tlalka, M., Bebber, D.P., Darrah, P.R., Watkinson, S.C., Fricker, M.D., 2008b. Quantifying dynamic resource allocation illuminates foraging strategy in *Phanerochaete velutina*. *Fungal Genet. Biol.* 45, 1111–1121.
- Trapnell, C., Williams, B.A., Pertea, G., Mortazavi, A., Kwan, G., Van Baren, M.J., Salzberg, S.L., Wold, B.J., Pachter, L., 2010. Transcript assembly and quantification by RNA-Seq reveals unannotated transcripts and isoform switching during cell differentiation. *Nat. Biotechnol.* 28, 511–515.
- Trinci, A.P.J., 1973. The hyphal growth unit of wild type and spreading colonial mutants of *Neurospora crassa*. *Arch. Mikrobiol.* 91, 127–136.
- Trinci, A.P.J., 1974. A study of the kinetics of hyphal extension and branch initiation of fungal mycelia. *J. Gen. Microbiol.* 81, 225–236.
- Tuller, M., Or, D., 2005. Water retention and characteristic curve. In: Hillel, D. (Ed.), *Encyclopedia of soils in the environment*, pp. 278–289.
- Umar, M.H., van Griensven, L.J.L.D., 1998. The role of morphogenetic cell death in the histogenesis of the mycelial cord of *Agaricus bisporus* and in the development of macrofungi. *Mycol. Res.* 102, 719–735.
- Urzúa, U., Kersten, P.J., Vicuña, R., 1998. Manganese peroxidase-dependent oxidation of glyoxylic and oxalic acids synthesized by *Ceriporiopsis subvermispora* produces extracellular hydrogen peroxide. *Appl. Environ. Microbiol.* 64, 68–73.
- Verma, R.K., Prabh, N.D., Sankaramakrishnan, R., 2014. New subfamilies of major intrinsic proteins in fungi suggest novel transport properties in fungal channels: Implications for the host-fungal interactions. *BMC Evol. Biol.* 14, 173.
- Visscher, H.R., 1988. Functions of casing soil. In: van Griensven, L.J.L.D. (Ed.), *The cultivation of mushrooms*. Darlington Mushroom Laboratories Ltd., Darlington, pp. 29.
- Vos, A.M., Heijboer, A., Boschker, H.T.S., Bonnet, B., Lugones, L.G., Wösten, H.A.B., 2017a. Microbial biomass in compost during colonization of *Agaricus bisporus*. *AMB Express* 7.
- Vos, A.M., Jurak, E., Pelkmans, J.F., Herman, K., Pels, G., Baars, J.J., Hendrix, E., Kabel, M.A., Lugones, L.G., Wösten, H.A.B., 2017b. H₂O₂ as a candidate bottleneck for mnp activity during cultivation of *Agaricus bisporus* in compost. *AMB Express* 7, 1–9.
- Vos, A.M., Jurak, E., de Gijssel, P., Ohm, R.A., Henrissat, B., Lugones, L.G., Kabel, M.A., Wösten, H.A.B., 2018. Production of α-1,3-L-arabinofuranosidase active on substituted xylan does not improve compost degradation by *Agaricus bisporus*. *PLoS One* 13, e0201090.
- Wallander, H., Massicotte, H.B., Nylund, J.-E., 1997. Seasonal variation in protein, ergosterol and chitin in five morphotypes of *Pinus sylvestris* L. ectomycorrhizae in a mature Swedish forest. *Soil Biol. Biochem.* 29, 45–53.
- Wallander, H., Ekblad, A., Godbold, D.L., Johnson, D., Bahr, A., Baldrian, P., Björk, R.G., Kieliszewska-Rokicka, B., Kjoller, R., Kraigher, H., Plassard, C., Rudawska, M., 2013. Evaluation of methods to estimate production, biomass and turnover of ectomycorrhizal mycelium in forests soils- A review. *Soil Biol. Biochem.* 57, 1034–1047.
- Wannet, W.J.B., Op den Camp, H.J.M., Wisselink, H.W., van der Drift, C., Van Griensven, L.J.L.D., Vogels, G.D., 1998. Purification and characterization of trehalose phosphorylase from the commercial mushroom *Agaricus bisporus*. *Biochim. Biophys. Acta* 1425, 177–188.
- Wannet, W.J.B., Aben, E.M.J., Van der Drift, C., Van Griensven, L.J.L.D., Vogels, G.D., Op den Camp, H.J.M., 1999. Trehalose phosphorylase activity and carbohydrate levels during axenic fruiting in three *Agaricus bisporus* strains. *Curr. Microbiol.* 39, 205–210.

- Wannet, W.J.B., Hermans, J.H.M., Van Der Drift, C., op Den Camp, H.J.M., 2000. HPLC detection of soluble carbohydrates involved in mannitol and trehalose metabolism in the edible mushroom *Agaricus bisporus*. *J. Agric. Food Chem.* 48, 287–291.
- Watkinson, S.C., 1971. The mechanism of mycelial strand induction in *Serpula lacrimans*: A possible effect of nutrient distribution. *New Phytol.* 70, 1079–1088.
- Watkinson, S.C., 1975. The relation between nitrogen nutrition and formation of mycelial strands in *Serpula lacrimans*. *Trans. Br. Mycol. Soc.* 64, 195–200.
- Watkinson, S.C., 1979. Growth of rhizomorphs, mycelial strands, coremia and sclerotia. In: Burnett JH and Trinci APJ (eds), *Fungal Walls and Hyphal Growth*. Cambridge University Press, Cambridge, UK, pp. 93–113.
- Watkinson, S.C., 1984. Morphogenesis of *Serpula lacrimans* colony in relation to its function in nature. In: Jennings DH and Rayner ADM (eds), *Ecology and Physiology of the Fungal Mycelium*. British Mycological Society Symposium, Cambridge University Press, Cambridge, UK, pp. 165–184.
- Watkinson, S.C., 1999. Metabolism and hyphal differentiation in large basidiomycete colonies. In: Gow NAR, Robson G, Gadd GM (eds), *The fungal colony*. Cambridge University Press, Cambridge, UK, pp 127–157.
- Wells, T.K., Hammond, J.B.W. and Dickerson, A.G., 1987. Variations in activities of glycogen phosphorylase and trehalase during the periodic fruiting of the edible mushroom *Agaricus bisporus* (Lange) Imbach. *New Phytol.* 105: 273–280.
- Wells, J.M., Hughes, C., Boddy, L., 1990. The fate of soil-derived phosphorus in mycelial cord systems of *Phanerochaete velutina* and *Phallus impudicus*. *New Phytol.* 114, 595–606.
- Wells, J.M., Boddy, L., 1995. Phosphorus translocation by saprotrophic basidiomycete mycelial cord systems on the floor of a mixed deciduous woodland. *Mycol. Res.* 99, 977–980.
- Whalley, W.R., Ober, E.S., Jenkins, M., 2013. Measurement of the matric potential of soil water in the rhizosphere. *J. Exp. Bot.* 64, 3951–3963.
- Whipps, J.M., Lewis, D.H., 1980. Methodology of a chitin assay. *Trans. Br. Mycol. Soc.* 74, 416–418.
- Wiebe, H., 1966. Matric potential of several plant tissues and biocolloids. *Plant Physiol.* 41, 1439–1442.
- Winkler, A., Arkind, C., Mattison, C.P., Burkholder, A., Knoche, K., Ota, I., 2002. Heat stress activates the yeast high-osmolarity glycerol mitogen-activated protein kinase pathway, and protein tyrosine phosphatases are essential under heat stress. *Eukaryot. Cell* 1, 163–173.
- Wood, D.A., 1979. A method for estimating biomass of *Agaricus bisporus* in a solid substrate, composted wheat straw. *Biotechnol. Lett.* 1, 255–260.
- Wood, D.A., 1980. Production, purification, and properties of extracellular laccase of *Agaricus bisporus*. *Microbiology* 117, 327–338.
- Wood, D.A., 1983. Lignocellulose degradation during the life cycle of *Agaricus bisporus*. *FEMS Microbiol. Lett.* 20, 421–424.
- Woolston, B.M., Schlagnhauser, C., Wilkinson, J., Larsen, J., Shi, Z., Mayer, K.M., Walters, D.S., Curtis, W.R., Romaine, C.P., 2011. Long-distance translocation of protein during morphogenesis of the fruiting body in the filamentous fungus, *Agaricus bisporus*. *PLoS One* 6.
- Worrall, J.J., Anagnost, S.E., Zabel, R.A., 1997. Comparison of wood decay among diverse lignicolous fungi. *Mycologia* 89, 199–219.
- Wosten, H.A.B., Moukha, S.M., Sietsma, J.H., Wessels, J.G.H., 1991. Localization of growth and secretion of proteins in *Aspergillus niger*. *J. Gen. Microbiol.* 137, 2017–2023.
- Wösten, H.A.B., 2001. Hydrophobins: multipurpose proteins. *Annu. Rev. Microbiol.* 55, 625–646.
- Xu, H., Cooke, J.E.K., Zwiazek, J.J., 2013. Phylogenetic analysis of fungal aquaporins provides insight into their possible role in water transport of mycorrhizal associations. *Botany* 91, 495–504.
- Xu, H., Navarro-Ródenas, A., Cooke, J.E.K., Zwiazek, J.J., 2016. Transcript profiling of aquaporins during basidiocarp development in *Laccaria bicolor* ectomycorrhizal with *Picea glauca*. *Mycorrhiza* 26.

-
- Xu, N., Hu, X., Xu, W., Li, X., Zhou, L., Zhu, S., Zhu, J., 2017. Mushrooms as efficient solar steam-generation devices. *Adv. Mat.* 29, 1606762.
- Zhang, X., Zhong, Y., Yang, S., Zhang, W., Xu, M., Ma, A., Zhuang, G., Chen, G., Liu, W., 2014. Diversity and dynamics of the microbial community on decomposing wheat straw during mushroom compost production. *Bioresour. Technol.* 170, 183–195.
- Zhang, J., Presley, G.N., Hammel, K.E., Ryu, J.S., Menke, J.R., Figueroa, M., Hu, D., Orr, G., Schilling, J.S., 2016. Localizing gene regulation reveals a staggered wood decay mechanism for the brown rot fungus *Postia placenta*. *Proc. Natl. Acad. Sci. USA* 113, 10968–10973.
- Zhang, J., Silverstein, K.A.T., Castaño, J.D., Figueroa, M., Schilling, J.S., 2019. Gene regulation shifts shed light on fungal adaption in plant biomass decomposers. *MBio* 10, 10–1128.

Nederlandse Samenvatting

Introductie

Agaricus bisporus wordt gekweekt om zijn witte champignons. De meeste van deze paddenstoelen worden geproduceerd in Azië, gevolgd door Europa. Nederland was in het verleden marktleider in de Europese Unie (EU) met een productie van 323.000 ton in 2013. Sinds 2013 is de champignonproductie in Nederland echter gedaald tot ~ 260.000 ton in 2020 (EU-marktaandeel van 18,4 %). Nederland werd hierdoor recentelijk door Polen ingehaald als grootste producent van champignons in de EU.

In Nederland wordt *A. bisporus* geteelt op een gecomposteerd mengsel van stro, paardenmest, gips en water. Roggekorrels gekoloniseerd met de schimmel, ook wel broed genoemd, worden vermengd met de compost om *A. bisporus* in dit substraat te introduceren. De verhouding tussen compost en broed zorgt ervoor dat het mycelium afkomstig van elke broedkorrel slechts 2 cm in elke richting kan groeien voordat het mycelium van een andere korrel tegenkomt. Wanneer de compost in 16 – 19 dagen doorgroeit is met mycelium wordt een deklaag op basis van turf, waaraan kalk is toegevoegd, aangebracht. De deklaag wordt gedurende 7 dagen gekoloniseerd, waarna de vorming van paddenstoelen wordt geïnduceerd. Dit gebeurt door de temperatuur te verlagen naar 18 °C en de concentratie CO₂ te verlagen door te ventileren, waarbij de luchtvochtigheid hoog gehouden wordt (rond de 90 % relatieve luchtvochtigheid). De paddenstoelen worden geogst in 2 tot 3 vluchten met tussenpozen van 7 – 8 dagen.

Voor paddenstoelvorming moeten voedingsstoffen en water vanuit het mycelium naar de paddenstoelen worden getransporteerd. Het doel van dit proefschrift was om de kolonisatie van de compost door *A. bisporus* te bestuderen evenals het transport van water en voedingsstoffen, zowel binnen het mycelium als naar de paddenstoelen. Het begrijpen van deze processen zou moeten resulteren in aanknopingspunten om paddenstoelproductie efficiënter te laten verlopen.

Kolonisatie van de compost door *A. bisporus*

Doorgaans gaat men ervan uit dat een goede kolonisatie van de compost door *A. bisporus* leidt tot hogere champignonopbrengst. Het kwantificeren van de mate van kolonisatie is echter niet simpel. De huidige methoden voor het meten van de biomassa in de compost zijn doorgaans gebaseerd op het destructief nemen van monsters gedurende de groei. Met gebruik van een scanner was de kolonisatie van *A. bisporus* in de compost te visualiseren (**Hoofdstuk 2, 5**). Het mycelium van *A. bisporus* is wit en contrasteert met de donkere achtergrond van de compost. Daarom is de toename van de gemiddelde grijswaarde van de compost een marker voor de mate van kolonisatie. Deze scantechniek toonde aan dat de hyfen van de commerciële *A. bisporus*-stam A15 in ongeveer 8 dagen een compostvolume van 12 x 12 x 1 cm koloniseerde. Hierna nam de kolonisatie van het substraat verder toe door het opvullen van de gaten tussen het bestaande netwerk (**Hoofdstuk 5**). De wildtype stam MES 01808 had de hoogste maximale kolonisatie, gevolgd door stammen 901 en A15. Alle negen geteste stammen koloniseerden het substraat gelijkmatig, met uitzondering van MES 01808, die een bimodale verdeling van de kolonisatie vertoonde. De hogere kolonisatie van MES 01808 kan worden verklaard

door gebieden die zeer dichtbegroeid zijn met mycelium, terwijl andere gebieden op vergelijkbare wijze gekoloniseerd zijn, zoals bijvoorbeeld A15 dit doet. Verder werd aangetoond dat de wildtype stammen MES 01651, MES 01717, MES 01919 en de commerciële stammen A15 en 901 een logistisch groeiprofiel volgen. De groei van de wildtype stammen MES 03828 en MES 01620 daarentegen kon worden beschreven met een exponentiële fase gevolgd door een lineaire fase voordat maximale kolonisatie werd bereikt, terwijl wildtype stammen MES 01537 en MES 01808 meerdere kolonisatiefasen vertoonden (**Hoofdstuk 5**).

Een positieve correlatie ($r^2 = 0.6$, $p < 0.05$) werd gevonden tussen de maximale kolonisatie en de gemiddelde opbrengst mits stam MES 01808, die de laagste opbrengst vertoonde, niet in de analyse werd meegenomen. Dit geeft aan dat kolonisatie een voorspellende waarde heeft voor de opbrengst van paddenstoelen. Daarnaast lijkt het erop dat groei die resulteert in een bimodale verdeling van kolonisatie een ongewenste eigenschap is voor commerciële paddenstoelenproductie.

De productie van CO₂, het verbruik van O₂ en de temperatuur werden gemeten tijdens de groei van *A. bisporus* in de compost (**Hoofdstuk 2**). Deze metingen lieten tijdelijke verhogingen van respiratie zien met een lengte van 2.5 - 5 uur en tussenliggende periodes variërend van slechts 13 uur (vroeg kolonisatie) tot wel 90 uur (late kolonisatie). Een temperatuurstijging van de compost tot 2 °C werd 30 minuten na het begin van een respiratiepiek gedetecteerd. De toename piekte 45 - 90 minuten later en het duurde 2 tot 8 uur voordat de temperatuur was genormaliseerd naar de temperatuur van voor de piek. Respiratie- en temperatuurpieken komen dus samen voor. De temperatuurstijging kan namelijk volledig verklaard worden door het O₂ verbruik (**Hoofdstuk 2**). Door de scanmethode te combineren met een temperatuursensor kon worden aangetoond dat de respiratie- en temperatuurpieken niet samenvielen met verhoogde groei in het geval van A15. Temperatuurpieken veroorzaakten weliswaar een piek in de gemeten grijswaarde, Echter kwam dit door condensatie en de daaropvolgende verdamping van water. Bij andere stammen, zoals bijvoorbeeld MES 01808, lijkt wel degelijk dat een periode van intensievere groei gepaard gaat met een temperatuurverhoging. Daarom wordt er van uitgegaan dat de tijdelijke toename van de grijswaarde mogelijk te associëren is met een toename van de groei in andere *A. bisporus* stammen, zoals bijvoorbeeld MES 01808 (**Hoofdstuk 5**).

Een infraroodcamera liet zien dat de temperatuurpieken zich met een snelheid van 1 mm min⁻¹ door het mycelium verplaatsen. Door temperatuursensoren op verschillende posities in de compost te plaatsen werd aangetoond dat de respiratiepieken van *A. bisporus* steeds meer synchroniseerden over een afstand van minstens 50 cm. Voor deze synchronisatie is hoogstwaarschijnlijk anastomose (samensmelting) van de hyfen van mycelia die afkomstig zijn van verschillende broedkorrels noodzakelijk (**Hoofdstuk 2**). De respiratiepieken synchroniseerden bijvoorbeeld wanneer twee stukken compost, beiden gekoloniseerd door A15, naast elkaar werden geplaatst. Daarentegen gebeurde dit niet wanneer de compost was gekoloniseerd door de incompatibele stammen A15 en Bisp015.

RNA-sequencing toonde aan dat genen van *A. bisporus* die coderen voor lignolytische enzymen het meest actief zijn vóór en tijdens de respiratiepieken. Genen die betrokken zijn bij de afbraak van (hemi-)cellulose en microbiële biomassa komen meer tot expressie tijdens en na de respiratiepieken, terwijl genen die voor suiker- en aminozuurtransporters coderen het meest actief zijn na een respiratiepiek. Hieruit werd

geconcludeerd dat ligninolytische activiteit door tijd gescheiden is van andere activiteiten zoals de afbraak van cellulose en microbiële biomassa. Deze temporele scheiding kan enzymen, zoals cellulases en enzymen die betrokken zijn bij de afbraak van bacteriële biomassa, beschermen tegen de extracellulaire zuurstofradicalen die worden geproduceerd tijdens ligninolytische activiteit van *A. bisporus*.

Transport van water en voedingsstoffen binnen het mycelium en naar de paddenstoelen

Om de transportcapaciteit en directionaliteit van het myceliumnetwerk van *A. bisporus* te bestuderen is er gebruik gemaakt van het radioactieve ^{14}C -aminoisoboterzuur (^{14}C -AIB) (**Hoofdstuk 3**). De translocatiesnelheid van ^{14}C -AIB was 3.68 en 3.47 mm * h⁻¹ in *A. bisporus* mycelium dat gekweekt was op respectievelijk compost en dekaarde. De translocatie was 1.8 maal sneller naar de groeiende periferie van *A. bisporus* wanneer het mycelium vanuit één richting in de compost werd gekweekt. Daarnaast was het gehalte ^{14}C -AIB in de paddenstoelen vijf keer hoger vergeleken met paddenstoelen die gekweekt waren op mycelium dat gemengd groeide. Bovendien nam de translocatieafstand toe wanneer het mycelium directioneel werd gegroeid, wat resulteerde in de vorming van meer zo gehete mycelium strengen. Dit suggereert dat het vormen van strengen belangrijk is voor een hoge transportcapaciteit.

Translocatie van ^{14}C -AIB naar de toppen van hyfen werd alleen waargenomen wanneer het mycelium van *A. bisporus* actief groeide. Dit wijst erop dat door groei geïnduceerde massastroom de belangrijkste component van translocatie is (**Hoofdstuk 3**).

Het mycelium zorgt voor een efficiënte stroom van water en voedingsstoffen naar de ontwikkelende paddenstoelen. In **Hoofdstuk 4** werd de bijdrage van de dekaarde en verschillende lagen van de compost aan het watertransport richting de paddenstoelen bestudeerd. De dekaarde bleek de belangrijkste bron van water te zijn, terwijl de bovenste, middelste en onderste compostlaag elk steeds minder water bijdroegen. Gelijktijdig werden gedurende het gehele teeltproces het waterpotentiaal (Ψ) en het osmotische potentiaal (Ψ_{osm}) bepaald in de dekaarde, de compostlagen en de vruchtlichamen. Water stroomt van gebieden met een hoge naar gebieden met een lage Ψ . Ψ bestaat uit verschillende componenten, onder andere uit Ψ_{osm} , het matrisch potentiaal (Ψ_{mat}) en het drukpotentiaal (Ψ_n). Ψ nam af in de dekaarde en alle compostlagen tijdens het teeltproces. Net als het watergehalte daalde Ψ het meest in de dekaardelaag, terwijl de onderste compostlaag het minst afnam. Uit de gegevens blijkt dat Ψ_{osm} van de compost- en dekaardelaag het waterpotentieel in het begin van de teelt grotendeels bepaalt, terwijl Ψ_{mat} in latere stadia steeds belangrijker wordt, vooral in de dekaarde. De Ψ van de dekaarde werd bijna volledig verklaard door Ψ_{osm} bij het enten en het ventileren. Daarentegen verklaarde Ψ_{osm} van de dekaarde slechts 51 % en 31 % van Ψ tijdens respectievelijk de eerste en tweede vlucht.

Op basis van de bevindingen in **Hoofdstuk 4** zijn nieuwe teeltstrategieën voor het gebruik van de dekaarde getest op het verhogen van de champignonopbrengst. Het vervangen van de dekaarde of het aanbrengen van een nieuwe laag bovenop de oude laag dekaarde na de tweede vlucht resulteerde in een 1.3 – 1.4 maal hogere totale opbrengst. Deze nieuwe teeltstrategieën waren echter niet kosteneffectief. Er was geen invloed op het relatieve drooggewicht van de paddenstoelen en de waterefficiëntie (d.w.z. de hoeveelheid

water uit het substraat die in de paddenstoelen wordt teruggevonden). De hoeveelheid droge stof in het substraat is niet beperkend voor de vorming van paddenstoelen. Daarom zou de bovengenoemde waterefficiëntie als extra parameter kunnen dienen om de teeltefficiëntie te beoordelen. Deze parameter omvat het water dat vanaf het begin in het substraat aanwezig is en het water dat door het bewateringsregime wordt toegevoegd. Het extra voordeel van deze parameter is dat er rekening wordt gehouden met de invloed van zowel de compost als de dekaarde.

Curriculum vitae

Koen Herman was born on the 17th of January 1993 in Leiden, the Netherlands. He followed his secondary education at the Bonaventura college in Leiden and graduated in 2011. In September 2011 he started the Bachelor Biology followed by the Master Environmental Biology at Utrecht University. As part of his studies, Koen completed two research internships, the first of which at the Microbiology group of Utrecht University. In this project, Koen worked under the supervision of prof. dr. Han Wösten and Dr. Aurin Vos on the dynamics of H₂O₂ production in compost colonised by *A. bisporus*. In his second internship, Koen worked under the supervision of Prof. Dr. John van der Oost and Dr. Richard Notebaart on the regulatory function of the MED13 protein on transcription initiation. Koen obtained his MSc degree in February 2018. In March 2018, Koen started his PhD at the Microbiology group of the Department of Biology at Utrecht University under the supervision of Prof. Dr. Han Wösten, Dr. Robert-Jan Bleichrodt, and Dr. Luis Lugones. The research on translocation of water and nutrients in *A. bisporus* was financially supported by NWO TTW and is described in this thesis.

List of Publications

- Herman, K.C.**, & Bleichrodt, R., 2022. Go with the flow: mechanisms driving water transport during vegetative growth and fruiting. *Fungal Biology Reviews*. 41, pp. 10–23.
- Herman, K.C.**, Vos, A.M., Bleichrodt, R.J., Ohm, R.A., Scholtmeijer, K., Schmitt, H., Lugones, L.G., Wösten, H.A.B., 2021. Cycling in degradation of organic polymers and uptake of nutrients by a litter-degrading fungus. *Environ. Microbiol.* 23, 224–238.
- Herman, K.C.**, Wösten, H.A.B., Fricker, M.D., Bleichrodt, R.J., 2020. Growth induced translocation effectively directs an amino acid analogue to developing zones in *Agaricus bisporus*. *Fungal Biol.* 124, 1013–1023.
- Vos, A.M., Jurak, E., Pelkmans, J.F., **Herman, K.C.**, Pels, G., Baars, J.J., Hendrix, E., Kabel, M.A., Lugones, L.G., Wösten, H.A.B., 2017. H₂O₂ as a candidate bottleneck for MnP activity during cultivation of *Agaricus bisporus* in compost. *AMB Express* 7, 1–9.

Dankwoord

Het dankwoord schrijven is het begin van het einde van een PhD, gelukkig eindigt het weer met een begin. Ik wist dat het zwaar zou worden toen ik aan dit project begon. Toch heb ik een aantal zaken flink onderschat. Achteraf gezien was stoppen een logischer besluit geweest. Een aantal mensen hebben ervoor gezorgd dat dit boekje er toch is gekomen. Iedereen die heeft bijgedragen en mij heeft gesteund in dit proces ben ik ontzettend dankbaar. Hopelijk kan ik in de toekomst iets meer trots zijn op dit werk.

Han, heel erg bedankt voor jouw onmisbare hulp bij zo een beetje alles. Zonder jouw eindeloze geduld, enthousiasme en optimisme was dit boekje er zeker niet gekomen. Inhoudelijk kunnen wij altijd goed van standpunt verschillen, maar op persoonlijk niveau wisten we elkaar wel altijd goed te vinden, waardoor alles te relativieren was. Bedankt dat jij het vertrouwen in een goede afloop behield, zelfs wanneer ik ervan overtuigd was dat dit niet meer mogelijk was. Luis, jij zorgde ervoor dat ik een nieuwsgierigheid ontwikkelde voor de microbiologie. Dat ik een promotie heb gedaan op dit vakgebied is dus zeker ook jouw verdienste. Bij jou kon ik terecht voor elke vraag. Wel met genoeg tijd voor het gesprek dat hieruit volgde, waarbij je niet alleen antwoord op de vraag, maar ook de meest uiteenlopende excentrieke feitjes mee kreeg. Eenmaal begonnen aan mijn PhD duurde het slechts 2 jaar voordat je erachter kwam dat jij ook mijn copromotor was. Gelukkig waren de supervisie taken al goed ingevuld. Robert-Jan, ik denk dat er geen persoon is waar ik meer van geleerd heb gedurende mijn PhD dan dat ik van jou deed. Of het nou gaat over microbiologie, radioactiviteit, microscopie, ImageJ, statistiek, arduino, macro's, wijn, of fermenteren, de lijst met zaken waar jij iets vanaf weet lijkt eindeloos. Met engelengeduld wilde je het me allemaal uitleggen en hier maakte ik ook zeker gebruik van. Bedankt voor jouw aandeel in dit boekje en ik weet zeker dat we in de toekomst hier nog vaker op gaan proosten.

Over proosten gesproken. Thierry en Elmar, bedankt dat jullie mijn paranimfen willen zijn. Een vriendschap die helemaal teruggaat naar de basisschool. Met enige regelmaat proosten we hierop en waren jullie mijn steun en toeverlaat op zulke avonden. Jullie hebben laten doorschemeren dat ik daar nog meer gebruik van mag maken en dat ga ik dan ook doen. Speaking of cheers. Cheers to all connoisseurs, Robert-Jan, Antonio, Freek and Auke. We have shared many great wines during our time at Microbiology and I am sure many more are still to come (looking at the picture of the Hermitage right now). Special thanks to Antonio for introducing me to cooking italian cuisine, mozzafiato!

Alle collega's van Microbiologie, bedankt voor jullie steun en input. Esther, samen hebben wij heel wat kilometers afgelegd! Deze tochten waren ideaal om even stoom af te blazen wanneer het allemaal wat teveel werd. Ik ben je erg dankbaar voor alle steun die je tijdens, naast en na mijn PhD hebt gegeven. Zonder jou was het echt niet hetzelfde geweest. Brigit, we kennen elkaar vanaf het begin van de studie en hebben binnen biologie ons eigen pad bewandeld. Toch wisten we elkaar altijd makkelijk te vinden en lagen we geregeld in een deuk van het lachen. Van La Chouffe in de put, langs commissieweekenden, naar wintersport met Fleur (die als een dolle naar beneden gaat) en William (keep on snowboarding!). Robin, heel erg bedankt dat ik met jou heb mogen samenwerken aan het Lipid Yeast project. Het was erg leuk om even lid te zijn van Fungal Genomics. Ik hoop dat er snel een doorbraak komt en dat de gisten natuurlijk liters olie gaan produceren. Bedankt Margot voor je hulp met studentenprojecten. Er is niet

echt iets concreets uit gekomen voor mijn project, maar dat doet niks af aan de prettige samenwerking. Beste roommies van O404, ik heb over de hele 4^e verdieping gezwerfd (in 4 jaar tijd heb ik 7 x van werkplek moeten verhuizen) maar de laatste sessie was hier, bedankt voor alle momenten van afleiding, internetclassics, relativering, banaantijd en het belachelijk maken van elkaar en elkaars onderzoek. Peter-Jan, ik hoop dat je in de Zweden een kantoor vindt dat groot genoeg is voor jou én je ego, dan komt het sowieso goed met jouw onderzoeks carrière. Erik (strijders!), veel succes met de laatste fase van je PhD. Geldt ook voor jou Marieke (HR!) en laat je niet gek maken door Peter-Jan. Geldt niet voor Emmeline, die wens ik succes met alle fasen van de PhD, maar in de korte tijd waarin ik je heb meegemaakt weet ik nu al dat dat helemaal goed gaat komen! Ioana, thanks for brightening up our sometimes grumpy office. Maarten ook jij was erbij in O404 en die relatief korte tijd is samen te vatten met: Pelkmans?! Over Pelkmans gesproken, heel erg bedankt Jordi. Zonder jou en later ook Femke zou het leven op het lab niet zo soepel verlopen als dat het nu doet. Het moge duidelijk zijn dat jullie jezelf onmisbaar hebben gemaakt.

Thanks Eline&Jésus (Broodje Ben!) for supporting me during corona times. Maryam, you are one of the toughest persons I know. I hope good times will find you where this quality won't always be necessary. Thanks Jun, I hope you are doing well with your family in China and let me know if you want me to kick your ass at tabletennis, Juan, Xiaoyi and all other staff, postdocs and PhDs: Charissa, Martin (Bedankt voor je hulp bij de statistiek & data analyse) Boris, Hans, Apostolos, Jeroen, (R)Ella, Stephanie, Jacq, Janieke, Maaïke en Nienke and Guus. Bram, bedankt voor je hulp bij de lay out!

Thanks to all members involved in the project. Jack, Francien, Lubos, Madalina, Eric, hopelijk komt ons manuscript nog tot een publicatie, and Johan. A big thank you to all co-authors. In het bijzonder, Aurin, heel erg bedankt. Jij hebt me zo'n beetje alle skills geleerd die ik nodig heb gehad op het lab. Zonder de tijd die jij in mij hebt geïnvesteerd zou ik niet ver zijn gekomen.

Partyknallers, Jeffrey, Bas, Arjan en Ties. Jullie hadden natuurlijk allang door dat mijn wetenschappelijke carrière niks werd en boden een alternatief. Bedankt voor deze muzikale uitlaatklep. Nog even een paar nummers schrijven en dan worden we in no time beroemd.

Lieve familie, volgens mij hebben jullie nog steeds geen flauw idee waar mijn PhD over gaat, mede omdat ik daar niet altijd graag over vertel, maar toch waren jullie er altijd voor me. Lieve ouders, Wijnand en Emmy, mien breur Thijs en Kiki (nu ook Herman). Jullie vormen de basis waarvan uit ik verder kon klimmen. Als er iets is wat ons bij elkaar brengt dan is het de liefde voor de wintersport. Het vooruitzicht op de volgende wintersport kan mij altijd op de been houden. Lieve schoonouders, Petra & Jan-Egbert, Edwin en Erica, Freek en Jet, Oma en Ria, Sophie, Tim en Frank, bedankt voor alle momenten die we samen hebben mogen meemaken.

Lieve Annerose, ik ben altijd heel gelukkig als ik bedenk hoeveel wij met elkaar gedeeld hebben. We hebben bijna het punt bereikt waarop we elkaar langer kennen dan niet. Niet al die tijd samen was makkelijk. De problemen waarmee ik soms thuiskwam wogen ook door op jou. Gelukkig weet jij als geen ander hoe je me scherp en vastberaden houdt om deze problemen op te lossen. Jouw onvoorwaardelijke steun de afgelopen jaren was dan ook onmisbaar. Één ding weet ik zeker en dat is dat ik met jou alles aankan wat de toekomst ons gaat brengen. We gaan nog veel meer samen meemaken dan we tot nu toe

gedaan hebben, en vanaf nu altijd samen met onze Luc.